Investigation into potential *Dirofilaria immitis* drug targets through rational anthelmintic synthesis and design

by

Autumn M. Collins

A thesis submitted to the
School of Graduate and Postdoctoral Studies in partial
fulfillment of the requirements for the degree of

Master of Science in Applied Bioscience

University of Ontario Institute of Technology (Ontario Tech University)

Oshawa, Ontario, Canada
April 2022

This Thesis Contains Confidential and Proprietary Information

© Autumn M. Collins, 2022

THESIS EXAMINATION INFORMATION

Submitted by: **Autumn M. Collins**

Master of Science in **Applied Biosciences**

Thesis title: Investigation into potential *Dirofilaria immitis* drug targets through rational anthelmintic synthesis and design

An oral defense of this thesis took place on April 5, 2022 in front of the following examining committee:

Examining Committee:

Chair of Examining Committee	Dr. Janice Strap
Research Supervisor	Dr. Jean-Paul Desaulniers
Research Co-supervisor	Dr. Sean Forrester
Examining Committee Member	Dr. Yuri Bolshan
Thesis Examiner	Dr. Hélène LeBlanc

The above committee determined that the thesis is acceptable in form and content and that a satisfactory knowledge of the field covered by the thesis was demonstrated by the candidate during an oral examination. A signed copy of the Certificate of Approval is available from the School of Graduate and Postdoctoral Studies.

Abstract

Dirofilaria immitis is a mosquito-transmitted parasitic nematode that can cause debilitating disease in dogs. *D. immitis* is present in Canada and over the years has increased in prevalence due to several factors including climate change. Anthelmintic resistance is becoming increasingly problematic and as such, the aim of this thesis was to synthesize several novel compounds and examine their activity on the anthelmintic receptor targets of interest, ACC-2 which is an acetylcholine-gated chloride channel unique to nematodes and the UNC-49 GABA receptor. In total, 22 compounds, 12 of which are novel, were synthesized, including imidazole-4-acetic acid like compounds, levamisole derivatives, and a levamisole dimer. Compounds **8**-**15** were tested on the Hco-ACC-2 receptor using electrophysiological techniques and all demonstrated various degrees of receptor activation. Compound **13,** which had the highest response, was further evaluated using computer-based ligand docking on a homology model of the Hco-ACC-2 receptor.

Keywords: *Dirofilaria immitis*; Anthelmintic; Heartworm; Levamisole; Imidazole-4-acetic acid

Authors Declaration

I hereby declare that this thesis consists of original work of which I have authored. This is a true copy of the thesis, including any required final revisions, as accepted by my examiners.

I authorize the University of Ontario Institute of Technology (Ontario Tech University) to lend this thesis to other institutions or individuals for the purpose of scholarly research. I further authorize University of Ontario Institute of Technology (Ontario Tech University) to reproduce this thesis by photocopying or by other means, in total or in part, at the request of other institutions or individuals for the purpose of scholarly research. I understand that my thesis will be made electronically available to the public.

The research work in this thesis that was performed in compliance with the regulations of Research Ethics Board/Animal Care Committee under **REB Certificate number/Animal care certificate file number 14290**.

Autumn M. Collins

Statement of Contributions

I hereby certify that I am the sole author of this thesis and that no part of this thesis has been published or submitted for publication. I have used standard referencing practices to acknowledge ideas, research techniques, or other materials that belong to others. Electrophysiology studies discussed in Chapter 3 were performed and data was collected by PhD Candidate Sierra Varley. Homology models of Dim-UNC-49 were based on unpublished sequences provided by Sierra Varley as part of a collaboration between Ontario Tech, Zoetis and the Institut National de la Recherche Agronomique.

Acknowledgements

I would like to first acknowledge our funding partner Zoetis, Inc, without their funding this project would have not been possible. It has been a pleasure to collaborate on this project with such a big industrial partner who is so involved and supportive. I hope this project opened the doors for future partnerships down the road.

To my supervisors Dr. Jean-Paul Desaulniers and Dr. Sean Forrester, thank you for taking a chance on a Forensic Chemistry student who had been out of the lab for a year. I was lucky enough to be in the Desaulniers lab for almost 4 years and am very fortunate for such a great opportunity to broaden my chemistry knowledge under his supervision. JP, thank you for listening to my fast-talking Monday updates, all my crazy scheme ideas, all your guidance and support especially over my master's period. Sean, thank you for letting me use the space in your lab and broaden my biology knowledge. Although we had less in person interactions then JP and myself, you were always there when I needed you and have always been very supportive. Through both of your supervision and guidance I have become a better scientist and I can't express my gratitude enough.

To my blended family of lab mates in both the Desaulniers (Matt, Andrew, Lidya, Golam, Ifrodet, Charlene and Makenzie) and Forrester (Sierra, Jen, Kristen and Sarah) lab groups, past and present, I appreciate all of you and I am so glad to have met you. Thank you all for shaping me into the scientist I am today. To my chemistry pals Ifrodet and Charlene. Ifrodet, thank you for all that you do from running the mass spec. to being a great friend and chemist. Charlene, thank you for all the great chemistry and personal talks and support. Without the both of you I don't think I would have been able to get through my masters with my sanity. I can't wait to see the great things you two will do. To my biology pals Sierra and Jen. Sierra, thank you

for your continual work on this project it means the world to me. Jen, thanks for being my desk mate and always being engaged and interested in my chemistry. I appreciate you both for your friendship and support.

To my family and friends for their immense support. To my parents, Heather and Terry (Step Mom - Annette), thank you for giving me the opportunity to go to a school 4 hours away from you, supporting me in every way you could and always believing in me. To my Aunt Amy and Pete, thank you for letting me live with you throughout my masters, making my lunch and always checking in on me. To Chris, thank you for the years of long-distance support, chemistry rants you half understand, advice and love. Without each and every one of your support I would not be where I am today.

Finally, to my committee members Dr. Yuri Bolshan, Dr. Hélène LeBlanc and Dr. Janice Strap. Thank you for your time and assistance in the completion of my Masters degree.

Table of Contents

THESIS EXAMINATION INFORMATION ..... **II**

ABSTRACT ..... **III**

AUTHORS DECLARATION ..... **IV**

STATEMENT OF CONTRIBUTIONS ..... **V**

ACKNOWLEDGEMENTS ..... **VI**

TABLE OF CONTENTS ..... **VIII**

LIST OF FIGURES ..... **XI**

LIST OF SCHEMES ..... **XIII**

LIST OF ABBREVIATIONS AND SYMBOLS ..... **XIV**

CHAPTER 1- INTRODUCTION **1**

1.1 *Dirofilaria Immitis* 1

1.2 Current Treatment Methods and Anthelmintic Resistance 4

1.2.1 Macrocyclic lactones- Ivermectin *4*

1.2.2 Melarsomine dihydrochloride- Diroban® *5*

1.2.4 Treatment Issues and Resistance *6*

1.3 Cys-Loop Receptors and Targets of Interest 7

1.3.1 $GABA_A$ Receptors and UNC-49 ..... *8*

1.3.2 Acetylcholine-gated Chloride Channels and ACC-2 ..... *9*

1.4 Nitrogen Containing Heterocycles 10

1.4.1 Imidazole-4-acetic acid (IMA) *10*

1.4.2 Levamisole *11*

1.5 Pharmacological Characterization 12

1.6 Homology Modeling and Computational Docking 13

1.7 Objectives 14

CHAPTER 2 - EXPERIMENTAL **15**

2.1 – General Synthetic Method 15

2.2- Synthesis and Characterization of Organic Compounds – Imidazole Like Compounds 15

2.2.1- 1-(azidomethyl)-2,4-dimethoxybenzene- Compound (1) *15*

2.2.2- 1-(2,4-dimethoxyphenyl)-1H-1,2,3-triazole-4-carboxylic acid- Compound (2) *16*

2.2.3- Methyl 1H-1,2,3-triazole-4-carboxylate – Compound (3) *17*

2.2.4 – 1H-1,2,3-triazole-4-carboxylic acid– Compound (4) *17*

2.2.5 – 2-(1-(2,4-dimethoxyphenyl)-1H-1,2,3-triazol-4-yl)acetic acid– Compound (5) *18*
2.2.6 – 2-(1H-1,2,3-triazol-4-yl)acetic acid – Compound (6) *19*
2.3- SYNTHESIS AND CHARACTERIZATION OF ORGANIC COMPOUNDS – LEVAMISOLE AND LEVAMISOLE DERIVATIVES 20
2.3.1- Extraction of Levamisole ((S)-6-phenyl-2,3,5,6-tetrahydroimidazo[2,1 b]thiazole) – Compound (7) *20*
2.3.2- Synthesis of (S)-7-methyl-6-phenyl-2,3,5,6-tetrahydroimidazo[2,1-b]thiazol-7-ium- Compound (8) *21*
2.3.3 – Synthesis of (S)-7-ethyl-6-phenyl-2,3,5,6-tetrahydroimidazo[2,1-b]thiazol-7-ium – Compound (9) *22*
2.3.4 – Synthesis of (S)-7-benzyl-6-phenyl-2,3,5,6-tetrahydroimidazo[2,1-b]thiazol-7-ium- Compound (10) *23*
2.3.5- Synthesis of (S)-7-((perfluorophenyl)methyl)-6-phenyl-2,3,5,6-tetrahydroimidazo[2,1-b]thiazol-7-ium – Compound (11) *24*
2.3.6- Synthesis of (S)-7-(4-bromobenzyl)-6-phenyl-2,3,5,6-tetrahydroimidazo[2,1-b]thiazol-7-ium – Compound (12) *25*
2.3.7- Synthesis of (S)-6-phenyl-7-(2-(trifluoromethyl)benzyl)-2,3,5,6-tetrahydroimidazo[2,1-b]thiazol-7-ium – Compound (13) *26*
2.3.8- Synthesis of (S)-6-phenyl-7-(4-(trifluoromethyl)benzyl)-2,3,5,6-tetrahydroimidazo[2,1-b]thiazol-7-ium – Compound (14) *27*
2.3.9- Synthesis of (S)-7-(4-nitrobenzyl)-6-phenyl-2,3,5,6-tetrahydroimidazo[2,1-b]thiazol-7-ium – Compound (15) *28*
2.3.10- Synthesis of (S)-7-(4-methylbenzyl)-6-phenyl-2,3,5,6-tetrahydroimidazo[2,1-b]thiazol-7-ium – Compound (16) *29*
2.3.11- Synthesis of (S)-7-(2-methylbenzyl)-6-phenyl-2,3,5,6-tetrahydroimidazo[2,1-b]thiazol-7-ium – Compound (17) *30*
2.3.12- Synthesis of (S)-7-allyl-6-phenyl-2,3,5,6-tetrahydroimidazo[2,1-b]thiazol-7-ium- Compound (18) *31*
2.3.13- Synthesis of (S)-6-phenyl-7-(prop-2-yn-1-yl)-2,3,5,6-tetrahydroimidazo[2,1-b]thiazol-7-ium- Compound (19) *32*
2.3.14- Synthesis of (S)-7-(4-(bromomethyl)benzyl)-6-phenyl-2,3,5,6-tetrahydroimidazo[2,1-b]thiazol-7-ium – Compound (20) *33*
2.3.14- Synthesis of (S)-7-(4-aminobenzyl)-6-phenyl-2,3,5,6-tetrahydroimidazo[2,1-b]thiazol-7-ium – Compound (21) *34*
2.4- SYNTHESIS AND CHARACTERIZATION OF ORGANIC COMPOUNDS – LEVAMISOLE DIMERS 35
2.4.1- Synthesis of (6S,6'S)-7,7'-(1,4-phenylenebis(methylene))bis(6-phenyl-2,3,5,6-tetrahydroimidazo[2,1-b]thiazol-7-ium) – Compound (22) *35*
2.5- ELECTROPHYSIOLOGICAL EVALUATION OF COMPOUNDS 36
2.6- HOMOLOGY MODELING AND COMPUTATIONAL DOCKING OF COMPOUNDS 37
CHAPTER 3- RESULTS AND DISCUSSION 39
3.1 – ORGANIC SYNTHESIS OF IMIDAZOLE – 4- ACETIC ACID LIKE COMPOUNDS 39

3.2 – ORGANIC SYNTHESIS OF LEVAMISOLE DERIVATIVES 43
3.3 – ORGANIC SYNTHESIS OF LEVAMISOLE DIMERS 48
3.4 Pharmacological Characterization 48
3.5 – HOMOLOGY MODELING DATA 52
3.5.1 Imidazole Like Compounds 54
3.5.2 Levamisole and Levamisole Derivatives 55
CHAPTER 4- CONCLUSIONS 59
CHAPTER 5- FUTURE DIRECTIONS 61
REFERENCES 63
APPENDICES 69
A1. CONFORMATIONAL NMR SPECTRA 69
A2. CONFORMATIONAL MS SPECTRA 93
A3. LEVAMISOLE NOVEL COMPOUND DATA 101

List of Figures

Chapter 1- Introduction

Figure 1.1 - *D. immitis* cycle of transmission. Figure was made in biorender……2

Figure 1.2- Structures of ivermectin and melarsomine dihydrochloride (Diroban)……...4

Figure 1.3 – GABA and $GABA_A$ Receptors**.** A: Structure of GABA. B: Pentameric structure of $GABA_A$ from a top and side view. C: $GABA_A$ receptor activation. Figure was made in biorender…….……..……7

Figure 1.4 - Structures of the vitamin thiamin, hormone melatonin, antibiotic levofloxacin and base pair thymine……..9

Figure 1.5 - Structure of imidazole-4-acetic acid (IMA)……...10

Figure 1.6 - Structure of levamisole……11

Chapter 3- Results and Discussion

Figure 3.1- Structures of Imidzaole-4-acetic acid, compound **4** and compound **6**……..…….39

Figure 3.2.1- S_N2 N-alkylation mechanism of free base levamisole and bromo substituents of interest to afford levamisole derivatives, compounds **8-20**…….……..…….43

Figure 3.4.1- Computer-generated trace for one run with each compound structure shown above the corresponding response……49

Figure 3.4.2- Summary of electrophysiology screening data for Acetylcholine, Levamisole and Compounds **8**-**10** at 500 μM. Percent response was normalized to Acetylcholine having a 100% response……49

Figure 3.4.3- Summary of electrophysiology screening data for acetylcholine, levamisole and compounds **10**-**15** at 500μM. Percent response was normalized to Acetylcholine having a 100% response……50

Figure 3.4.4- Compounds **13, 14, 16, 17** with each of the benzyl group positions labeled….51

Figure 3.5.1- Homology models of Dim-UNC-49B (top) and Hco-ACC-2 (bottom) with labeled extracellular domain, binding pocket and transmembrane domain…….……52

Figure 3.5.2: Binding Pocket of Dim-UNC-49 (left) and Hco-ACC-2 (right) with relevant amino acids exposed. Part of loop C has been removed for visualization purposes. Loop A (yellow), Loop B (blue), Loop C (red), Loop D (orange), Loop E (green), Loop F (purple) and for ACC-2 Loop G (magenta) have been highlighted in different colors for identification purposes…….53

Figure 3.5.3- Homology model and computational docking of imidazole-4-acetic acid (top left), compound **4** (top right) and compound **6** (bottom) in Dim-UNC-49B……..…..….54

Figure 3.5.2.1- Homology model and computational docking of Compound **7** in the homomeric Hco-ACC-2 channel with distances and amino acids expressed. Part of loop C has been removed for visualization purposes..……..…….55

Figure 3.5.2.2- Homology model and computational docking of Compound **13** in the homomeric Hco-ACC-2 channel with distances and amino acids expressed. Part of loop C has been removed for visualization purposes..……..…….56

Figure 3.5.2.3- Homology model and computational docking of Compound **15** in the homomeric Hco-ACC-2 channel with distances and amino acids expressed. Part of loop C has been removed for visualization purposes……..57

Figure 4- Structures of all 22 compounds synthesized……...……..59

List of Schemes

Chapter 3- Results and Discussion

Scheme 3.1.1: Original scheme of compound **4**……..40

Scheme 3.1.2: Synthesis of compound **6**……..…41

Scheme 3.1.3- Synthesis of Compound **4**……42

Scheme 3.2.1- General scheme for compounds **8-20**. Compounds 8+9 used 1.2 eq of the alkyl iodine source and THF as the solvent. Compounds 10-17 used 1.1 eq of the respective alkyl bromide and THF as the solvent. Compounds 18 and 19 used 1.2 eq of the respective alkyl bromide and DMF as the solvent. Finally compound 20 used 1.2 eq of 1,4-bis(bromomethyl)benzene and acetone as the solvent……..……44

Scheme 3.2.2- Synthesis of compound **21** using approximately 7 eq of Zn and acetic acid in a H_2O and Methanol solvent system……...…46

Scheme 3.3- Synthesis of compound **22** was done with 1.2 eq of 1,4-bis(bromomethyl)benzene and 2.0 eq of compound **7**……47

List of Abbreviations and Symbols

ACC	Acetylcholine-gated chloride channel
ACN	Acetonitrile
Biotage	Isolera One Biotage purification instrument
CDCl3	Deuterated chloroform
CuAAC	Copper-catalyzed azide–alkyne cycloaddition
Cys-loop	Cysteine loop
DCM	Dichloromethane
dd	doublet of doublets
Dim	Dirofilaria immitis
DMF	N,N-dimethylformamide
DMSO	Dimethyl sulfoxide
DMSO-d_6	Deuterated dimethyl sulfoxide
DOPE	Discrete optimized protein energy
dt	doublet of triplets
ECD	Extracellular domain
eq	Equivalents
EtOAc	Ethyl acetate
GABA	γ-Aminobutyric acid
Glu (E)	Glutamic acid
H2O	Water
HCl	Hydrochloric acid
Hco	*Haemonchus contortus*
IMA	Imidzaole-4-acetic acid
J	Coupling constant (Hz)
L#	Larval stage 1-5
Lev	Levamisole
m	Multiplet
m/z	Mass to charge ratio
MeOD	Deuterated methanol
MeOH	Methanol
MHz	Megahertz
miVAc	GeneVac miVac Quattro concentrator
Na2SO4	Sodium sulfate
NaOH	Sodium hydroxide
NMR	Nuclear magnetic resonance
pH	Potential hydrogen
Phe (F)	Phenylalanine

Q-TOF LC/MS	Quadrupole time of flight liquid chromatography mass spectrometry
rt.	Room temperature
t	Triplet
tButOH	Tert-butyl alcohol
TEA	Triethylamine
TFA	Trifluoracetic acid
THF	Tetrahydrofuran
Thr (T)	Threonine
TLC	Thin-layer chromatography
TMD	Transmembrane domain
Trp (W)	Tryptophan
Tyr (Y)	Tyrosine
UNC	Uncoordinated

Chapter 1- Introduction

1.1 *Dirofilaria Immitis*

Dirofilaria immitis, formally named *Filaria canis cordis*, was first discovered in 1856 by Dr. Joseph Leidy (1). *D. immitis* is a parasitic, elongated roundworm from the Nematoda phylum. This parasite affects 30 mammalian species including the feline and canine family, however the most prevalent host are dogs (2,3). This parasite has also been identified as a zoonotic infection as it is able to be transmitted from animals to humans, however, cases of this are rare (4,5). The first report of a human dirofilariasis infection was found in a child in 1887 where worms were located in the left ventricle of the heart (4,5). Since the human body is not the natural host for this parasite the worms will eventually die. However, they can block the pulmonary arteries resulting in nodule formations in the lungs that can be detected in a computerized tomography (CT) scan (4). *D.immitis* can also cause peripheral eosinophoilia in humans, which is an increased amount of white blood cells due parasitic infection (4). Although peripheral eosinophoilia is present in only 6.5-15% of cases, it can become life threatening (4)

The *D. immitis* cycle of transmission occurs through the use of the mosquito vector (**figure 1.1**). The cycle starts when a mosquito bites an infected dog and ingests microfilariae produced from adult female worms (2). These microfilariae then mature within the mosquito for approximately two weeks until they reach larval stage 3 (L3). At this stage, the mosquitos are able to transmit the parasite to a new host. The mosquito then bites the host leaving the larvae on the skin. These larvae can then enter the host via the puncture wound left by the mosquito (5). Forty-five to sixty days after these larvae have been deposited, the stage 5 larvae, also known as immature adults, enter the

bloodstream which clogs the pulmonary arteries (5). The immature adults continue to mature, mate and, in the process, migrate to the heart. After approximately one hundred and ninety days microfilaria appear in the blood stream and the process of transmission is able to repeat (5). If this parasite is left untreated it can cause multiple system dysfunction affecting the pulmonary circulation, heart, liver, and kidneys and as result my lead to the death of the host (5).

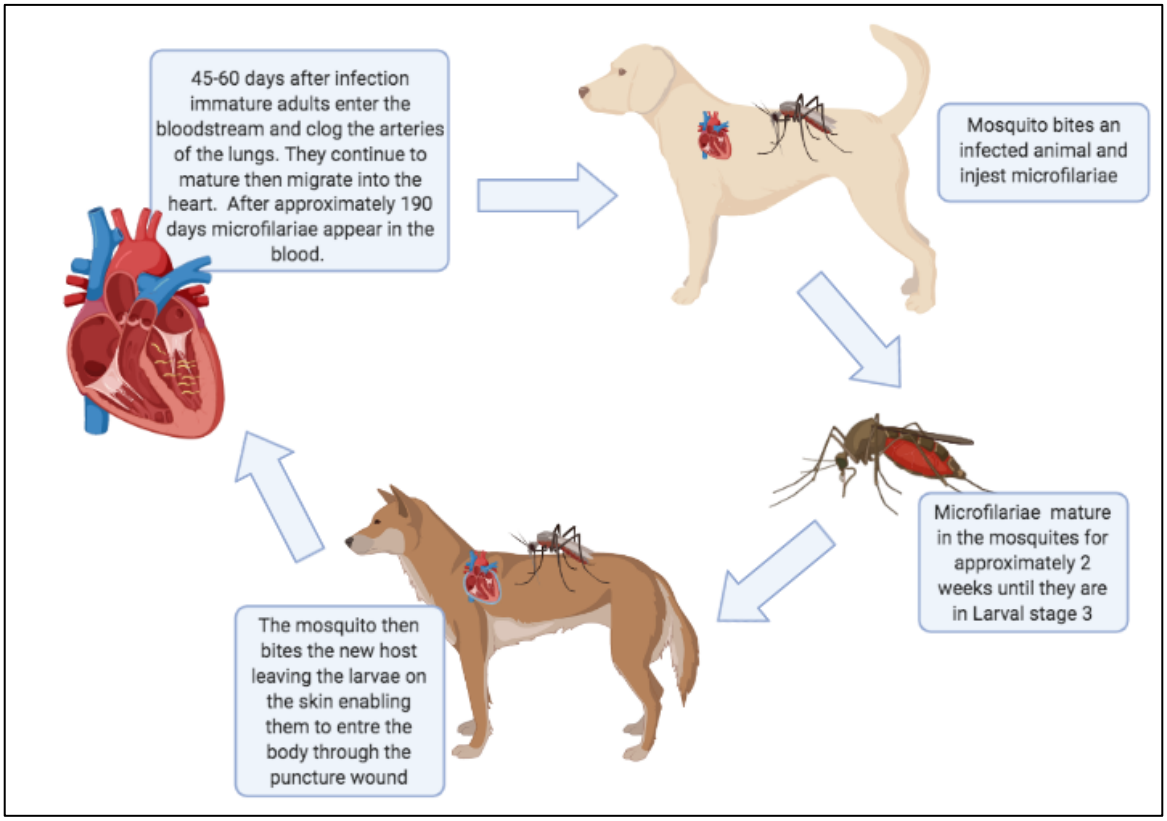

Figure 1.1 - *Dirofilaria immitis* cycle of transmission. Figure was made in biorender.

Throughout the *D. immitis* life cycle a species of bacteria, *Wolbachia*, is produced and concentrated within the hypodermal latera cords for males and in both the hypodermal latera cords and reproductive organs of females (6). This bacteria is essential for the nematodes survival (6–8). The *Wolbachia* bacteria is released into the host with the death of the parasite (9). This can cause adverse effects to the host after being treated

for *D. immitis* (9). *Wolbachia* can cause inflammatory effects in canines effecting there kidneys, lungs and liver (8). However, there are treatment methods available to decrease this bacteria in the dog thus reducing the inflammatory effects (9).

Although *D. immitis* was discovered in 1856, its first case in Canada was reported in 1977 (10). Since that time there has been an increased number of cases (10). In Canada, with a sampling size of 86,251 dogs, the positivity rate of *D. immitis* in 2008 was determined to be 0.22% (11). Five years later, with a sampling size of 115,636 dogs, this percentage has doubled to 0.42% (10).

This increase in the *D. immitis* positivity rate in Canada could be due to several factors. As it is well known, our world temperature is increasing every year due to global warming, over 68 years (1948-2016), Canada's overall mean temperature has increased 1.7 ^{o}C (12). This increase has been observed more in northern Canada with an average increase of 2.3 ^{o}C (12). With this increase, we are also seeing *D. immitis* in more northern parts of Canada than previously reported (13). In order for the microfilariae to mature in the mosquito to larval stage 3 (L3) the temperature must be above 14^{o}C (13). With the rise in temperature, mosquitos are now able to live longer, increase their population and have a larger length of time to infect a new host.

Some additional reasons for the increase in positivity rate that has been presented include is the improper administration of preventative medication to dogs or other pets, accompanying there owners on vacations and/or lack of veterinary visits (14–16). A survey published in 2013 in the United States, in sampling population of 50,000 people, determined that 18.7% of owners have not taken their dog to a veterinarian in 2011 (17). This means that there is only a small percentage of owners using this preventative

medication. This also brings up a point of how accurate the case count is if there is only a small percentage of dogs being brought to a veterinary clinic.

1.2 Current Treatment Methods and Anthelmintic Resistance

Anthelmintics are a class of drugs that are used to treat parasitic helminth infections (18). Current treatment methods of *D. immitis* are primarily prescribed as preventative measures. Macrocyclic lactones, such as ivermectin, along with Melarsomine dihydrochloride, (Diroban®- Zoetis), are the drugs currently used in combination as preventative measures and parasite removal (19). The structures of these molecules can be found in **figure 1.2** below.

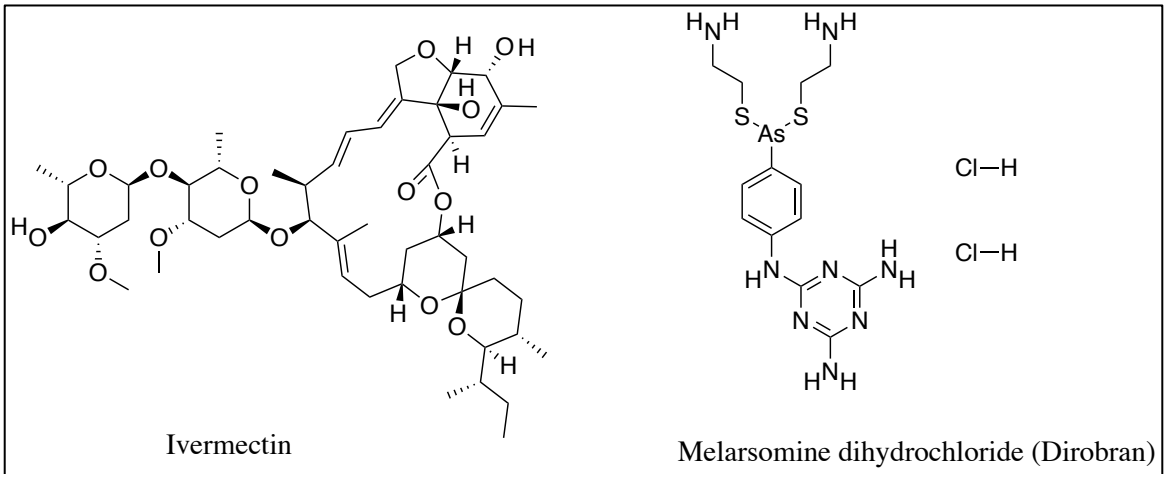

Figure 1.2 - Structures of ivermectin and melarsomine dihydrochloride (Diroban®).

1.2.1 Macrocyclic lactones- Ivermectin

Macrocyclic lactones are a group of anthelmintics known for treating filarial nematode infections in both animals and humans, however, currently ivermectin is the only one approved to be used in humans (20). The mode of action of ivermectin is through direct activation of glutamate-gated chloride channels by enhancing the action of glutamate (21). In *Caenorhabditis elegans* and *Haemonchus contortus*, ivermectin has

been shown to cause paralysis and inhibition of pharyngeal pumping in the worms (22). Ivermectin has also been show to prevent the secretion of immunomodulatory proteins in *Brugia malayi*, one of the filarial nematodes that cause elephantiasis in humans (23). This results in leaving the parasite vulnerable to be attacked by the hosts immune system (23). Thus the treatment of ivermectin reduces the microfilariae in the blood, which results in a reduced chance of microfilariae being consumed by the vector and continuing the cycle of transmission (20). In 6 to 8 months, ivermectin has been shown to clear circulating microfilariae from dogs infected with *D. immitis* from the blood (24). Ivermectin is very effective at killing up to stage four larvae. However, after this point the efficacy declines (25,26). This is why the need for additional drugs is needed in these preventative treatments.

1.2.2 Melarsomine dihydrochloride- Diroban®

Melarsomine dihydrochloride, known by its marketed name as Diroban®, is an anthelmintic used to kill worms from larval stage 5 (L5) to the adult worms and used in mild to severe cases of infection (27). This is currently the only approved drug treatment for adult worms in *D. immitis* (26,28). According to Diroban's product label, the exact mode of action of this therapeutic in *D. immitis* is unknown (27). Since the drug is used to kill parasitic worms there is a risk of pulmonary thromboembolism post-treatment(26).

1.2.3 Tetracycline- Doxycycline

Doxycycline, a tetracycline antibiotic compound, along with macrocyclic lactones together were studied to determine the effectiveness of this combination (7). Doxycycline targets the bacteria *Wolbachia* which is essential for filarial worms survival (7,29). Without these bacteria the worms are unable to grow and continue their lifecycle. When

looking at the adult worm burden, it was found that when doxycycline was administered daily (10mg/kg day) and ivermectin were administered weekly (6μg/kg) together it was 78.3% effective at minimizing the amount of adult worms present (7). Doxycycline by itself was only 8.7% effective at minimizing the amount of adult worms present (7).

1.2.4 Treatment Issues and Resistance

Although the above treatment methods have shown past success in the treatment of *D. immitis* there are still additional considerations. As mentioned above for treatments targeting adult worms, there is a risk of pulmonary thromboembolism which could result in the death of the dog or severe health complications (26). As well, doxycycline is only effective at early stages in the heartworm life cycle and will only be effective if the *Wolbachia* bacteria is present (7). In addition, for macrocyclic lactones, like ivermectin, to be approved for commercial use it has to show that it has a 100% efficacy in preventing *D. immitis* infections (19). Ivermectin however was first FDA approved under the name Mectizan in 1987 (30). Since this approval there have been reports to the FDA about its loss of efficacy starting as early as 1998 (31). As mentioned before this could be due to inconsistent treatment administration by the dog owner and/or anthelmintic resistance (19).

Anthelmintic resistance is when the drug treatment, used to kill the parasite of interest, is no longer effective. Resistance to macrocyclic lactones are well known and have been found in other species of parasitic nematodes (32). For this reason and the reasons stated above, the need for new treatment strategies is evident.

1.3 Cys-Loop Receptors and Targets of Interest

When looking to synthesize new anthelmintics, we must first determine a target of interest. Cys-loop ligand gated ion channels (LGICs) are a group of membrane-spanning proteins that are responsible for neurotransmission in the nervous system (33). This family includes, but is not limited to, nicotinic acetylcholine receptors (nAChR) and gamma-aminobutyric acid receptors ($GABA_A$ and $GABA_C$) (33). Nematodes contain a wide variety of cys-loop receptors that are found on both muscle and throughout the nervous system making them attractive targets for future anthelmintics (34).

Members of the cys-loop receptor family all have a similar structure, which contains five subunits surrounding a ion-conducting pore (33). These subunits are made of an extracellular domain, N-terminal ligand-binding domain and a transmembrane domain (35). The ligand-binding domain of two subunits make up the agonist binding site (35). This binding site is made up of three loops from one subunit, domains A-C, and 3 beta pleated sheets from the other subunit, domains D-F (35). These subunits can be either homomeric or heteromeric meaning that they can contain all of the same subunit or made up of more than one subunit type. In some cys-loop receptors, the different combinations of subtypes results in receptors with different functionality and pharmacology (36).

1.3.1 $GABA_A$ Receptors and UNC-49

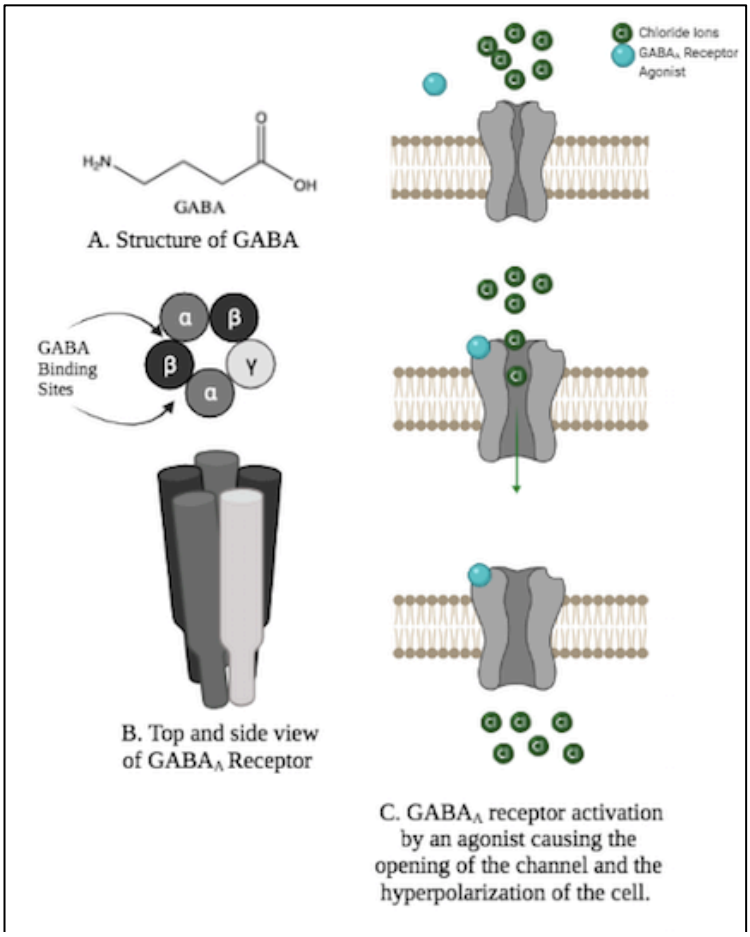

Figure 1.3 – GABA and $GABA_A$ receptors. A: Structure of GABA. B: Pentameric structure of $GABA_A$ from a top and side view. C: $GABA_A$ receptor activation. Figure was made in biorender.

$GABA_A$ is an example of a receptor whose subtypes can create various pharmacological outcomes (36). The structure of this receptor can be illustrated in **figure 1.3 B**. With respect to the mammalian $GABA_A$ receptor, the binding site is found between the alpha and beta subunit interface (37). When an agonist binds to this site it causes the opening of the pour and chloride ions are able to enter the cell causing a hyperpolarization (38). This can be seen in **figure 1.3 C**.

Cys-loop GABA receptors are also found in nematodes including parasitic nematodes. However, these nematode receptors have been discovered to exhibit some key differences compared to those in mammals. In nematodes, these receptors have key roles in locomotion, muscle contraction and defecation (39). When looking into more specific $GABA_A$ receptors, UNC-49 is one receptor that has potential as a future drug target. The UNC-49 receptor has been shown to have some structural differences in comparison to mammalian receptors (36,39). These receptors have also been found at neuromuscular junctions and play an important role in locomotion (40).

UNC-49 is made up of 3 alternatively spliced protein subunits; UNC-49A, UNC-49B and UNC-49C, however, only UNC-49B and UNC-49C contribute to receptor formation (41). The UNC-49B subunit can assemble as a homomeric channel with itself or it can assemble with UNC-49C to form a heteromeric channel (36,39). The *unc-49* gene has been found to be present not only in *C. elegans* but also parasitic nematodes such as *H. contortus* and *D. immitis.* This makes it a sensible target of interest when investigating new receptor targets.

1.3.2 Acetylcholine-gated Chloride Channels and ACC-2

A cys-loop receptor that is only found in invertebrate organisms such as nematodes is the acetylcholine-gate chloride (ACC) (42). These are similar in structure to cys-loop GABA receptors and are found in a wide range of parasitic nematodes. They have also been said to be promising targets for anthelmintic discovery as the activation of ACC-2 in expressing tissues was lethal or resulted or delayed the deployment of *C. elegans* larvae (43). This gives ACC-2 potential to be a larvicide which makes them an attractive target for future anthelmintics (43).

1.4 Nitrogen Containing Heterocycles

Nitrogen containing heterocycles are cyclic compounds of various sizes containing nitrogen in the ring structure. Compounds containing these heterocycles in their structure have been found to be used for applications in medicinal chemistry such as anti-inflammatory, antiviral and antiparasitic treatments (44,45). These compounds are also found naturally in vitamins, hormones and even antibiotics (45). This structure can even be found in our own DNA and RNA base pairs (46). Some specific examples of these structures can be shown in the **figure 1.4** below.

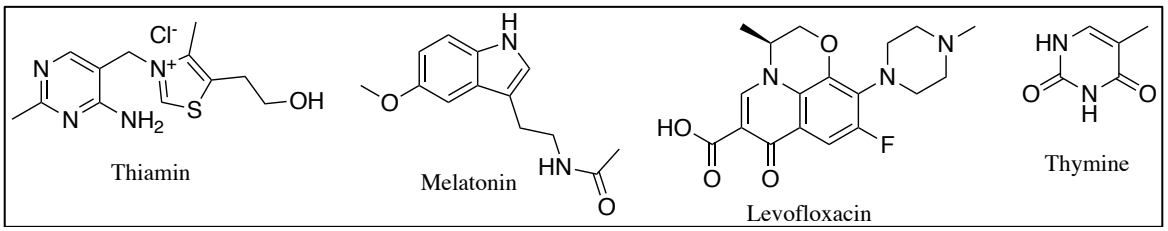

Figure 1.4 - Structures of the vitamin thiamin, hormone melatonin, antibiotic levofloxacin and base pair thymine.

Some of the things that make these compounds so attractive is their ability to act as a general Bronsted acid and base (46). They are also able to bind to many biological targets due to their ability to bind to protein targets through non-covalent interactions including hydrogen bonding and pi-stacking interactions (46). In 2014, it was determined that out of the FDA approved drugs, 59% of them contain nitrogen containing heterocycles in their structure (47).

1.4.1 Imidazole-4-acetic acid (IMA)

Imidazole-derived structures are used in many current anthelmintics (44). A specific imidazole containing compound of interest is imidazole-4-acetic acid (IMA), shown in **figure 1.5**.

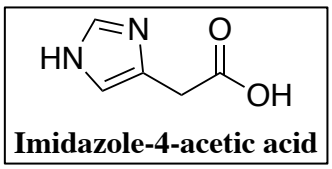

Figure 1.5 - Structure of imidazole-4-acetic acid (IMA)

IMA is actually a naturally occurring metabolite in the brain and is thought to be an oxidation product of histamine (38). The imidazole ring of IMA is important for bioactivity and it does not impede on the ability of the compound to bind to targets (44). Its structure also contains a monocarboxylic acid which adds an additional element for hydrogen bonding. IMA is also a known partial agonist in $GABA_A$ receptors in mammals (38). However, it has been shown to be a full agonist of the UNC-49 receptor of the parasite *H. contortus* (39).

1.4.2 Levamisole

Another compound of particular interest is Levamisole. Levamisole's structure also contains a nitrogen heterocycle imidazole ring illustrated in **figure 1.6** (44).

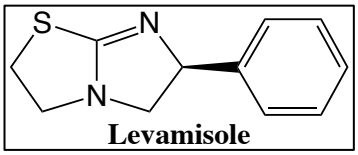

Figure 1.6 - Structure of levamisole.

Levamisole's mode of action is through the activation of nAChRs which causes paralysis of the worm (44). Levamisole sensitive receptors include, UNC-29, UNC-38, UNC-63, LEV-1, LEV-8 and ACR-8 (34,48). Levamisole is also a known partial agonist for the Hco-ACC-2 receptor. Levamisole has been used as a microfilaricidal drug and also as an adulticidal drug (49). Levamisole is ineffective at killing *D. immitis* microfilariae at a concentration of 5mg/kg twice daily. At an increased concentration of 20mg/kg twice

daily, levamisole was able to kill microfilariae, as well as, adult worms (49). However, at a concentration of 20mg/kg, increased toxicity of levamisole is observed with the host experiencing many symptoms including vomiting, weight loss and diarrhoea to name a few (49). It was found that at a dosage of 10mg/kg twice a day was the ideal dose killing both microfilariae and adult worms while causing little toxic effects to the dog (49).

Levamisole has also been used for other treatments such as rheumatoid arthritis as well as has been shown to have immunomodulatory effects (50,51). Levamisole was unfortunately removed as a treatment for humans in 2000 due to its side effects such as agranulocytosis (50,51). Recently, levamisole has been found as an additive in cocaine and one hypothesis is that it increases the cocaine-induced euphoria (51). However, this can cause a the blood infection agranulocytosis and vasculitis(51).

1.5 Pharmacological Characterization

Receptors such as UNC-49 and ACCs can be evaluated as potential targets using both currently available small molecules as well as novel small molecules. These molecules can be evaluated as agonists which activate or open the receptor channel causing a flow of ion current into the cell. This current that occurs during activation can be evaluated and recorded through electrophysiology techniques. This evaluation method involves expressing the receptor of interest onto a single cell such as *Xenopus laevis*, African clawed frog, oocytes (39). Electrodes are then placed into the oocyte to measure the change in current. The compounds of interest are then washed over these oocytes and any changes in current will be recorded on the computer in the form of traces. The compound is then washed away, and the oocyte can then be tested again.

There are major advantages to this type of evaluation. One advantage is the ability to screen compounds quickly and evaluate their effectiveness on the receptor of choice. Using this method, compounds are able to be compared to each other using the same oocyte which expresses a single receptor of interest. As well, the same compound can also be evaluated at different concentrations. From this information a dose response curve is able to be produced. This dose response curve can then be compared to known controls of the receptors and the effectiveness of the compound can be evaluated.

When looking at a rational drug design approach, electrophysiology enables the testing of molecules at any stage in the synthesis process. This data can then be evaluated, and other molecules can be designed based on your results. This is a more efficient method used instead of making a large number of molecules and testing all of them at one time.

1.6 Homology Modeling and Computational Docking

Another tool used to further evaluate how compounds of interest may interact with the receptors binding pocket is through homology modeling and computational docking. Using the sequence of the receptor of interest, we are able to align it to a known crystalized receptor that has similarities in the sequence of the binding pocket (39). With additional coding we are then able to place our molecule in the receptor and investigate the interactions between amino acids in the binding pocket and our compound of interest.

Some interactions that can be identified and analyzed include pi-cation interactions, pi-stacking interactions, hydrogen bonding and ionic bonding. Pi-cationic interactions occur between a benzene ring and a nitrogen or oxygen. The bond length measured to determine if this interaction is likely to occur is usually no longer than 6 Å

(52). An amino acid capable of participating in this type of interaction is tryptophan. This interaction has also been shown to be important in the nACh receptor (52). Pi-pi (π–π) stacking non-covalent interactions occur between two aromatic rings containing pi orbitals (53). A few examples of amino acids that participate in this type of interaction are tryptophan, phenylalanine and tyrosine (53). Hydrogen bonding interactions occur between a hydrogen and an electronegative element such as nitrogen and oxygen. If there is a proper acceptor-donor pair within 2.7 to 3.3 Å, the bond is accepted as a hydrogen bond (54).

1.7 Objectives

With the information presented above it is easy to see the importance and need for novel anthelmintics with new modes of action. For this project, the goal is to use rational drug design and investigate potential anthelmintics in our receptors of interest. This has been broken down into 3 main objectives. The first objective is to synthesize two imidazole-4-acetic acid like compounds. These compounds would contain an additional nitrogen in the ring and by doing this our hope is to increase their efficacy in the $GABA_A$ Dim-UNC-49 receptor. The second objective is to create a levamisole derivative library using a rational drug design. This objective will look at adding modifications to the levamisole structure itself. This is to evaluate each modified levamisole's efficacy to using the Hco-ACC-2 receptor and compare each derivative to levamisole. The rationale is to synthesize molecules that have better efficacy than levamisole. The final objective will be to synthesize a proof-of-concept levamisole dimer. This will be a novel molecule that may exhibit activity at the receptor and novel anthelmintic properties.

Chapter 2 - Experimental

2.1 – General Synthetic Method

All starting materials and solvents used in this thesis were purchased from the chemical manufacturer TCI or Sigma-Aldrich, unless indicated otherwise. These chemicals were used without any further purification. Reactions were concentrated using a rotary evaporator or with a GeneVac miVac Quattro concentrator. All purifications of products were completed via flash column chromatography using Silicycle Siliaflash P60 (230-400 mesh) manually or automatically using an Isolera One Biotage Purification Instrument. To confirm products ^{1}H, ^{13}C and ^{19}F NMRs were performed in various deuterated solvents using a Bruker Ascend 400 (400 MHz) NMR spectrometer. Further confirmation of products was also done in some cases using an Agilent Technologies 6545 Q-TOF LC/MS.

2.2- Synthesis and Characterization of Organic Compounds – Imidazole Like Compounds

2.2.1- 1-(azidomethyl)-2,4-dimethoxybenzene- Compound (1)

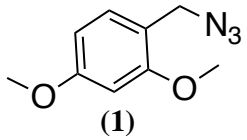

(1)

To a 100 mL round bottom flask, 57 mL of anhydrous DCM was added. 1.0 mL of 2,4-dimethoxybenzyl alcohol (0.89 g, 6.5 mmol, 1.00 eq) was then added and the reaction was stirred. 1.28 g of sodum azide (19.8 mmol, 3.00 eq) was then added slowly. Once the compound was dissolved, 2.25 g of triphenyl phosphine (8.6 mmol, 1.30 equivalents) was then added. Finally, 3.28 g of carbon tetrabromide (9.8 mmol, 1.50 equivalents) was added. The mixture was stirred for 48 hours at room temperature. Once

completed the reaction was dried via the rotary evaporator before being purified via flash column chromatography with 10% hexanes in DCM. The resulting oil afforded compound 1 (0.90 g, 71.0%). 1H NMR (400 MHz, CDCl3) δ 7.18 (d, J = 8.1 Hz, 1H), 6.50 (dt, J = 8.1, 2.3 Hz, 2H), 4.31 (s, 2H), 3.87 (s, 3H), 3.84 (s, 3H). 13C NMR (101 MHz, CDCl3) δ 161.28, 158.84, 131.05, 116.33, 104.10, 98.65, 55.51, 55.41, 49.90.

2.2.2- 1-(2,4-dimethoxyphenyl)-1*H*-1,2,3-triazole-4-carboxylic acid- Compound (2)

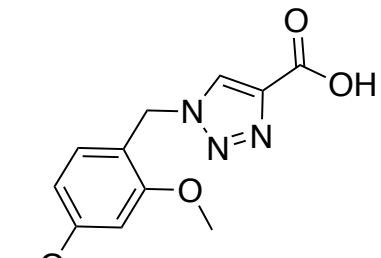

(2)

To a 20 mL scintillation vial, 16 mL of *t*BuOH: H2O were added in a 1:1 ratio. To this 0.234 g of compound **1** (1.21 mmol, 1.00 eq) was added and stirred. 0.024 g of copper (II) acetate (0.12 mmol, 0.10 eq) were then added along with 0.051 g of sodium L-ascorbate (0.24 mmol, 0.20 eq) and let to dissolve. Finally, 96 μL of propiolic acid (0.08 g, 1.21 mmol, 1.00 eq) was added. The whole reaction was then let to stir overnight at room temperature. Once finished the reaction was then placed on the mivac to concentrate. The dried reaction then underwent an extraction with H_2O and DCM. The aqueous layer was then collected and concentrated on the miVac. The crude product was then purified using silica gel chromatography with a gradient of MeOH and DCM (1% to 10% MeOH in DCM) to afford compound **2** as a white solid (0.065 g, 20.3%). ^{1}H NMR (400 MHz, MeOD) δ 8.26 (s, 1H), 7.29 (d, *J* = 8.3 Hz, 1H), 6.62 – 6.53 (m, 2H), 5.54 (s,

2H), 3.86 (s, 3H), 3.82 (s, 3H).^{13}C NMR (101 MHz, MeOD) δ 162.16, 158.67, 139.89, 131.25, 127.70, 114.74, 104.61, 98.22, 54.65, 54.49, 49.06, 47.81, 47.59, 47.38.

2.2.3- Methyl 1*H*-1,2,3-triazole-4-carboxylate – Compound (3)

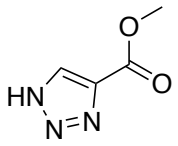

(3)

To a 10mL round bottom flask of 10 mL of ACN, 0.708 g of methyl propiolate (8.42 mmol, 1.00 eq) and 1.94 g of trimethylsilyl azide (16. 84 mmol, 2.00 eq) were added. The reaction was then refluxed and let stir for 72 hours. After the reaction was done stirring, 4 mL of MeOH was added and the reaction was placed on the rotary evaporator to dry. The reaction was washed with DCM and filtered. The orange crystals remaining afforded compound 3 (0.514 g, 48.0 %). ^{1}H NMR (400 MHz, DMSO-d_6) δ 8.55 (s, 1H), 3.84 (s, 3H). ^{13}C NMR (101 MHz, DMSO-d_6) δ 161.42, 138.45, 131.73, 52.24.

2.2.4 – 1*H*-1,2,3-triazole-4-carboxylic acid– Compound (4)

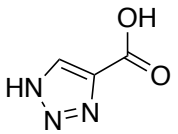

(4)

To a 10 mL round bottom flask 0.200 g of compound **3** (1.57 mmol, 1.00 eq), 0.126 g of NaOH (3.15 mmol, 2.00 eq) was added in 1.97 mL of H_2O. The reaction was then refluxed for 3 hours. After 3 hours, the reaction was let to cool to room temperature. The cooled reaction then underwent an extraction with H_2O and DCM. The aqueous fraction was then acidified with HCl dropwise until it reached a pH of 2. This aqueous

fraction was then further extracted with EtOAc. The organic phase was then dried with Na_2SO_4 and further dried on the rotary evaporator to afford compound **4** as a white solid (0.039g, 22.0%).^{1}H NMR (400 MHz, D_2O) δ 8.33 (s, 1H). ^{13}C NMR (101 MHz, DMSO-d_6) δ 162.33, 139.35, 131.91.

2.2.5 – 2-(1-(2,4-dimethoxyphenyl)-1*H*-1,2,3-triazol-4-yl)acetic acid– Compound (5)

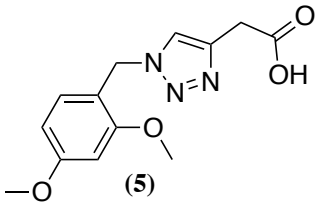

(5)

To a 10 mL round bottom flask, 2 mL of *t*BuOH:H_2O were added in a 1:1 ratio. To this 0.090 g of compound **1** (0.47 mmol, 1.00 eq) was added and stirred. 90 µL of TEA (0.07 g, 0.70 mmol, 1.5 eq) we added. 0.042 g of copper (II) acetate (0.23 mmol, 0.50 eq) were then added along with 0.049 g of sodium L-ascorbate (0.28 mmol, 0.60 eq) and let to dissolve. Finally, 0.047 g of but-3-ynoic acid (0.56 mmol, 1.20 eq) was added. The whole reaction was then let to stir overnight at room temperature. Once finished the reaction was then placed on the mivac to concentrate. The dried reaction then underwent an extraction with H_2O and DCM. The aqueous layer was then collected and concentrated on the miVac. This product was then purified by the biotage with a gradient of MeOH and DCM (1% to 10% MeOH in DCM) to afford compound **5** as a white solid (0.057g, 47.9%). ^{1}H NMR (400 MHz, DMSO-d_6) δ 7.78 – 7.77 (m, 1H), 7.17 – 7.13 (m, 1H), 6.62 – 6.60 (m, 1H), 6.54 – 6.51 (m, 1H), 5.42 – 5.40 (m, 2H), 3.81 (s, 3H), 3.76 (s, 3H), 3.63 – 3.61 (m, 2H).^{13}C NMR (101 MHz, DMSO-d_6) δ 172.00, 161.44, 158.53, 140.78, 131.42, 123.67, 116.24, 105.43, 99.06, 56.12, 55.76, 48.28, 31.87.

2.2.6 – 2-(1*H*-1,2,3-triazol-4-yl)acetic acid – Compound (6)

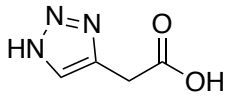

(6)

To a 50 mL round bottom flask, 0.113g of compound **5** (0.41 mmol, 1.00 eq) was added. 4.60 mL of TFA (58.2 mmol, 143eq) was then added along with 0.12 mL of THF (0.103 g, 1.43 mmol. 3.50 eq) to the flask. The reaction was then stirred at 50^{o}C for 1.5 hours. The reaction was then cooled to room temperature before the addition of 5 mL of MeOH. The reaction was then dried on the rotary evaporator. Once dried, the reaction was extracted using H_2O and DCM and the aqueous fraction was placed on the miVac to dry overnight. The remaining white crystal product was not purified any further giving us compound **6** (0.037 g, 72.5%). ^{1}H NMR (400 MHz, Acetone) δ 7.72 (s, 1H), 3.81 (d, J = 4.8 Hz, 2H). ^{13}C NMR (101 MHz, Acetone) δ 170.79, 133.08, 133.20, 30.58.

2.3- Synthesis and Characterization of Organic Compounds – Levamisole and Levamisole Derivatives

2.3.1- Extraction of Levamisole ((S)-6-phenyl-2,3,5,6-tetrahydroimidazo[2,1 b]thiazole) – Compound (7)

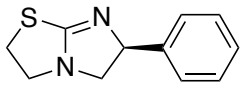

(7)

To a 250 mL Erlenmeyer flask, 1.082 g of levamisole hydrochloride (4.27 mmol, 1.00 eq) was added. 25 mL of ethyl ether was then added along with 5 mL of NaOH (8.75 M) and 7.5 mL of H_2O. The reaction was manually stirred until the levamisole hydrochloride was dissolved. An extraction was then preformed with diethyl ether and H_2O. The organic fraction was then dried with Na_2SO_4 and further dried with the rotary evaporator. The resulting clear oil was the free base levamisole, compound **7** without further purification (0.916 g, 99.7%). ^{1}H NMR (400 MHz, MeOD) δ 7.39 – 7.25 (m, 5H), 5.41 (t, J = 9.0 Hz, 1H), 3.79 – 3.69 (m, 2H), 3.64 (ddd, J = 11.0, 6.6, 4.5 Hz, 1H), 3.44 (ddd, J = 9.0, 6.6, 4.5 Hz, 1H), 3.21 (td, J = 8.7, 6.6 Hz, 1H), 3.06 – 3.00 (m, 1H). ^{13}C NMR (101 MHz, MeOD) δ 176.00, 142.61, 128.16, 127.14, 126.31, 75.97, 57.86, 48.71, 33.85. + ESI Scan m/z calculated for $C_{11}H_{12}N_2S$: 205.0799, found 205.0867 [M+H]+

2.3.2- Synthesis of (S)-7-methyl-6-phenyl-2,3,5,6-tetrahydroimidazo[2,1-b]thiazol-7-ium- Compound (8)

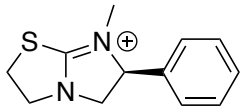

(8)

In a 10 mL round bottom flask containing a solution of 5.0 mL of THF, 0.202 g of compound **7** (0.99 mmol, 1.00 eq) was added and stirred. After the mixture was dissolved, 75 μL of iodomethane (0.172 g, 1.21 mmol, 1.23 eq) was added and stirring continued. A condenser was then set up above the reaction and the reaction was refluxed. After 24 hours, the reaction was left to cool and THF was removed using a rotary evaporator. The dried reaction then underwent an extraction with H_2O and DCM. The aqueous layer was then collected and concentrated on the miVac to afford an oil. This oil was then purified by the biotage with a gradient of MeOH and DCM (1% to 10% MeOH in DCM) to afford compound **8** as a clear oil (0.18 g, 84.3 %). ^{1}H NMR (400 MHz, MeOD) δ 7.57 – 7.42 (m, 5H), 5.66 – 5.59 (m, 1H), 4.33 (t, J = 10.4 Hz, 1H), 4.13 (dd, J = 7.9, 6.9 Hz, 2H), 4.02 – 3.90 (m, 2H), 3.83 – 3.76 (m, 1H), 2.94 (s, 3H). ^{13}C NMR (101 MHz, MeOD) δ 177.75, 135.33, 129.65, 129.24, 127.61, 72.93, 54.66, 48.74, 36.75, 32.56. + ESI Scan m/z calculated for $C_{12}H_{15}N_2S^+$: 219.0956, found 219.0950 [M+H]+

2.3.3 – Synthesis of (*S*)-7-ethyl-6-phenyl-2,3,5,6-tetrahydroimidazo[2,1-*b*]thiazol-7-ium – Compound (9)

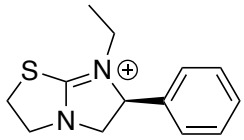

(9)

In a 10 mL round bottom flask containing a solution of 5.0 mL of THF, 0.253 g of compound 7 (1.23 mmol, 1.00 eq) was added and stirred. After the mixture was dissolved, 119 µL of iodoethane (0.229 g, 1.47 mmol, 1.20 eq) was added and stirring continued. A condenser was then set up above the reaction and the reaction was refluxed. After 24 hours, the reaction was left to cool and THF was removed using a rotary evaporator. The dried reaction then underwent an extraction with H2O and DCM. The aqueous layer was then collected and concentrated on the miVac to afford an oil. This oil was then purified by using the biotage with a gradient of MeOH and DCM (1% to 10% MeOH in DCM) to afford compound **9** as a clear oil (0.10g, 32.4%). ^{1}H NMR (400 MHz, MeOD) δ 7.61 – 7.44 (m, 5H), 5.75 (dd, J = 10.3, 9.0 Hz, 1H), 4.33 (s, 1H), 4.16 – 4.10 (m, 2H), 3.95 (d, J = 7.4 Hz, 2H), 3.86 – 3.76 (m, 1H), 3.37 (d, J = 1.0 Hz, 1H), 3.27 – 3.16 (m, 1H), 1.15 (t, J = 7.3 Hz, 3H). ^{13}C NMR (101 MHz, MeOD) δ 176.88, 135.59, 129.69, 129.24, 127.73, 70.73, 53.43, 48.42, 42.01, 36.63, 11.30. + ESI Scan m/z calculated for C13H17N2S+: 233.1112, found 233.1113 [M+H]+

2.3.4 – Synthesis of (*S*)-7-benzyl-6-phenyl-2,3,5,6-tetrahydroimidazo[2,1-*b*]thiazol-7-ium- Compound (10)

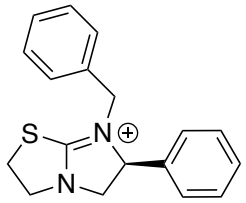

(10)

In a 50 mL round bottom flask containing a solution of 5.3 mL of THF, 0.22 g of compound **7** (1.07 mmol, 1.00 eq) was added and stirred. After the mixture was dissolved, 141 μL of benzyl bromide (0.201 g, 1.18 mmol, 1.10 eq) was added and stirring continued. A condenser was then set up above the reaction and the reaction was refluxed. After 24 hours, the reaction was left to cool and THF was removed using a rotary evaporator. The dried reaction then underwent an extraction with water and DCM. The aqueous layer was then collected and concentrated on the miVac to afford an oil. This oil was then purified by using silica gel chromatography with a gradient of MeOH and DCM (1% to 12% MeOH in DCM) to afford compound **10** as a clear yellow oil (0.30 g, 94.3 %). ^{1}H NMR (400 MHz, MeOD) δ 7.55 – 7.47 (m, 10H), 7.41 – 7.35 (m, 6H), 7.23 – 7.17 (m, 4H), 5.60 – 5.53 (m, 2H), 4.51 (d, J = 15.1 Hz, 2H), 4.32 (dd, J = 17.0, 6.5 Hz, 3H), 4.35 – 4.23 (m, 4H), 4.08 (dd, J = 7.8, 5.6 Hz, 4H), 4.01 – 3.89 (m, 4H), 3.84 (dd, J = 10.4, 9.4 Hz, 2H). ^{13}C NMR (101 MHz, MeOD) δ 177.31, 135.16, 132.16, 129.77, 129.25, 128.80, 128.02, 71.43, 54.54, 50.54, 48.25, 36.70. + ESI Scan m/z calculated for $C_{18}H_{19}N_2S^+$: 295.1269, found 295.1252 [M+H]+

2.3.5- Synthesis of (*S*)-7-((perfluorophenyl)methyl)-6-phenyl-2,3,5,6-tetrahydroimidazo[2,1-*b*]thiazol-7-ium – Compound (11)

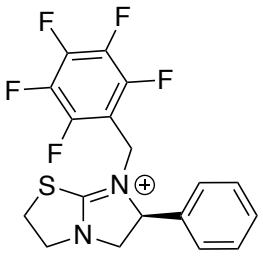

(11)

In a 50 mL round bottom flask containing a solution of 7.6 mL of THF, 0.311 g of compound **7** (1.52 mmol, 1.00 eq) was added and stirred. After the mixture was dissolved, 252 µL of 1-(bromomethyl)-2,3,4,5,6-pentafluorobenzene (0.436 g, 1.67 mmol, 1.10 eq) was added and stirring continued. A condenser was then set up above the reaction and the reaction was refluxed. After 24 hours, the reaction was left to cool and THF was removed using a rotary evaporator. The dried reaction then underwent an extraction with H_2O and DCM. The aqueous layer was then collected and concentrated on the miVac to afford an oil. This oil was then purified by using silica gel chromatography with a gradient of MeOH and DCM (1% to 12% MeOH in DCM) to afford compound 11 as a clear yellow oil (0.550 g, 93.8 %). ^{1}H NMR (400 MHz, MeOD) δ 7.43 (ddd, J = 6.6, 5.6, 2.8 Hz, 5H), 5.65 (d, J = 1.1 Hz, 1H), 4.73 (s, 1H), 4.61 (d, J = 15.7 Hz, 1H), 4.35 (t, J = 10.6 Hz, 1H), 4.19 (t, J = 7.3 Hz, 2H), 4.02 (dd, J = 7.6, 4.8 Hz, 2H), 3.81 (dd, J = 10.6, 9.0 Hz, 1H). ^{13}C NMR (101 MHz, MeOD) δ 178.05, 146.52, 144.00, 135.39, 129.70, 128.90, 128.33, 127.67, 126.81, 107.45, 71.95, 54.87, 48.59, 39.01, 36.89. 19F NMR (377 MHz, MeOD) δ -141.88, -155.49, -164.23. + ESI Scan m/z calculated for $C_{18}H_{14}F_5N_2S^+$: 385.0798, found 385.0207 [M+H]+

Confidential and Proprietary Information

2.3.6- Synthesis of (*S*)-7-(4-bromobenzyl)-6-phenyl-2,3,5,6-tetrahydroimidazo[2,1-*b*]thiazol-7-ium – Compound (12)

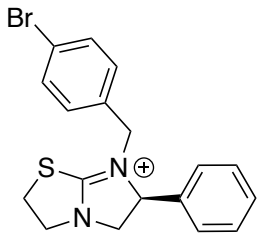

(12)

In a 50 mL round bottom flask containing a solution of 8.1 mL of THF, 0.330 g of compound **7** (1.61 mmol, 1.00 eq) was added and stirred. After the mixture was dissolved, 0.444 g of 1-bromo-4-(bromomethyl)benzene (1.78 mmol, 1.10 eq) was added and stirring continued. A condenser was then set up above the reaction and the reaction was refluxed. After 24 hours, the reaction was left to cool and THF was removed using a rotary evaporator. The dried reaction then underwent an extraction with H_2O and DCM. The aqueous layer was then collected and concentrated on the miVac to afford an oil. This oil was then purified by using silica gel chromatography with a gradient of MeOH and DCM (1% to 12% MeOH in DCM) to afford compound **12** as a clear yellow oil (0.422 g, 69.9 %). ^{1}H NMR (400 MHz, MeOD) δ 7.55 – 7.47 (m, 7H), 7.13 (d, J = 8.4 Hz, 2H), 5.59 (dd, J = 10.2, 9.4 Hz, 1H), 4.48 (d, J = 15.3 Hz, 1H), 4.37 – 4.26 (m, 2H), 4.13 – 4.06 (m, 2H), 4.02 – 3.91 (m, 2H), 3.85 (dd, J = 10.5, 9.3 Hz, 1H). ^{13}C NMR (101 MHz, MeOD) δ 177.41, 135.05, 131.85, 130.64, 129.81, 129.27, 127.99, 122.76, 71.53, 54.51, 49.88, 36.75. + ESI Scan m/z calculated for $C_{18}H_{18}BrN_2S^+$: 373.0374, found 373.0453 and 375.0434 [M+H]+

Confidential and Proprietary Information

2.3.7- Synthesis of (*S*)-6-phenyl-7-(2-(trifluoromethyl)benzyl)-2,3,5,6-tetrahydroimidazo[2,1-*b*]thiazol-7-ium – Compound (13)

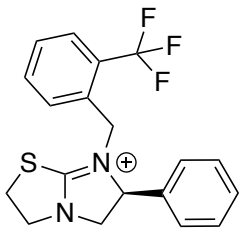

(13)

In a 50 mL round bottom flask containing a solution of 18.5 mL of THF, 0.757 g of compound **7** (3.70 mmol, 1.00 eq) was added and stirred. After the mixture was dissolved, 0.444 g of 2-(trifluoromethyl)benzyl bromide (4.08 mmol, 1.10 eq) was added and stirring continued. A condenser was then set up above the reaction and the reaction was refluxed. After 24 hours, the reaction was left to cool and THF was removed using a rotary evaporator. The dried reaction then underwent an extraction with H_2O and DCM. The aqueous layer was then collected and concentrated on the miVac to afford an oil. This oil was then purified by using silica gel chromatography with a gradient of MeOH and DCM (1% to 12% MeOH in DCM) to afford compound **13** as a clear yellow oil (0.97 g, 72.0 %). ^{1}H NMR (400 MHz, MeOD) δ 7.70 (dd, J = 23.4, 7.7 Hz, 2H), 7.61 – 7.51 (m, 2H), 7.46 (s, 5H), 5.65 (dd, J = 10.5, 8.8 Hz, 1H), 4.65 (s, 1H), 4.62 (s, 1H), 4.39 (t, J = 10.6 Hz, 1H), 4.13 – 4.08 (m, 2H), 4.05 – 3.96 (m, 2H), 3.92 (dd, J = 10.6, 8.7 Hz, 1H). ^{13}C NMR (101 MHz, MeOD) δ 177.88, 134.85, 132.61, 130.71, 130.06, 129.80, 129.16, 127.90, 126.32, 122.55, 71.98, 54.51, 48.45, 48.35, 36.80. ^{19}F NMR (377 MHz, MeOD) δ -61.00. + ESI Scan m/z calculated for $C_{19}H_{18}F_3N_2S^+$: 363.1143, found 363.0507 [M+H]+

Confidential and Proprietary Information

2.3.8- Synthesis of (*S*)-6-phenyl-7-(4-(trifluoromethyl)benzyl)-2,3,5,6-tetrahydroimidazo[2,1-*b*]thiazol-7-ium – Compound (14)

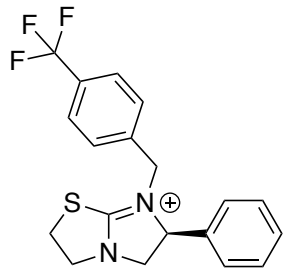

(14)

In a 50 mL round bottom flask containing a solution of 7.3 mL of THF, 0.300 g of compound **7** (1.47 mmol, 1.00 eq) was added and stirred. After the mixture was dissolved, 0.386 g of 4-(trifluoromethyl)benzyl bromide (1.62 mmol, 1.10 eq) was added and stirring continued. A condenser was then set up above the reaction and the reaction was refluxed. After 24 hours, the reaction was left to cool and THF was removed using a rotary evaporator. The dried reaction then underwent an extraction with H_2O and DCM. The aqueous layer was then collected and concentrated on the miVac to afford an oil. This oil was then purified by using silica gel chromatography with a gradient of MeOH and DCM (1% to 12% MeOH in DCM) to afford compound **14** as a clear yellow oil (0.215 g, 40.1 %). ^{1}H NMR (400 MHz, MeOD) δ 7.66 (d, J = 8.1 Hz, 2H), 7.51 – 7.45 (m, 5H), 7.41 (d, J = 8.1 Hz, 2H), 5.62 (dd, J = 10.4, 9.3 Hz, 1H), 4.62 (d, J = 15.6 Hz, 1H), 4.42 (d, J = 15.6 Hz, 1H), 4.36 (t, J = 10.5 Hz, 1H), 4.17 – 4.11 (m, 2H), 4.06 – 3.95 (m, 2H), 3.89 (dd, J = 10.5, 9.2 Hz, 1H). ^{13}C NMR (101 MHz, MeOD) δ 177.58, 136.98, 135.00, 130.75, 130.43, 129.81, 129.27, 128.10, 125.51, 122.63, 71.72, 54.54, 50.02, 48.46, 48.38, 36.90. ^{19}F NMR (377 MHz, MeOD) δ -64.26. + ESI Scan m/z calculated for $C_{19}H_{18}F_3N_2S^+$: 363.1143, found 363.0503 [M+H]+

Confidential and Proprietary Information

2.3.9- Synthesis of (*S*)-7-(4-nitrobenzyl)-6-phenyl-2,3,5,6-tetrahydroimidazo[2,1-*b*]thiazol-7-ium – Compound (15)

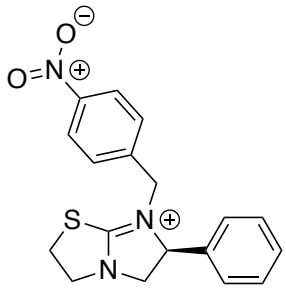

(15)

In a 50 mL round bottom flask containing a solution of 24.5 mL of THF, 1.0 g of compound **7** (4.91 mmol, 1.00 eq) was added and stirred. After the mixture was dissolved, 1.17 g of 1-(bromomethyl)-4-nitrobenzene (5.40 mmol, 1.10 eq) was added and stirring continued. A condenser was then set up above the reaction and the reaction was refluxed. After 24 hours, the reaction was left to cool and THF was removed using a rotary evaporator. The dried reaction then underwent an extraction with H_2O and DCM. The aqueous layer was then collected and concentrated on the miVac to afford an oil. This oil was then purified by using silica gel flash chromatography with a gradient of MeOH and DCM (1% to 12% MeOH in DCM) to afford compound **15** as a clear yellow oil (1.37 g, 82.0 %). ^{1}H NMR (400 MHz, MeOD) δ 8.21 – 8.17 (m, 2H), 7.53 – 7.44 (m, 7H), 5.66 (dd, J = 10.3, 9.3 Hz, 1H), 4.67 (d, J = 15.9 Hz, 1H), 4.49 (d, J = 15.9 Hz, 1H), 4.39 (t, J = 10.5 Hz, 1H), 4.19 – 4.13 (m, 2H), 4.08 – 3.97 (m, 2H), 3.92 (dd, J = 10.6, 9.2 Hz, 1H). ^{13}C NMR (101 MHz, MeOD) δ 177.69, 148.08, 139.90, 134.92, 129.84, 129.63, 129.23, 128.17, 123.56, 71.84, 54.52, 49.82, 48.47, 36.98. + ESI Scan m/z calculated for $C_{18}H_{18}N_3O_2S^+$: 340.1120, found 340.0579 [M+H]+

Confidential and Proprietary Information

2.3.10- Synthesis of (S)-7-(4-methylbenzyl)-6-phenyl-2,3,5,6-tetrahydroimidazo[2,1-b]thiazol-7-ium – Compound (16)

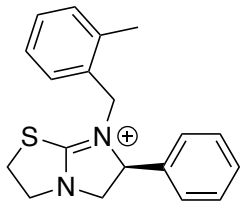

(16)

In a 50 mL round bottom flask containing a solution of 7.4 mL of THF, 0.303 g of compound **7** (1.48 mmol, 1.00 eq) was added and stirred. After the mixture was dissolved, 219 μL of alpha-bromo-o-xylene (0.302 g, 1.63 mmol, 1.10 eq) was added and stirring continued. A condenser was then set up above the reaction and the reaction was refluxed. After 24 hours, the reaction was left to cool and THF was removed using a rotary evaporator. The dried reaction then underwent an extraction with H_2O and DCM. The aqueous layer was then collected and concentrated on the miVac to afford an oil. This oil was then purified by using the automated biotage with a gradient of MeOH and DCM (1% to 10% MeOH in DCM) to afford compound **16** as a clear yellow oil (0.346 g, 75.3 %). ^{1}H NMR (400 MHz, MeOD) δ 7.56 – 7.37 (m, 5H), 7.34 – 7.28 (m, 1H), 7.23 – 7.11 (m, 3H), 5.56 (dd, J = 10.4, 8.9 Hz, 1H), 4.43 – 4.29 (m, 3H), 3.93 (dddd, J = 27.6, 19.5, 8.8, 5.4 Hz, 5H), 2.15 (s, 3H). ^{13}C NMR (101 MHz, MeOD) δ 176.87, 137.89, 135.31, 130.59, 129.76, 129.41, 129.20, 127.92, 126.15, 71.77, 54.44, 48.72, 48.25, 36.46, 17.91. + ESI Scan m/z calculated for $C_{19}H_{21}N_2S^+$: 309.1425, found 309.1457 [M+H]+

Confidential and Proprietary Information

2.3.11- Synthesis of (*S*)-7-(2-methylbenzyl)-6-phenyl-2,3,5,6-tetrahydroimidazo[2,1-*b*]thiazol-7-ium – Compound (17)

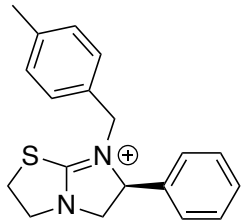

(17)

In a 50 mL round bottom flask containing a solution of 7.4 mL of THF, 0.303 g of compound **7** (1.48 mmol, 1.00 eq) was added and stirred. After the mixture was dissolved, 0.302 g of alpha-bromo-p-xylene (1.63 mmol, 1.10 eq) was added and stirring continued. A condenser was then set up above the reaction and the reaction was refluxed. After 24 hours, the reaction was left to cool and THF was removed using a rotary evaporator. The dried reaction then underwent an extraction with water and DCM. The aqueous layer was then collected and concentrated on the miVac to afford an oil. This oil was then purified by using silica gel chromatography with a gradient of MeOH and DCM (1% to 12% MeOH in DCM) to afford compound **17** as a clear yellow oil (0.252 g, 67.6 %). 1H NMR (400 MHz, MeOD) δ 7.56 – 7.49 (m, 5H), 7.20 (d, J = 7.8 Hz, 2H), 7.08 (d, J = 8.0 Hz, 2H), 5.56 (dd, J = 10.3, 9.5 Hz, 1H), 4.44 (d, J = 14.9 Hz, 1H), 4.37 – 4.18 (m, 2H), 4.11 – 4.02 (m, 2H), 4.01 – 3.77 (m, 10H), 2.35 (s, 3H). 13C NMR (101 MHz, MeOD) δ 177.18, 139.09, 135.23, 129.74, 129.34, 129.25, 128.99, 128.90, 128.02, 71.38, 54.54, 50.30, 48.47, 48.26, 36.67, 19.83. + ESI Scan m/z calculated for $C_{19}H_{21}N_2S^+$: 309.1425, found 309.1470 [M+H]+

Confidential and Proprietary Information

2.3.12- Synthesis of (*S*)-7-allyl-6-phenyl-2,3,5,6-tetrahydroimidazo[2,1-*b*]thiazol-7-ium- Compound (18)

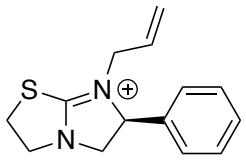

(18)

To a 50mL round bottom flask of 11.9 mL of acetone, 0.204 g of compound **7** (0.98 mmol, 1.00 eq) was added and stirred. 78 µL of allyl bromide (0.111 g, 1.08 mmol, 1.10 eq). The reaction was then stirred at 60 °C for 22 hours. After the reaction was done stirring it was let to cool to room temperature then concentrated on the rotary evaporator. This oil was then purified by using the biotage with a gradient of MeOH and DCM (1% to 10% MeOH in DCM) to afford compound **18** as a clear oil (0.227 g, 92.6 %). ^{1}H NMR (400 MHz, DMSO-d_6) δ 7.58 – 7.44 (m, 5H), 5.66 (t, J = 9.7 Hz, 2H), 5.26 (ddd, J = 10.1, 5.7, 1.3 Hz, 2H), 4.29 (t, J = 10.4 Hz, 1H), 4.11 – 4.00 (m, 2H), 3.94 – 3.83 (m, 3H), 3.77 (dd, J = 10.4, 8.9 Hz, 1H), 3.68 (d, J = 6.7 Hz, 1H). ^{13}C NMR (101 MHz, DMSO-d_6) δ 177.07, 136.34, 130.29, 130.07, 129.60, 128.70, 121.07, 71.09, 54.86, 49.10, 37.87. + ESI Scan m/z calculated for $C_{14}H_{17}N_2S^+$: 245.1112, found 245.1130 [M+H]+

Confidential and Proprietary Information

2.3.13- Synthesis of (*S*)-6-phenyl-7-(prop-2-yn-1-yl)-2,3,5,6-tetrahydroimidazo[2,1-*b*]thiazol-7-ium- Compound (19)

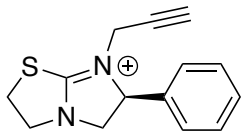

(19)

To a 50mL round bottom flask of 11.9 mL of acetone, 0.205 g of compound **7** (1.00 mmol, 1.00 eq) was added and stirred. 96 µL of propargyl bromide (0.128 g, 1.08 mmol, 1.10 eq). The reaction was then stirred at 60 ºC for 22 hours. After the reaction was done stirring it was let to cool to room temperature then concentrated on the rotary evaporator. This oil was then purified by using the biotage with a gradient of MeOH and DCM (1% to 10% MeOH in DCM) to afford compound **19** as a clear oil (0.215 g, 92.0 %). ^{1}H NMR (400 MHz, DMSO-d_6) δ 7.60 – 7.41 (m, 5H), 5.68 (t, *J* = 9.9 Hz, 1H), 4.33 (t, *J* = 10.4 Hz, 1H), 4.25 (dd, *J* = 18.3, 2.6 Hz, 1H), 4.13 – 4.03 (m, 2H), 4.01 – 3.84 (m, 3H), 3.77 (dd, *J* = 10.3, 9.6 Hz, 1H), 3.65 (t, *J* = 2.5 Hz, 1H). ^{13}C NMR (101 MHz, DMSO-d_6) δ 177.36, 135.75, 130.12, 129.58, 128.72, 79.06, 75.52, 71.03, 54.80, 48.71, 38.08, 36.48. + ESI Scan m/z calculated for $C_{14}H_{15}N_2S^+$: 243.0956, found 243.0986 [M+H]+

Confidential and Proprietary Information

2.3.14- Synthesis of (*S*)-7-(4-(bromomethyl)benzyl)-6-phenyl-2,3,5,6-tetrahydroimidazo[2,1-b]thiazol-7-ium – Compound (20)

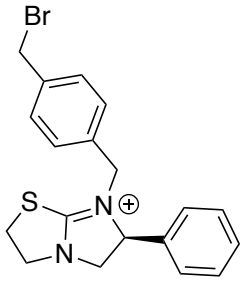

(20)

To a 50 mL round bottom flask, 0.200g of compound **7** (0.97 mmol, 1.00 eq) was added and along with 12 mL of acetone. To this stirring reaction, 0.310 g of 1,4-bis(bromomethyl)benzene (1.17 mmol, 1.20 eq) was added and stirring continued. A condenser was then set up above the reaction and the reaction was refluxed for 21.5 hours. The reaction heat was then turned off and the reaction was left to cool to room temperature. Once cooled, the reaction was gravity filtered and washed with additional acetone. The filtrate was collected and dried using a rotary evaporator. The dried reaction was then purified by using silica gel chromatography with a gradient of MeOH and DCM (1% to 15% MeOH in DCM) to afford compound **20** as a clear yellow oil (0.304 g, 80.0 %). 1H NMR (400 MHz, DMSO-d_6) δ 7.62 – 7.41 (m, 7H), 7.18 (d, J = 8.0 Hz, 2H), 5.60 (t, J = 9.6 Hz, 1H), 4.71 (s, 2H), 4.49 (d, J = 15.6 Hz, 1H), 4.31 (t, J = 10.4 Hz, 1H), 4.22 (d, J = 15.6 Hz, 1H), 4.08 – 4.00 (m, 2H), 3.92 – 3.85 (m, 2H), 3.79 (dd, J = 10.1, 9.2 Hz, 1H).13C NMR (101 MHz, DMSO-d_6) δ 177.14, 138.95, 136.11, 133.48, 130.14, 130.11, 129.63, 129.35, 128.84, 71.20, 54.89, 49.97, 48.61, 37.97, 34.28.+ ESI Scan m/z calculated for $C_{19}H_{20}BrN_2S^+$: 387.0531, found 387.0573 [M+H]+

Confidential and Proprietary Information

2.3.14- Synthesis of (*S*)-7-(4-aminobenzyl)-6-phenyl-2,3,5,6-tetrahydroimidazo[2,1-*b*]thiazol-7-ium – Compound (21)

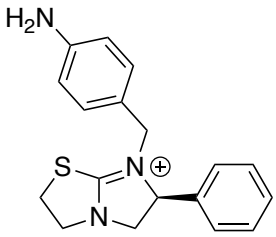

(21)

To a 50 mL round bottom flask containing a mixture of MeOH and H_2O (98:2), 0.108 g of compound 15 (0.32 mmol, 1.00 eq) was added and the reaction was stirred. 0.134g of zinc (2.05 mmol, 6.40 eq) and 0.12 mL of acetic acid was then added to the reaction. The reaction was then stirred at room temperature for one hour. After completion, an extraction was done on the reaction using H2O and DCM. The aqueous layer was then collected and concentrated on the miVac to afford an oil. This oil was then purified by the biotage with a gradient of MeOH and DCM (1% to 10% MeOH in DCM) to afford compound 21 as a clear oil (0.038 g, 38.6 %). ^{1}H NMR (400 MHz, MeOD) δ 7.56 – 7.48 (m, 5H), 6.91 (d, J = 8.4 Hz, 2H), 6.68 (d, J = 8.5 Hz, 2H), 5.56 – 5.49 (m, 1H), 4.29 (d, J = 10.5 Hz, 1H), 4.27 (s, 1H), 4.11 (d, J = 14.6 Hz, 1H), 4.03 – 3.97 (m, 2H), 3.93 – 3.87 (m, 1H), 3.78 (s, 2H). ^{13}C NMR (101 MHz, MeOD) δ 176.84, 149.15, 135.44, 130.40, 129.69, 129.25, 127.88, 119.59, 114.73, 71.24, 54.54, 50.42, 36.43. + ESI Scan m/z calculated for $C_{18}H_{20}N_3S^+$: 310.1378, found 310.1200 [M+H]+

Confidential and Proprietary Information

2.4- Synthesis and Characterization of Organic Compounds – Levamisole Dimers

2.4.1- Synthesis of (6*S*,6'*S*)-7,7'-(1,4-phenylenebis(methylene))bis(6-phenyl-2,3,5,6-tetrahydroimidazo[2,1-*b*]thiazol-7-ium) – Compound (22)

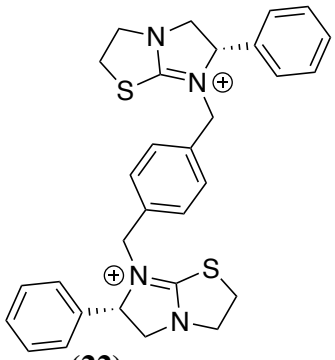

(22)

To a 50 mL round bottom flask, 0.143 g of compound **7** (0.70 mmol, 2.20 eq) was added and along with 8.5 mL of acetone. To this stirring reaction, 0.084 g of 1,4-bis(bromomethyl)benzene (0.32 mmol, 1.00 eq) was added and stirring continued. A condenser was then set up above the reaction and the reaction was refluxed for 20 hours. The reaction heat was then turned off and the reaction was left to cool to room temperature. Once cooled, the reaction was gravity filtered and washed with additional acetone. The crystals collected were dried using a rotary evaporator to remove any additional acetone. No further purification was done to these white crystals affording compound **22** (0.121 g, 74.2 %). ^{1}H NMR (400 MHz, MeOD) δ 7.58 – 7.47 (m, 5H), 7.22 (s, 2H), 5.63 (t, J = 9.9 Hz, 1H), 4.50 (d, J = 15.3 Hz, 1H), 4.40 (t, J = 10.5 Hz, 1H), 4.30 (d, J = 15.3 Hz, 1H), 4.17 – 4.07 (m, 2H), 4.06 – 3.92 (m, 2H), 3.88 (dd, J = 10.4, 9.4 Hz, 1H). ^{13}C NMR (101 MHz, MeOD) δ 177.31, 135.18, 133.26, 129.77, 129.41,

Confidential and Proprietary Information

129.27, 128.23, 71.55, 54.59, 50.08, 48.53, 37.02. + ESI Scan m/z calculated for $C_{30}H_{32}N_4S_2^{2+}$: 256.1034, found 256.1013 [M+H]+

2.5- Electrophysiological Evaluation of Compounds

Some of the synthesized compounds, **8-15**, were evaluated *in vitro*. To do this *X. laevis* oocytes were injected with 50 nL of the receptor of interest, *hco-acc-2,* copy RNA as well as 3 accessory proteins, *unc-50*, *unc-74* and *ric-3.1* by members of the Forrester Lab (42). The injected oocytes were then stored in a supplemented ND-96 solution, containing pyruvic acid and antibiotic gentamycin, and incubated at 18 °C for up to 72 hours. After this time, the oocytes express the homomeric receptor of interest on their outer membrane and are now able to be used in two-electrode voltage clamp electrophysiology.

Two-electrode voltage clamp electrophysiology was done by the insertion of two glass electrodes into the oocyte. These electrodes were connected to a Axoclamp 900A voltage clamp (Molecular Devices, Sunnyvale, CA, USA). The first electrode was used to induce a current into the oocyte and the second electrode was used to measure any current change during the testing of each compound. Each electrode was backfilled with 3M KCl and contained Agl AgCl wires (42). Each oocyte was held at a potential of -60mV before a compound is tested. In preparation to be tested, acetylcholine, levamisole and compounds **8**-**15** were then dissolved in ND-96 solution to give a final concentration of 500 μM. Each compound was then washed over the oocyte using the RC-1Z recording chamber (Warner Instruments Inc., Hamdan, CT, USA) and the change in current was recorded. The oocyte was washed with ND-96 solution in between each compound to return the potential to -60 mV. The changes in current for each run were recorded

Confidential and Proprietary Information

in Clampex Software v10.2 (Molecular Devices) giving us a trace for each of the compounds tested. This process was repeated for 7 eggs and data from the traces for each run were analyzed. The data was then summarized into bar graphs showing the percent response of each compound in comparison to a full agonist, acetylcholine. This was summarized using Graphpad Prism Software v5.0 (San Diego, CA, USA).

2.6- Homology Modeling and Computational Docking of Compounds

The synthesised compounds of interest were also evaluated using homology modeling and computational docking as a way to hypothesize how they would bind to their respective receptors of interest. In order to do this the sequence of the receptor of interest is compared to a database of templates on SWISS-MODEL. These templates are assessed by their likeness to the sequence of interest as well as the amino acids present in the binding loops. The template used for Dim-UNC-49 was the glutamate-gated chloride channel from the organism Caenorhabditis elegans, also known in the protein data bank as 3RIF. The template used for the Hco-ACC-2 receptor was the alpha-1 glycine receptor from the organism Danio rerio, also known in the protein data bank as 3JAD (42). Modeller 9.24 was then used to align our receptor sequence to the template. This was then further assessed by using the discrete optimized protein energy score or the DOPE score. The lower the DOPE score the better the alignment of the template to our sequence of interest. AutoDock Tools version 1.5.6 was then used to define the binding pocket for each receptor respectively (55).

Our compounds of interest were then drawn in ChemDraw 3D and docked in the binding pocket using AutoDock Vina. This output gives the compound in 9 different conformations. The receptor and conformations were visualized using Chimera (56).

These conformations were evaluated based on the position of the molecule in the pocket as well as the possible interactions with the surrounding amino acids. Chimera allows the user to measure distances from amino acids to the compounds of interest (56). These distances enable us to hypothesize whether an interaction is most likely occurring or not.

Chapter 3- Results and Discussion

3.1 – Organic synthesis of imidazole – 4- acetic acid like compounds

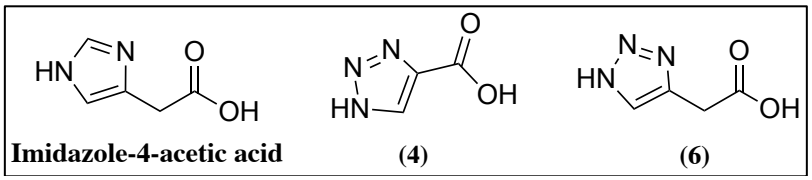

Imidazole-4-acetic acid **(4)** **(6)**

Figure 3.1- Structures of imidzaole-4-acetic acid, compound **4** and compound **6**.

In this thesis the synthesis of compounds similar to that of imidazole-4-acetic acid (IMA) were explored. It is known that nitrogen-containing heterocycles are ideal biomolecular scaffolds for molecules of interest for biological purposes. In the case of IMA there are only two nitrogen atoms present in its structure (**figure 3.1**). Our compounds **4** and **6** were designed to include an additional nitrogen in the ring with the thought that this could increase activity potentially in our receptor of interest, UNC-49 (**figure 3.1**). This triazole structure has a lot of benefits as it is able to participate in hydrogen bonding and it is said to have high chemical stability (57,58). The synthesis of these molecules was rather challenging and had rather low yields for most steps in the process. The first scheme (**scheme 3.1.1**) that was attempted, started with 2,4-dimethoxybenzyl alcohol undergoing the Appel reaction in order to remove the alcohol group and replace it with an azide group. This reaction took about 2 days to stir and was a rather well yielding reaction to produce compound **1** at 71%.

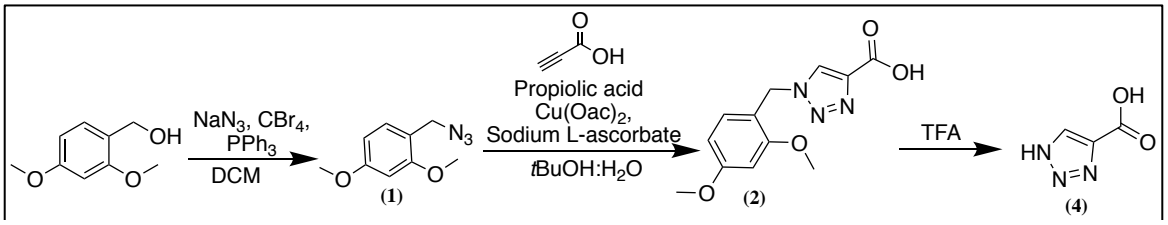

Scheme 3.1.1: Original scheme of compound **4**

For the next portion of scheme 3.1.1, the copper-catalyzed click reaction also known as the copper-catalyzed azide–alkyne cycloaddition (CuAAC) was performed. This reaction requires two functional groups, an alkyne and an azide, to be on the reactants of interest to create a triazole ring connecting the two molecules. Compound **1** was used as the azide source in the schemes for both compounds 4 and 6, **scheme 3.1.1** and **3.1.2** respectively. The synthesis of compound 2 used propiolic acid as the alkyne source needed. Many copper catalyst sources were explored for this scheme including copper (II) sulfate pentahydrate and copper (I) iodine. However, these copper sources resulted in no reaction. Copper (II) acetate was found to give the desired product and was used as the copper source for the remaining click reactions. Due to the copper source being a copper (II), it was reduced by the addition of sodium L-ascorbate in the reaction. The reaction of compound 2 was not high yielding and gave a yield of 20.3%. This was rather unexpected as the click reaction is said to be robust and high yielding (58). Due to this low yield, compound **4** was never successfully synthesised as described in **scheme 3.1.1**. This low yield could be due to the fact that a base was not added into the reaction scheme. Unsaturated carboxylic acids have been said to have chemical compatibility issues due to their acidic nature (59). This could be why we are seeing a low yield. A method that could be used in the future is removing our copper source and adding 5% of (2-nitrophenyl)boronic acid with our 2,4-dimethoxy benzyl alcohol and our propiolic acid

Confidential and Proprietary Information

in 1,2-dichloroethane. Hall et al. showed that the addition of 5% of (2-nitrophenyl)boronic acid to a similar reaction was able to return a 94% yield which was a major increase to the 20% yield that was shown without this catalyst (59).

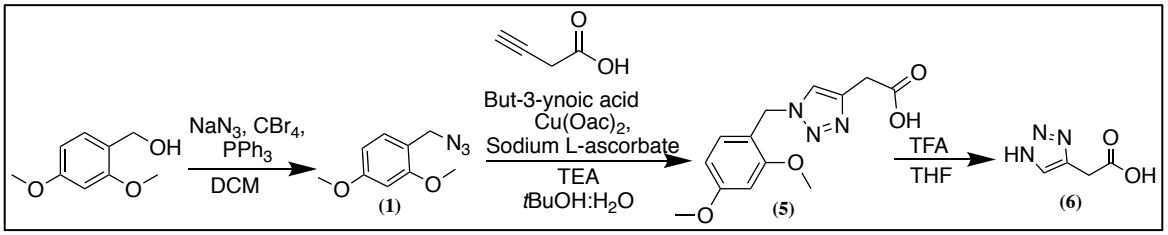

Scheme 3.1.2: Synthesis of compound **6**

The low yield observed in the synthesis of compound **2**, was also noted in the synthesis of compound **5** using a different alkyne source, but-3-ynoic acid (**scheme 3.1.2**). Due to this compound having more similarities to our compound of interest, IMA, optimization was done to try and increase the yield of compound **5**. The synthesis of compound **2** did not include the addition of a base which can be sometimes seen in click reactions. As a part of the optimization, this was added into the scheme of compound **5**, as well the equivalents of our copper source and our reducing agent were changed. With these changes we were able to get the yield of compound **5** from 31 to 47%.

The reaction optimization did not produce a great yield, but it did give us enough product to move on to the final step in our reaction (**scheme 3.1.2**). This step was a cleavage reaction of the 2,4-methoxy ring from the nitrogen in the triazole ring. This reaction proceeded very quickly and gave us a yield of 72.5%. Compound **6** was not purified any further as there were only 37 mg of this compound, and due to the polarity of the molecule it would be rather difficult to purify both manually and using the biotage. The NMR of compound **6** was okay and although it did have some impurities the large signal peaks corresponded to our compound of interest.

Confidential and Proprietary Information

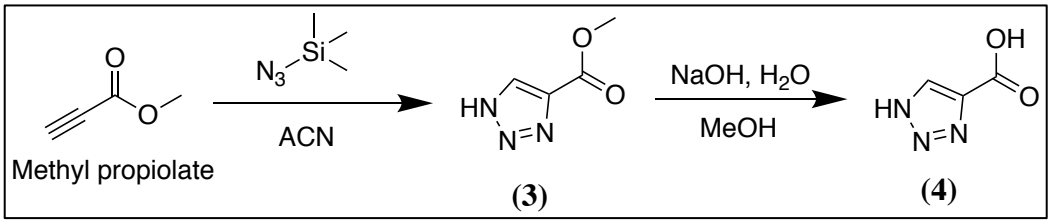

Scheme 3.1.3- Synthesis of Compound **4**.

In researching alternative schemes to create compound **4**, an article by Sibgatulin et al, (60) from 2009 was found. This paper described an alternative method of creating a triazole ring without the use of a copper catalyst. This scheme started differently than what was used previously to synthesize this compound. In this scheme (**scheme 3.1.3),** we used methyl propiolate and trimethylsilyl azide to create our triazole ring. This reaction took 3 days to react but resulted in a yield of 48% for compound **3**. This was lower than the 77% reported but the reaction produced enough product to continue on to compound **4**.

To synthesize compound **4**, compound **3** underwent ester hydrolysis changing the carboxylate to the desired carboxylic acid. This reaction, just like compound **6**, was rather quick in comparison to the other reactions and only took 3 hours resulting in a 22% yield. This was a lower yield then presented in the literature (60). This lower yield could be due to the acidification step. pH strips were used in this step and a pH meter would have given a more accurate reading of the pH in the solution. If the pH of the solution was not 2 then some of the compound may have stayed in the aqueous layer and therefore was not a part of the yield collected from the organic layer.

3.2 – Organic synthesis of Levamisole Derivatives

In this portion of the thesis, fourteen levamisole derivatives were synthesised, including eleven of which were novel to the best of our knowledge. The synthesis of these compounds all used the N-alkylation S_N2 mechanism with a base solvent. This mechanism starts with the lone pair of electrons on the nitrogen of interest, attacking the carbon directly attached to the bromine atom. At the same time, the bromine atom, which is the leaving group in this reaction, leaves this carbon. This then leaves the molecule of interest with a positively charged nitrogen at the point of the substitution and a negatively charged bromine atom. This mechanism can be observed in **figure 3.2.1.**

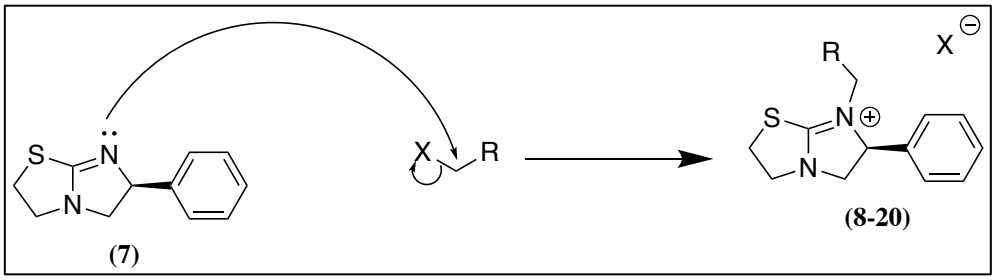

Figure 3.2.1- S_N2 N-alkylation mechanism of free base levamisole and bromo substituents of interest to afford levamisole derivatives, compounds **8-20**.

In order to do these substitutions, the synthesis was first started with the purchased chemical, levamisole hydrochloride. This compound was then extracted with diethyl ether, NaOH and water to produce the free base levamisole, compound 7 at a yield of 99%. The procedure for this extraction along with compounds 8-10 were synthesised using similar methods to a paper published by Hansen, et al. (50) in 2012 (**scheme 3.2.1**). Contrary to Hansen, et al., the compounds synthesised in this thesis were purified by using silica gel chromatography or by the biotage not using an HPLC as was done in the literature (50). The yields of these compounds were 33.4% for compound **9**, 84.3% for

compound **8** and 94.3% for compound **10**. Overall, this reaction procedure worked well and produced decent yields for the compounds of interest.

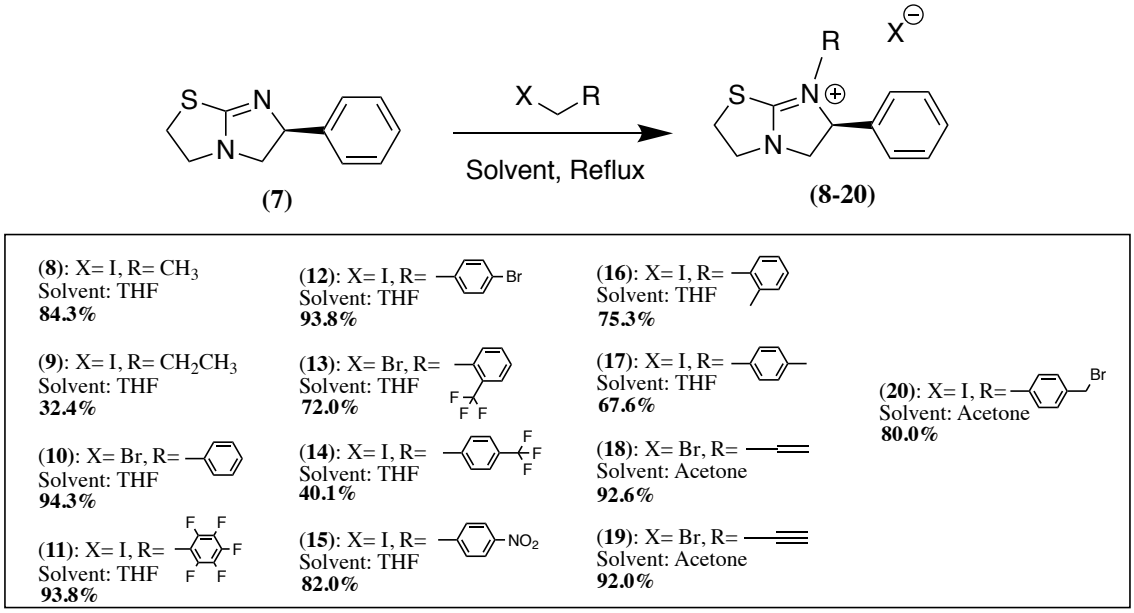

Scheme 3.2.1- General scheme for compounds **8-20**. Compounds **8+9** used 1.2 eq of the alkyl iodine source and THF as the solvent. Compounds **10-17** used 1.1 eq of the respective alkyl bromide and THF as the solvent. Compounds **18** and **19** used 1.1 eq of the respective alkyl bromide and acetone as the solvent. Finally compound **20** used 1.2 eq of 1,4-bis(bromomethyl)benzene and acetone as the solvent.

With this optimized procedure, further modifications for the free base levamisole, compound 7, were explored. These modifications included a pentafloro benzene ring, a 4-bromo benzene ring, a 2-trifluoromethyl benzene ring, a 4-trifluoromethyl benzene ring and 4-nitro benzene ring. These modifications were also successfully synthesised following scheme 3.2.1 at rather decent yields ranging from 40.1% to 93.8% with most compound's yields being above 69%. This range in yields could be due to a few reasons such as experience working with levamisole compounds as well as the type of functional groups present on the benzyl bromide source. Compounds **11,13,14,15** have electron withdrawing groups. This, in theory, should make **14** have a better yield as this would

Confidential and Proprietary Information

make the carbon slightly positive for the nitrogen attack. However, this is not what we see in this case.

Through further investigation into the binding pocket, homology modeling and the compounds structures, two more compounds were synthesised, compounds **16** and **17**. These compounds have very similar structures with compounds **13** and **14** but instead of having a tri-fluorinated methyl group, compounds **16** and **17** just have a methyl group on the 2 and 4 positions of the benzene ring respectively. These compounds were synthesised to be used as a type of control to see if the tri-fluorinated methyl groups on compounds **13** and **14** were creating activity in the binding pocket or if the 2 and 4 positions on the benzene ring are important for receptor activity. Compounds **16** and **17** also had decent yields at 75.3% and 67.6% respectively.

The last objective, of the thesis was to at create a dimer of levamisole. During this process it was noted that we did not have any compounds currently that could be used directly and easily for dimerization. Because of this the addition of an allyl and propargyl group to compound 7 was explored. These compounds **18** and **19** were originally synthesised using DMF as the solvent instead of THF which was previously used for compounds **8-17** (**scheme 3.2.1**). This change of solvent enabled us to increase the temperature at which the reaction could be refluxed. However, these reactions did not work as well as the previous compounds and gave yields of 10.0% and 30.4% respectively. This was hypothesised to be due to a couple of factors including equivalents of the respective linker and temperature. The synthesis of by-products with both nitrogen's becoming substituted decreased the yield of our desired product. This was due to linkers being added at 1.2 eq instead of 1.1 eq. Another factor was that although the

synthesis did not work in THF, levamisole seems to degrade at higher temperatures and the use of DMF did not appear to be the best solvent to use. With this being said, a different solvent, acetone was then used in the synthesis of compound **18** and compound **19** with 1.1 eq of the bromide source, allyl and propargyl bromide respectively. This increased the yields to 92.6 % for compound **18** and 92.0% for compound **19**.

Additionally compound **19** contains an alkyne functional group which, as described in chapter 3.1, is used in the copper-catalyzed click reaction. As was observed compound **10,** containing an aromatic ring, worked well within the binding pocket. Thus, the addition of a triazole ring instead of a benzene ring to the levamisole base structure may increase the amount of available nitrogen's present for hydrogen bonding in the binding pocket. As well the triazole ring is able to be functionalized by other functional groups such as carboxylic acids, aliphatic chains, alcohols and many other groups. This opens the doors to a wide range of modifications that may enhance the efficacy of these novel molecules within the binding pocket by increasing the opportunities for hydrogen bonding.

Through the synthesis of all of the levamisole derivatives, it was found that it was ideal to keep reactions at 60 °C or below for optimal yield. The synthesis of compound **20** is another example of where acetone could be used as a substitution to THF (**scheme 3.2.1)**. This compound was synthesized at an 80.0% yield and still used 1.2 eq of its bromine source. This molecule was synthesized in the process of creating a dimer of levamisole with a benzene ring in the middle. This procedure was adapted from Musilek, et al. (61) where 1,4-bis(bromomethyl)benzene was used in a non-symmetrical synthesis.

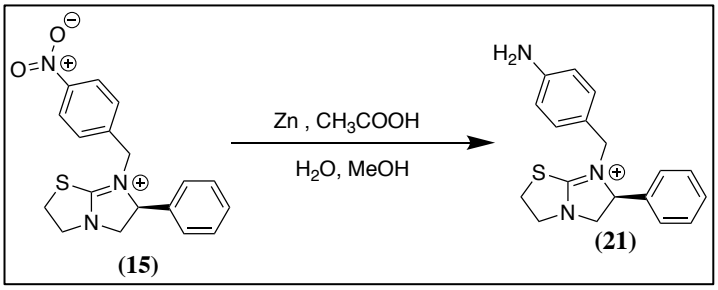

Scheme 3.2.2- Synthesis of compound **21** using approximately 7 eq of Zn and acetic acid in a H_2O and methanol solvent system.

Compound **21** was a derivative that was also synthesized with later reactions in mind. This was synthesized by the reduction of compound **15** using around 7 equivalents of zinc and acetic acid (**scheme 3.2.2**). This reaction was rather short, only taking an hour to produce compound 21 at a 38.6% yield. The reaction was monitored via TLC to see when the conversion of the NO_2 to NH_2 was complete. This was visualized between 1 hour and 1 hour and 20 minutes. The longer this reaction stirred the more degradation of the compound itself is observed. When looking at the ^1H NMR's for both compound **15** and compound **21**, a clear difference can be observed in the aromatic region. In compound **15** the hydrogens closest to the nitro group are present between 8.17 and 8.21 as a multiplet with the remainder of the aromatic hydrogens at 7.44 – 7.53. In compound **21**, there is a shift where two doublets are present at 6.68 and 6.91 and the peak previously observed at 8.17-8.21 is no longer present.

Confidential and Proprietary Information

3.3 – Organic synthesis of Levamisole Dimers

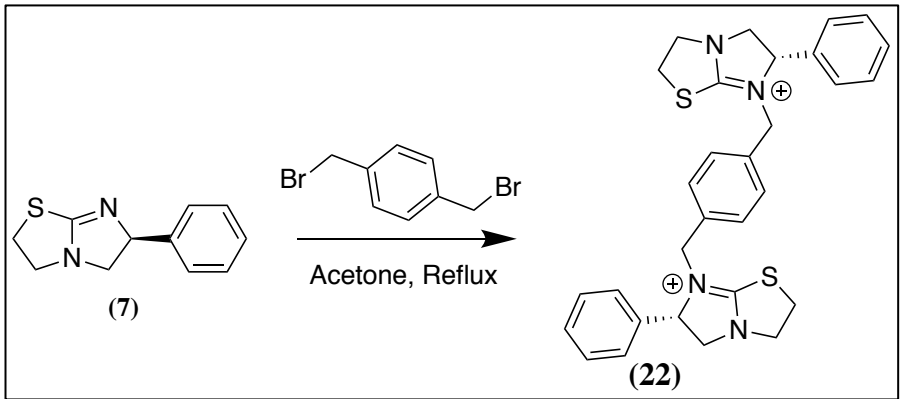

Scheme 3.3- Synthesis of compound **22** was done with 1.0 eq of 1,4-bis(bromomethyl)benzene and 2.2 eq of compound **7**.

In the literature in order to synthesize compound **22**, it was suggested to do this synthesis in two reactions. The first reaction is using acetone and 1,4-bis(bromomethyl)benzene to get to compound **20** then using DMF and levamisole in the second reaction to get to compound **22** (61). As mentioned before, DMF does not work well with levamisole in types of reactions involving a reflux and this was unsuccessful. However, compound **20** was successfully synthesized using the first reaction scheme. This scheme was then adapted slightly and the equivalents of compound **7** were increased to 2.2 instead of 1 eq used in compound **20 (scheme 3.3**). From this scheme compound **22** was successfully synthesised with a 74.5% yield. This scheme was also tried with other linkers such as 1,2-dibromoethane and 1,6-dibromohexane however these were not found to be successful under these conditions.

3.4 Pharmacological Characterization

In order to have a rational drug design, compounds must be tested and evaluated based on their efficacy. From this information, additional compounds can then be synthesised. In this thesis, *X. laevis* oocytes were used to express receptors of interest and

Confidential and Proprietary Information

an electrophysiology system was used to evaluate each compounds effectiveness at generating a response. The imidazole like compounds, compounds **4** and **6**, were not tested due to their difficulty to dissolve in an appropriate solution and poor yield. The levamisole derivatives, compounds **8**-**15,** however, were easily dissolved in the ND-96 solvent and there was a sufficient amount of each compound in order for pharmacological evaluation.

To start the screening, compounds **8**, **9**, and **10** were evaluated in the Hco-ACC-2 homomeric channel at a concentration of 500 μM. In our compounds of interest, the nitrogen with known interactions in the binding pocket is modified (42). Compounds **8-10** were screened in order to first determine if there was any activity at our receptor of interest. This approach also determined what modifications produce favorable efficacy. Acetylcholine, a known full agonist for the Hco-ACC-2 receptor, was used as a control in this evaluation (42). The 500 μM concentration was chosen as it is above 250 μM, which is the concentration responsible for producing a maximal response for acetylcholine in the Hco-ACC-2 receptor (42). Levamisole, a partial agonist of Hco-ACC-2, compound **8**, **9** and **10** were evaluated and normalized to Acetylcholine's response in the receptor (42). The changes in the current produced by each compound are computer-generated into traces as shown in **figure 3.4.1.** From multiple runs and traces, the percent response was normalized to acetylcholine having 100% response in the receptor. The summary results of this can be observed in **figure 3.4.2**.

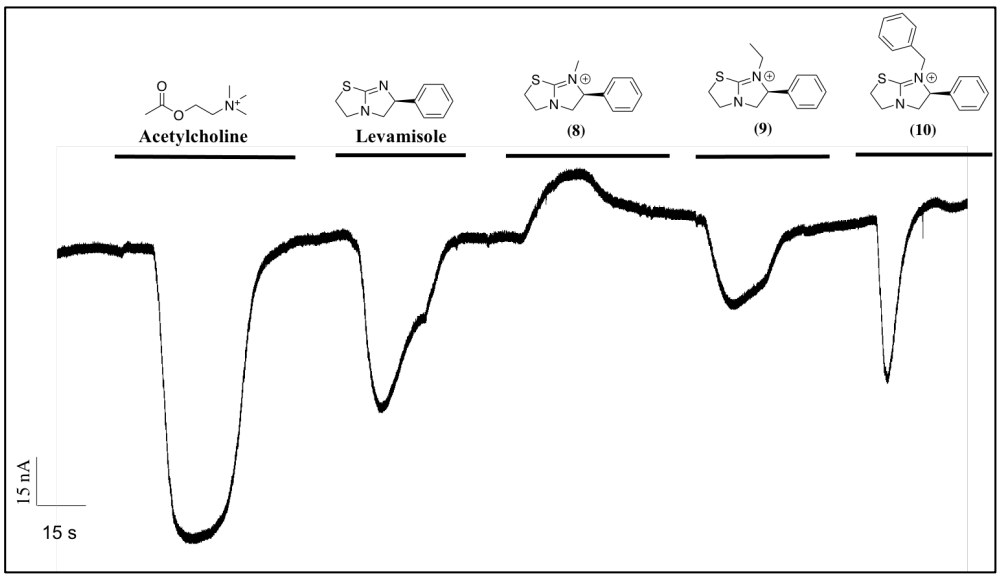

Figure 3.4.1- Clampex Software v10.2 generated trace for one run with each compound structure shown above the corresponding response.

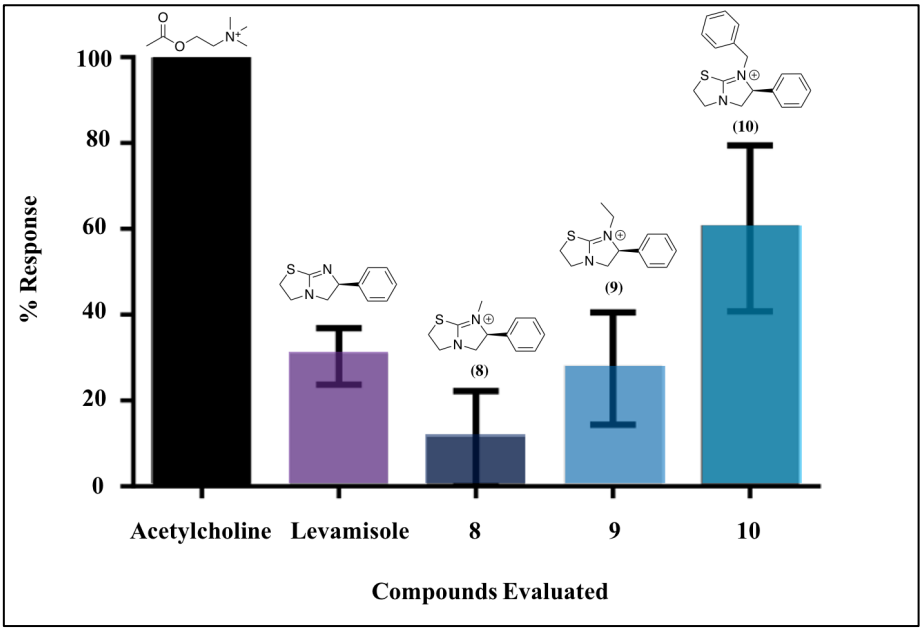

Figure 3.4.2- Summary of electrophysiology screening data for Acetylcholine, Levamisole and Compounds **8**-**10** at 500 µM. Percent response was normalized to Acetylcholine having a 100% response.

Compounds **8, 9** and **10** were able to generate a response in the Hco-ACC-2 receptor. After evaluating the data further, it was determined that perusing levamisole

Confidential and Proprietary Information

compounds with additional benzene modifications would be the next step as compound **10** was determined to have the highest response at 62%.

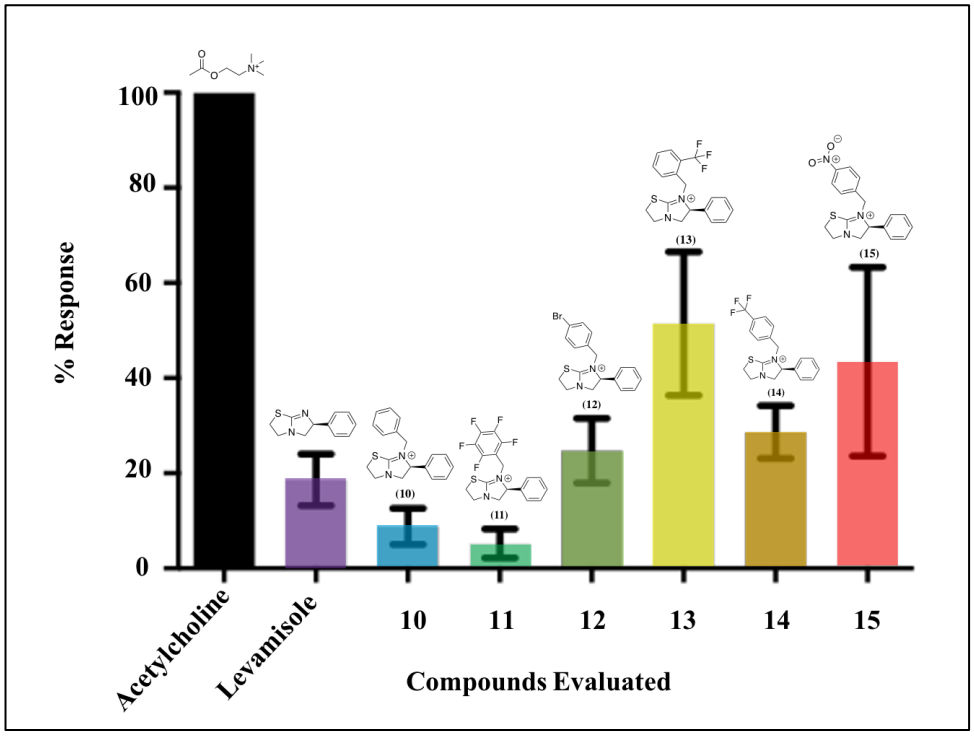

Figure 3.4.3- Summary of electrophysiology screening data for acetylcholine, levamisole and compounds **10**-**15** at 500 μM. Percent response was normalized to Acetylcholine having a 100% response.

Once synthesis was completed for compounds **11** – **15,** they were evaluated in the Hco-ACC-2 homomeric channel alongside acetylcholine, levamisole and compound **10**. This data is summarized in **figure 3.4.2**, where all of the compounds tested (**11-15)** were able to generate a response. The lowest response (8.8%) was observed from compound **11**, which contained a fully fluorinated benzene ring. The greatest response was seen from compound **13**, which contained a trifluoromethyl group at the two position, produced the greatest response at 55.4% of the acetylcholine response.

Interestingly enough, although compound **13** had a rather large response, compound **14**, in comparison, produced less of a response despite containing a

Confidential and Proprietary Information

trifluoromethyl group (**figure 3.4.4)**. This brings up an interesting point about the placement of functional groups on the benzene ring (**figure 3.4.4**). With the data presented so far, it looks as if the two position on the benzene ring may enable for more interactions between the compounds of interest and the surrounding amino acids in the binding pocket.

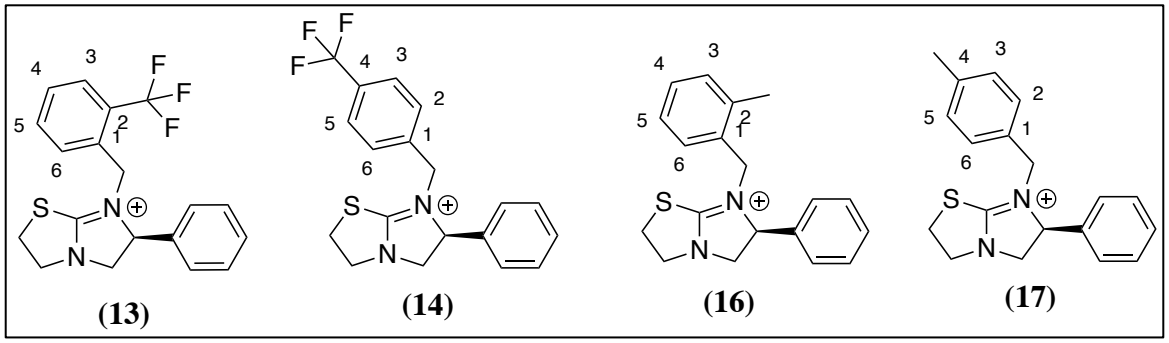

Figure 3.4.4- Compounds **13, 14, 16, 17** with each of the benzyl group positions labeled.

With this in mind compounds **16** and **17** were synthesised. These compounds were synthesized with a neutral functional group on the benzene ring which is not electron withdrawing like present on compounds **13** and **14**. This was done to determine the importance of placement of functional groups on the 2 position of the benzene ring. These modifications can be seen in compound **13** and **16** where a trifluoromethyl group and the methyl group on the 2 position are present on the benzene ring respectively (**figure 3.4.4**).

3.5 – Homology Modeling Data

Homology modeling was completed for both Dim-UNC-49B homomer and Hco-ACC-2 homomer. Compounds **4**, **6** and imidazole-4-acetic acid were modeled in Dim-UNC-49B and Compounds **7-19** were modelled in Hco-ACC-2.

Confidential and Proprietary Information

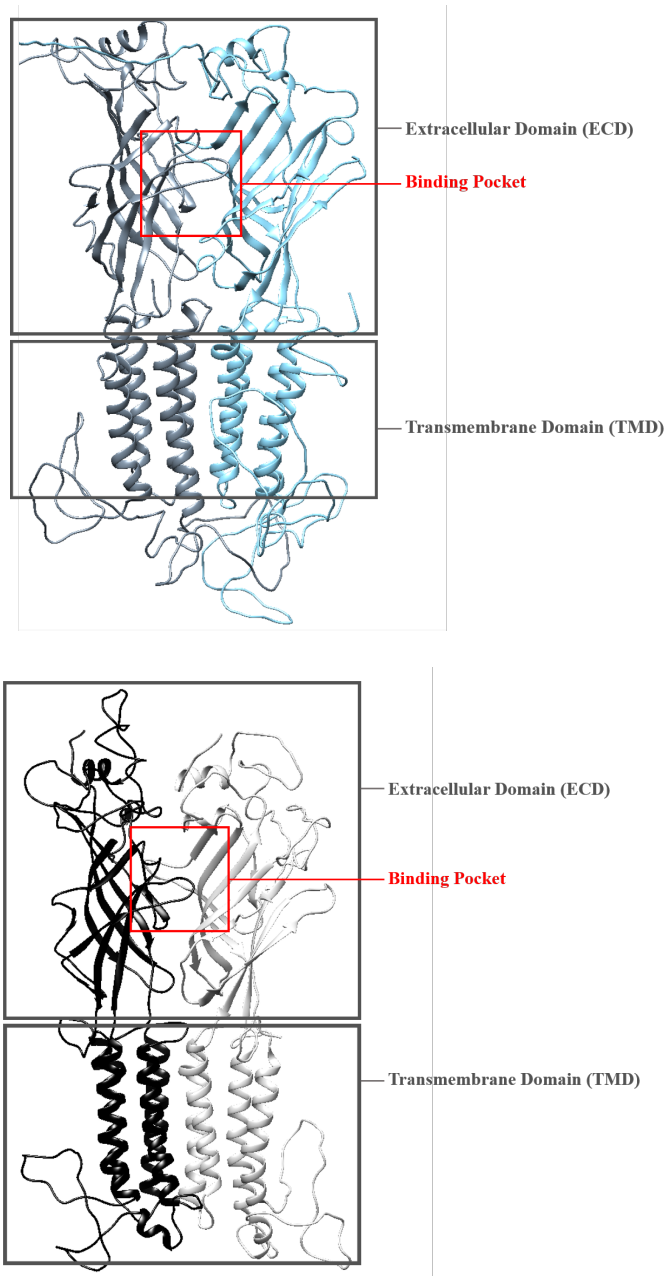

Figure 3.5.1- Homology models of Dim-UNC-49B (top) and Hco-ACC-2 (bottom) with labeled extracellular domain, binding pocket and transmembrane domain.

Due to both receptors being from the cys-loop receptor family the general structure of each homomeric channel looks rather similar. This can be seen in the **figure 3.5.1** where the extracellular domain, which includes the binding pocket, and the transmembrane domain have been highlighted in both receptors. Where these receptors

Confidential and Proprietary Information

differ is by the amino acids present in the binding pocket (**figure 3.5.2**). For Dim-UNC-49B the amino acids found to be important were: T236, Y241, Y87, E188. For Hco-ACC-2 the following amino acids were found to be important in the binding pocket: W248, F200, Y243, Y102, W83.

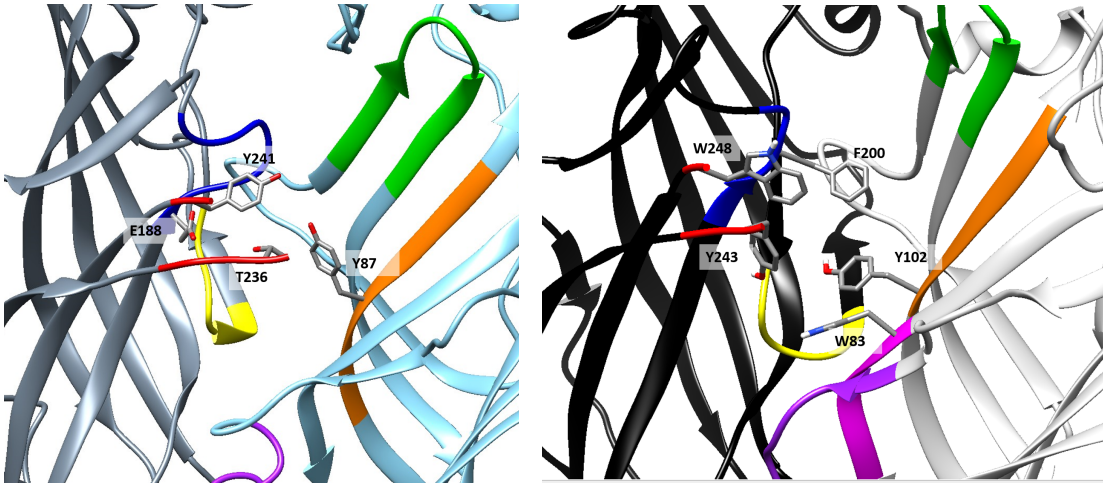

Figure 3.5.2- Binding Pocket of Dim-UNC-49 (left) and Hco-ACC-2 (right) with relevant amino acids exposed. Part of loop C has been removed for visualization purposes. Loop A (yellow), Loop B (blue), Loop C (red), Loop D (orange), Loop E (green), Loop F (purple) and for ACC-2 Loop G (magenta) have been highlighted in different colors for identification purposes.

3.5.1 Imidazole Like Compounds

Although we were not able to test compounds **4** and **6** using electrophysiology, they were able to be modelled to hypothesize the interactions with the binding pocket. Both of the compounds were able to make hydrogen bonds with at least two of the important amino acids present in the binding pocket. This suggests that compounds **4** and **6** would be able to dock in our receptor of interest.

Confidential and Proprietary Information

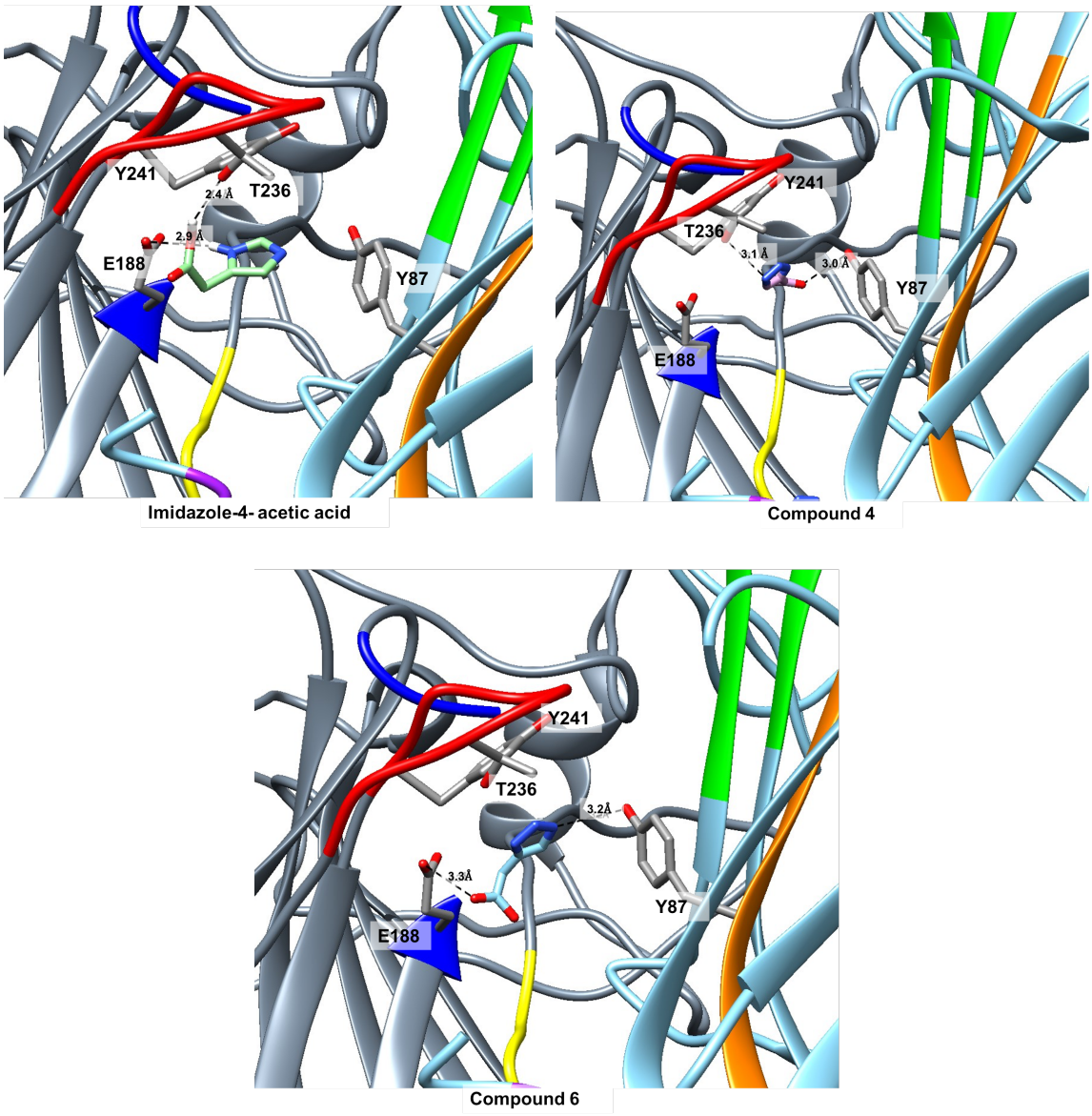

Figure 3.5.3- Homology model and computational docking of imidazole-4-acetic acid (top left), compound **4** (top right) and compound **6** (bottom) in Dim-UNC-49B. Part of loop B has been removed for visualization purposes.

3.5.2 Levamisole and Levamisole Derivatives

Compounds **7-19** were all modelled in the homomeric Hco-ACC-2 channel. All of the compounds showed a pi-cationic interaction with W248 and the positively charged quaternary amine on our compounds of interest. This is the same interaction that is observed in the docking of levamisole itself (**figure 3.5.2.1**).

Confidential and Proprietary Information

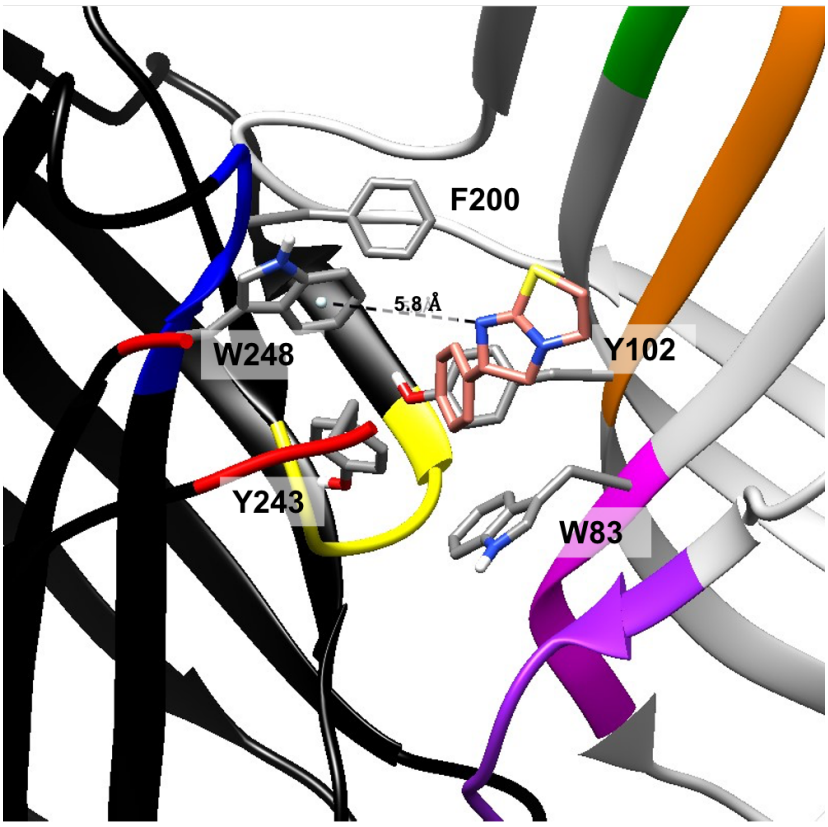

Figure 3.5.2.1- Homology model and computational docking of Compound **7** in the homomeric Hco-ACC-2 channel with distances and amino acids expressed. Part of loop C has been removed for visualization purposes.

This also aligns with our electrophysiology data where all of the compounds tested were able to elicit a response. Compound **13**, modeled in **figure 3.5.2.2**, shows an additional interaction with W83 which was not noted in any of the other models. This interaction could be the reason that this compound had a greater percent response than the other compounds tested.

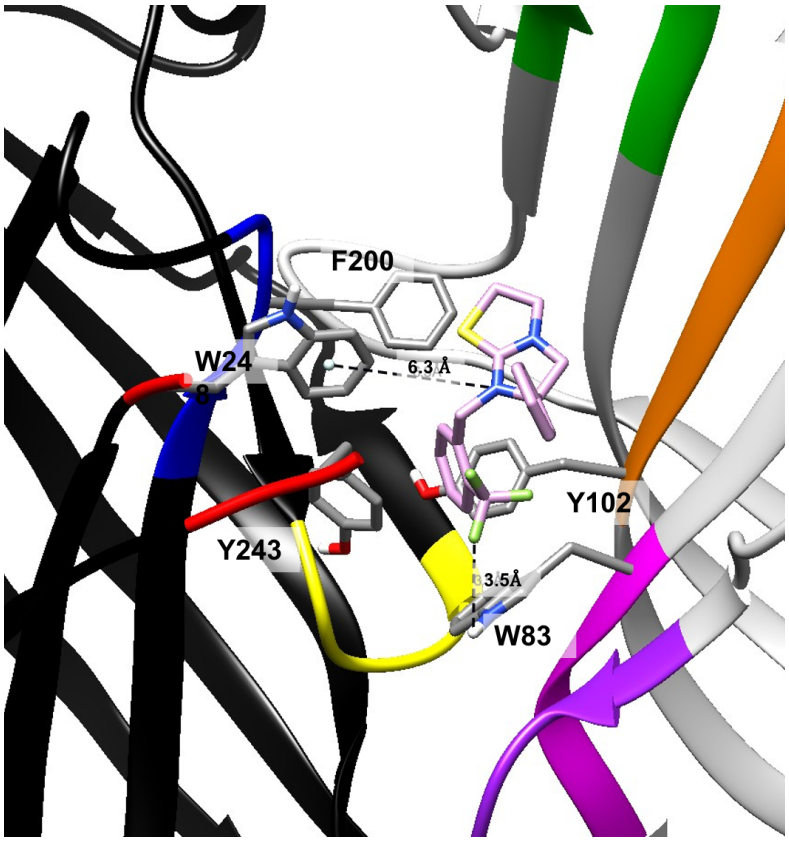

Figure 3.5.2.2- Homology model and computational docking of Compound **13** in the homomeric Hco-ACC-2 channel with distances and amino acids expressed. Part of loop C has been removed for visualization purposes.

Another interaction that may be taking place for compound **13** is pi-stacking between the modified benzene ring and the tyrosine (Y102) residue. Compound **15** is also situated in the binding pocket to pi-stack with the tyrosine residue (Y102) as this is a known interaction with this amino acid that can occur (**figure 3.5.2.3**) (53).

Confidential and Proprietary Information

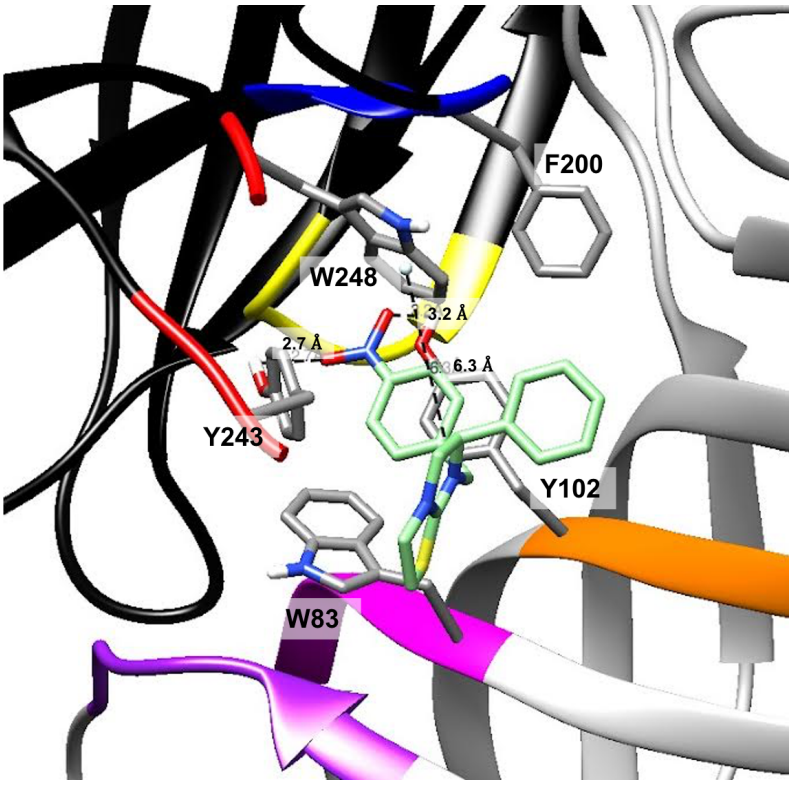

Figure 3.5.2.3- Homology model and computational docking of Compound **15** in the homomeric Hco-ACC-2 channel with distances and amino acids expressed.
Part of loop C has been removed for visualization purposes.

As well, compound **15** could be hydrogen bonding with tyrosine as the bond length between the oxygen of the NO_2 group and the hydrogen on tyrosine (Y102) and tyrosine (Y243) has a bond length of 3.2 Å and 2.7 Å respectively. Compound **15** also had the second highest percent response at 43% indicating some of these interactions could be responsible.

Confidential and Proprietary Information

Chapter 4- Conclusions

D. immitis' prevalence in Canada is growing due to many factors including anthelmintic resistance. Due to this the need for new anthelmintics is increasing. Throughout this project, 22 compounds containing nitrogen containing heterocycles were successfully synthesized including imidazole-4-acetic acid like derivatives, levamisole derivatives and a levamisole dimer. In total, 12 of the 22 synthesized compounds were determined to be novel and could not be located in the SciFinder® database (**figure 4**).

All of the compounds tested *in vitro* had activity within the Hco-ACC-2 receptor, with compound **13** showing the highest activity at 55.4%. Through the testing of this molecule, it was also recognized the potential importance of the 2 position on the benzene ring with interactions in the Hco-ACC-2 receptor. Future results that emerge from testing compound **16** in the Hco-ACC-2 receptor will be able to better solidify this finding on whether the 2 position of the modification or the modification itself, trifluoromethyl group, is important.

From the continuation of testing and evaluation of the remaining novel compounds in a *D.immitis* levamisole receptor we will gain a more complete understanding of their potential as promising nematicides. Overall, this project has synthesized 14 novel compounds and some of which have been shown to have promising results for being potential anthelmintics for *D. immitis*.

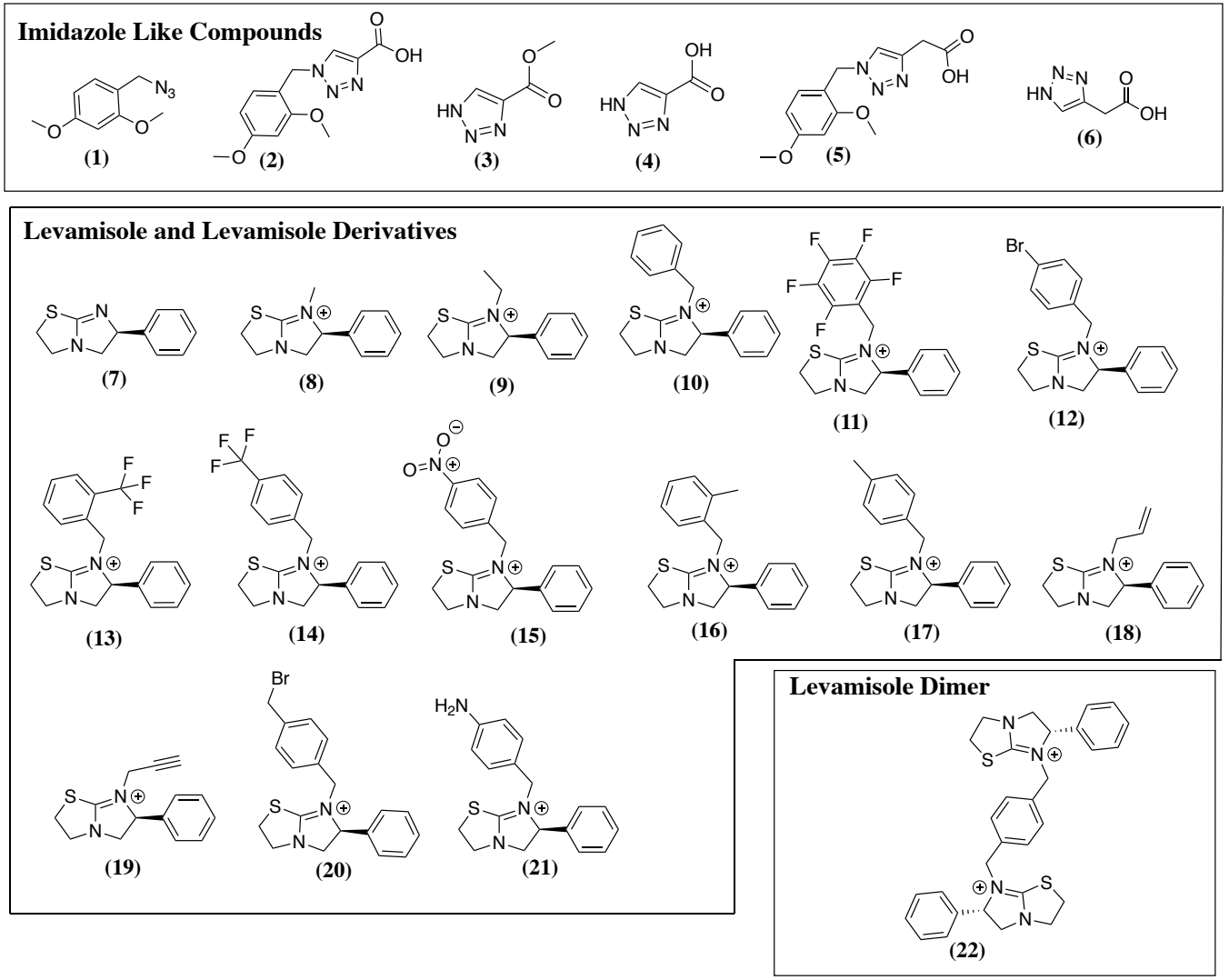

Figure 4- Structures of all 22 compounds synthesized.

Confidential and Proprietary Information

Chapter 5- Future Directions

In the preliminary results obtained so far using our electrophysiology technique, it is evident that this project has great potential and the compounds synthesized should continue to be explored and further evaluated.

All of the electrophysiology testing in this project thus far has been done in Hco-ACC-2 receptor, however due to the differences between the parasites it would be preferable to test these compounds in our organism of interest, *D. immitis*. As well, levamisole is only a partial agonist in the ACC-2 receptor so evaluation using the *D. immitis* levamisole receptor (which are another family of cys-loop receptors, the ACh-gated cation channels), where levamisole is likely a full agonist, would be ideal In the meantime, compounds **7-22** could be tested on a levamisole receptor from the parasitic nematode *H. contortus* that has been extensively characterized (34).

When looking into the specific compounds themselves, compound **13** should be further evaluated in vivo to determine their physiological effects on the *D. immitis* worm. Levamisole is known to cause the paralysis of parasitic nematodes, but it would be interesting to see if compound **13** shows similar effects or if other nematocidal effects are observed (44). Compound **22** should be used as a template to create dimers where there is a different receptor agonist replacing one of the levamisole molecules. For example, replacing one of the levamisole with an IMA, a full agonist for the UNC-49 receptor. This could be done in two steps by first synthesizing compound **20** then in a second reaction adding the new agonist of choice. This scheme in theory should make a new dimer.

The synthesis of these novel levamisole derivatives also have good potential as pharmacological tools for the characterization of acetylcholine receptors from other parasitic nematodes. There are several parasites where these receptors have been characterized and shown to have pharmacological and possibly functional differences (34). It is likely that these modified levamisole derivatives described in this thesis may be used to further characterize and understand the cholinergic nervous system across the nematode phyla.

References

1. Academy of Natural Sciences of Philadelphia. Proceedings of the Academy of Natural Sciences of Philadelphia. [Internet]. Vol. v.8 (1856). Philadelphia,Academy of Natural Sciences of Philadelphia; 1856. 544 p. Available from: https://www.biodiversitylibrary.org/item/18246

2. Godel C, Kumar S, Koutsovoulos G, Ludin P, Nilsson D, Comandatore F, et al. The genome of the heartworm, Dirofilaria immitis, reveals drug and vaccine targets. FASEB J. 2012;26(11).

3. Verma S, Kulke D, McCall JW, Martin RJ, Robertson AP. Recording drug responses from adult Dirofilaria immitis pharyngeal and somatic muscle cells. Int J Parasitol Drugs Drug Resist [Internet]. 2021;15(December 2020):1–8. Available from: https://doi.org/10.1016/j.ijpddr.2020.12.002

4. Malik D, Amaraneni A, Singh S, Roach R. Man's best friend: How humans can develop Dirofilaria immitis infections. IDCases [Internet]. 2016;4:43–5. Available from: http://dx.doi.org/10.1016/j.idcr.2016.03.003

5. Grieve RB, Lok JB, Glickman LT. Epidemiology of canine heartworm infection. Epidemiol Rev. 1983;5(1):220–46.

6. Rossi MID, Aguiar-Alves F, Santos S, Paiva J, Bendas A, Fernandes O, et al. Detection of Wolbachia DNA in blood from dogs infected with Dirofilaria immitis. Exp Parasitol. 2010;126(2):270–2.

7. McCall JW, Genchi C, Kramer L, Guerrero J, Dzimianski MT, Supakorndej P, et al. Heartworm and Wolbachia: Therapeutic implications. Vet Parasitol. 2008;158(3):204–14.

8. Taylor MJ, Bandi C, Hoerauf A. Wolbachia bacterial endosymbionts of filarial nematodes. Adv Parasitol. 2005;60(05):245–84.

9. Taylor MJ, Cross HF, Ford L, Makunde WH, Prasad GBKS, Bilo K. Wolbachia bacteria in filarial immunity and disease. Parasite Immunol. 2001;23(7):401–9.

10. Herrin BH, Peregrine AS, Goring J, Beall MJ, Little SE. Canine infection with Borrelia burgdorferi, Dirofilaria immitis, Anaplasma spp. and Ehrlichia spp. in Canada, 2013-2014. Parasites and Vectors. 2017;10(1).

11. Villeneuve A, Goring J, Marcotte L, Overvelde S. Seroprevalence of Borrelia burgdorferi, Anaplasma phagocytophilum, Ehrlichia canis, and Dirofilaria immitis among dogs in Canada. Can Vet J. 2011;52(5):527–30.

12. Zhang, X., Flato, G., Kirchmeier-Young, M., Vincent, L., Wan, H., Wang, X., Rong, R., Fyfe, J., Li, G., Kharin, V.V. (2019): Changes in Temperature and Precipitation Across Canada; Chapter 4 in Bush, E. and Lemmen, D.S. (Eds.) Canada's Changing Climate Re pp 112-193. Temperature and Precipitation Across Canada.

13. McGill E, Berke O, Peregrine AS, Weese JS. Epidemiology of canine heartworm (Dirofilaria immitis) infection in domestic dogs in Ontario, Canada: Geographic distribution, risk factors and effects of climate. Geospat Health. 2019;14(1):17–24.

14. McGill E, Berke O, Weese JS, Peregrine A. Heartworm infection in domestic dogs in Canada, 1977-2016: Prevalence, time trend, and efficacy of prophylaxis. Can Vet J = La Rev Vet Can [Internet]. 2019;60(6):605–12. Available from: http://www.ncbi.nlm.nih.gov/pubmed/31156260%0Ahttp://www.pubmedcentral.nih.gov/articlerender.fcgi?artid=PMC6515813

15. Snyder DE, Wiseman S, Cruthers LR, Slone RL. Ivermectin and Milbemycin Oxime in Experimental Adult Heartworm (Dirofilaria immitis) Infection of Dogs. J Vet Intern Med. 2011;25(1):61–4.

16. Kryda K, Holzmer S, Everett WR, McCall JW, Mahabir SP, McTier TL, et al. Preventive efficacy of four or six monthly oral doses of 24 μg/kg moxidectin compared to six monthly doses of Heartgard® plus or Interceptor® plus against macrocyclic lactone-resistant heartworm (Dirofilaria immitis) strains in dogs. Parasites and Vectors [Internet]. 2020;13(1):1–11. Available from: https://doi.org/10.1186/s13071-020-04178-z

17. Burns K. Vital statistics: AVMA report details pet ownership, veterinary care [Internet]. American Vetrinary Medical Association. 2013 [cited 2022 Apr 10]. Available from: https://www.avma.org/javma-news/2013-02-01/vital-statistics

18. Holden-Dye L, Walker RJ. Anthelmintic drugs and nematicides: studies in Caenorhabditis elegans. WormBook. 2014;(1995):1–29.

19. Geary TG, Bourguinat C, Prichard RK. Evidence for macrocyclic lactone anthelmintic resistance in dirofilaria immitis. Top Companion Anim Med. 2011;26(4).

20. Wolstenholme AJ, Maclean MJ, Coates R, McCoy CJ, Reaves BJ. How do the macrocyclic lactones kill filarial nematode larvae? Invertebr Neurosci [Internet]. 2016 Sep 9;16(3):7. Available from: http://link.springer.com/10.1007/s10158-016-0190-7

21. Wolstenholme AJ. Glutamate-gated chloride channels. J Biol Chem. 2012;287(48):40232–8.

22. Geary TG, Sims SM, Thomas EM, Vanover L, Davis JP, Winterrowd CA, et al. Haemonchus contortus: Ivermectin-Induced Paralysis of the Pharynx. Exp Parasitol [Internet]. 1993 Aug;77(1):88–96. Available from: https://linkinghub.elsevier.com/retrieve/pii/S0014489483710647

23. Moreno Y, Nabhan JF, Solomon J, MacKenzie CD, Geary TG. Ivermectin disrupts the function of the excretory- secretory apparatus in microfilariae of Brugia malayi. Proc Natl Acad Sci U S A. 2010;107(46):20120–5.

24. Bowman DD, Atkins CE. Heartworm Biology, Treatment, and Control. Vet Clin North Am - Small Anim Pract. 2009;39(6):1127–58.

25. McCall JW. The safety-net story about macrocyclic lactone heartworm preventives: A review, an update, and recommendations. Vet Parasitol. 2005;133(2-3 SPEC. ISS):197–206.

26. Maxwell E, Ryan K, Reynolds C, Pariaut R. Outcome of a heartworm treatment protocol in dogs presenting to Louisiana State University from 2008 to 2011: 50 cases. Vet Parasitol [Internet]. 2014;206(1–2):71–7. Available from: http://dx.doi.org/10.1016/j.vetpar.2014.05.033

27. Treatment CH. Treatment Record with DIROBAN ® (melarsomine dihydrochloride). 2020;(January).

28. Lucchetti C, Genchi M, Venco L, Menozzi A, Serventi P, Bertini S, et al. Differential ABC transporter gene expression in adult Dirofilaria immitis males and females following in vitro treatment with ivermectin, doxycycline or a combination of both. Parasites and Vectors [Internet]. 2019;12(1):1–9. Available from: https://doi.org/10.1186/s13071-019-3645-y

29. Kozek WJ. What is new in the Wolbachia/Dirofilaria interaction? Vet Parasitol. 2005;133(2-3 SPEC. ISS):127–32.

30. Ashour DS. Ivermectin: From theory to clinical application. Int J Antimicrob Agents [Internet]. 2019;54(2):134–42. Available from: https://doi.org/10.1016/j.ijantimicag.2019.05.003

31. Hampshire VA. Evaluation of efficacy of heartworm preventive products at the FDA. Vet Parasitol. 2005;133(2-3 SPEC. ISS):191–5.

32. Bourguinat C, Keller K, Blagburn B, Schenker R, Geary TG, Prichard RK. Correlation between loss of efficacy of macrocyclic lactone heartworm anthelmintics and P-glycoprotein genotype. Vet Parasitol [Internet]. 2011;176(4):374–81. Available from: http://dx.doi.org/10.1016/j.vetpar.2011.01.024

33. Thompson AJ, Lester HA, Lummis SCR. The structural basis of function in Cys-loop receptors. Vol. 43, Quarterly Reviews of Biophysics. 2010. 449–499 p.

34. Choudhary S, Kashyap SS, Martin RJ, Robertson AP. Advances in our understanding of nematode ion channels as potential anthelmintic targets. Int J Parasitol Drugs Drug Resist [Internet]. 2022;18(June 2021):52–86. Available from: https://doi.org/10.1016/j.ijpddr.2021.12.001

35. Pless SA, Lynch JW. Illuminating the structure and function of Cys-loop receptors. Clin Exp Pharmacol Physiol. 2008;35(10):1137–42.

36. Hernando G, Bouzat C. Caenorhabditis elegans neuromuscular junction: GABA receptors and ivermectin action. PLoS One. 2014;9(4).

37. Wongsamitkul N, Maldifassi MC, Simeone X, Baur R, Ernst M, Sigel E. α subunits in GABAA receptors are dispensable for GABA and diazepam action. Sci Rep [Internet]. 2017;7(1):1–11. Available from: http://dx.doi.org/10.1038/s41598-017-15628-7

38. Tunnicliff G. Pharmacology and function of imidazole 4-acetic acid in brain. Gen Pharmacol. 1998;31(4):503–9.

39. Kaji MD, Kwaka A, Callanan MK, Nusrat H, Desaulniers JP, Forrester SG. A molecular characterization of the agonist binding site of a nematode cys-loop GABA receptor. Br J Pharmacol. 2015;172(15):3737–47.

40. Accardi M V., Forrester SG. The Haemonchus contortus UNC-49B subunit possesses the residues required for GABA sensitivity in homomeric and heteromeric channels. Mol Biochem Parasitol [Internet]. 2011;178(1–2):15–22. Available from: http://dx.doi.org/10.1016/j.molbiopara.2011.04.002

41. Bamber BA, Beg AA, Twyman RE, Jorgensen EM. The Caenorhabditis elegans unc-49 Locus Encodes Multiple. 1999;19(13):5348–59.

42. Habibi SA, Callanan M, Forrester SG. Molecular and pharmacological characterization of an acetylcholine-gated chloride channel (ACC-2) from the parasitic nematode Haemonchus contortus. Int J Parasitol Drugs Drug Resist [Internet]. 2018;8(3):518–25. Available from: https://doi.org/10.1016/j.ijpddr.2018.09.004

43. Wever CM, Farrington D, Dent JA. The validation of nematode-specific acetylcholine-gated chloride channels as potential anthelmintic drug targets. PLoS One. 2015;10(9):1–21.

44. Blanco MG, Vela Gurovic MS, Silbestri GF, Garelli A, Giunti S, Rayes D, et al. Diisopropylphenyl-imidazole (DII): A new compound that exerts anthelmintic activity through novel molecular mechanisms. PLoS Negl Trop Dis. 2018;12(12):1–23.

45. Heravi MM, Zadsirjan V. Prescribed drugs containing nitrogen heterocycles: an overview. RSC Adv. 2020;10(72):44247–311.

46. Kerru N, Gummidi L, Maddila S, Gangu KK, Jonnalagadda SB. A review on recent advances in nitrogen-containing molecules and their biological applications. Molecules. 2020;25(8).

47. Vitaku E, Smith DT, Njardarson JT. Analysis of the structural diversity, substitution patterns, and frequency of nitrogen heterocycles among U.S. FDA approved pharmaceuticals. J Med Chem. 2014;57(24):10257–74.

48. Boulin T, Fauvin A, Charvet CL, Cortet J, Cabaret J, Bessereau JL, et al. Functional reconstitution of Haemonchus contortus acetylcholine receptors in Xenopus oocytes provides mechanistic insights into levamisole resistance. Br J Pharmacol. 2011;164(5):1421–32.

49. Carlisle CH, Atwell RB, Robinson S. The effectiveness of levamisole hydrochloride against the microfilaria of Dirofilaria immitis. Aust Vet J. 1984;61(9):282–4.

50. Hansen AN, Bendiksen CD, Sylvest L, Friis T, Staerk D, Jørgensen FS, et al. Synthesis and Antiangiogenic Activity of N-Alkylated Levamisole Derivatives. PLoS One. 2012;7(9).

51. Lee KC, Ladizinski B, Federman DG. Complications associated with use of levamisole-contaminated cocaine: An emerging public health challenge. Mayo Clin Proc [Internet]. 2012;87(6):581–6. Available from: http://dx.doi.org/10.1016/j.mayocp.2012.03.010

52. Gallivan JP, Dougherty DA. Cation-π interactions in structural biology. Proc Natl Acad Sci [Internet]. 1999 Aug 17;96(17):9459–64. Available from: https://pnas.org/doi/full/10.1073/pnas.96.17.9459

53. Chen T, Li M, Liu J. π-π Stacking Interaction: A Nondestructive and Facile Means in Material Engineering for Bioapplications. Cryst Growth Des. 2018;18(5):2765–83.

54. McRee DE. Practical Protein Crystallography [Internet]. Second Edi. Practical Protein Crystallography. Elsevier; 1999. 266 p. Available from: https://linkinghub.elsevier.com/retrieve/pii/B9780124860520X50003

55. Morris GM, Huey R, Lindstrom W, Sanner MF, Belew RK, Goodsell DS, et al. AutoDock4 and AutoDockTools4: Automated Docking with Selective Receptor Flexibility. J Comput Chem. 2009;32:174–82.

56. Pettersen EF, Goddard TD, Huang CC, Couch GS, Greenblatt DM, Meng EC, et al. UCSF Chimera - A visualization system for exploratory research and analysis. J Comput Chem. 2004;25(13):1605–12.

57. Haldón E, Nicasio MC, Pérez PJ. Copper-catalysed azide-alkyne cycloadditions (CuAAC): An update. Org Biomol Chem. 2015;13(37):9528–50.

58. Hein JE, Fokin V V. ChemInform Abstract: Copper-Catalyzed Azide-Alkyne Cycloaddition (CuAAC) and Beyond: New Reactivity of Copper(I) Acetylides. ChemInform. 2010;41(28):no-no.

59. Zheng H, McDonald R, Hall DG. Boronic acid catalysis for mild and selective [3+2] dipolar cycloadditions to unsaturated carboxylic acids. Chem - A Eur J. 2010;16(18):5454–60.

60. Sibgatulin DA, Bezdudny A V., Mykhailiuk PK, Voievoda NM, Kondratov IS, Volochnyuk DM, et al. Novel synthetic approaches to (Trifluoromethyl)triazoles. Synthesis (Stuttg). 2010;(7).

61. Musilek K, Holas O, Kuca K, Jun D, Dohnal V, Dolezal M. Synthesis of a novel series of non-symmetrical bispyridinium compounds bearing a xylene linker and evaluation of their reactivation activity against tabun and paraoxon-inhibited acetylcholinesterase. J Enzyme Inhib Med Chem. 2007;22(4):425–32.

Appendices

A1. Conformational NMR Spectra

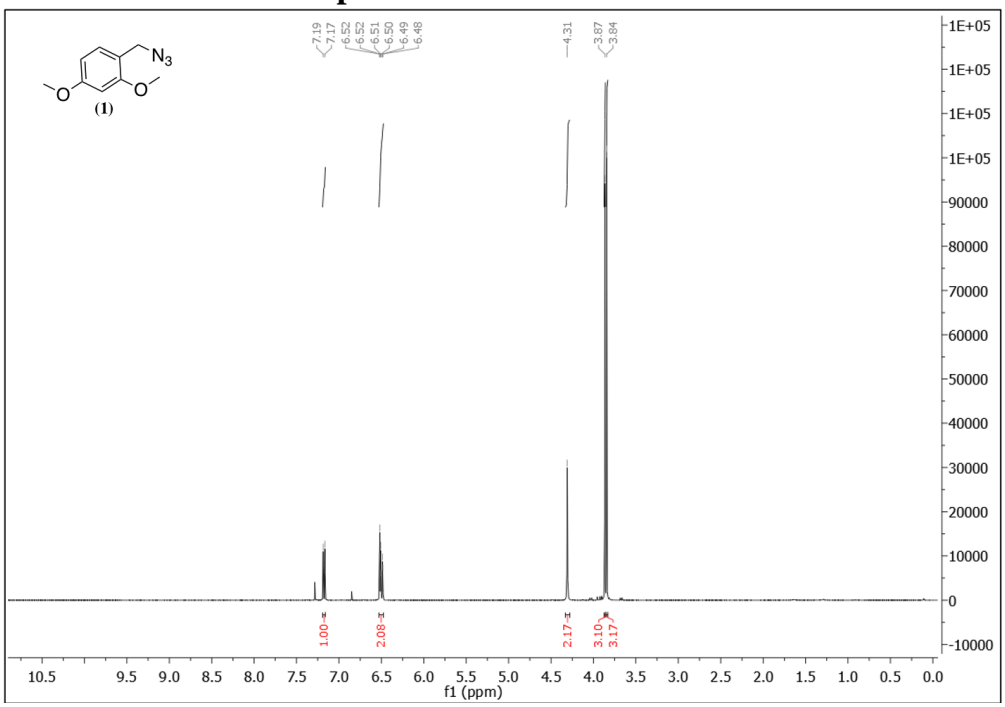

A1.1 ^{1}H NMR Spectrum of 1-(azidomethyl)-2,4-dimethoxybenzene – **(1)** in $CDCl_3$ at 400 MHz.

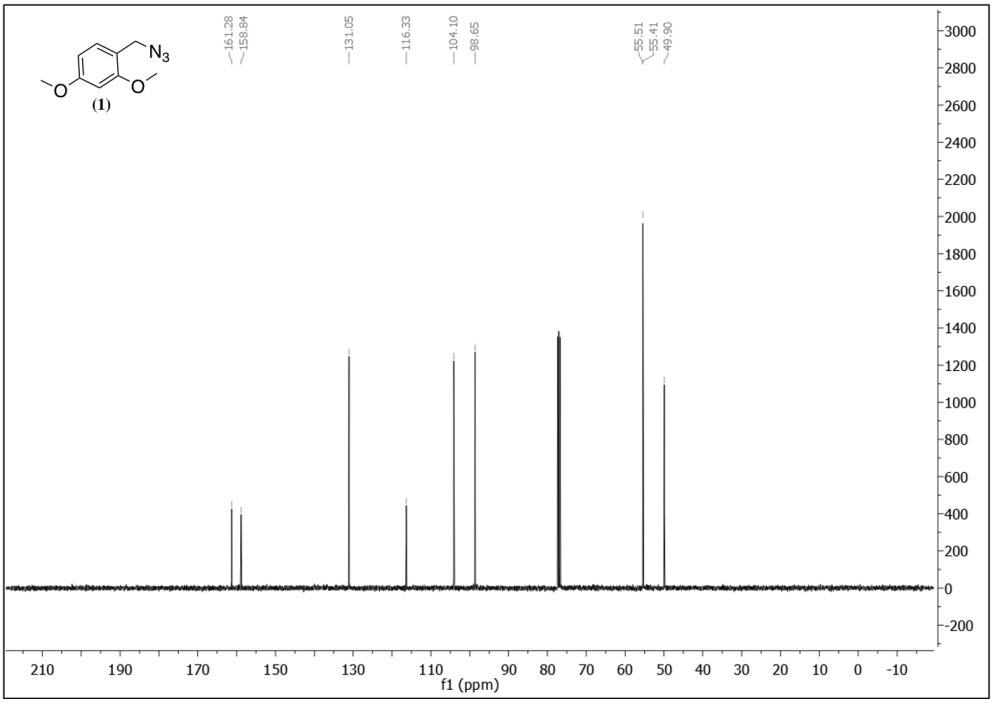

A1.2 ^{13}C NMR Spectrum of 1-(azidomethyl)-2,4-dimethoxybenzene – (1) in $CDCl_3$ at 101 MHz

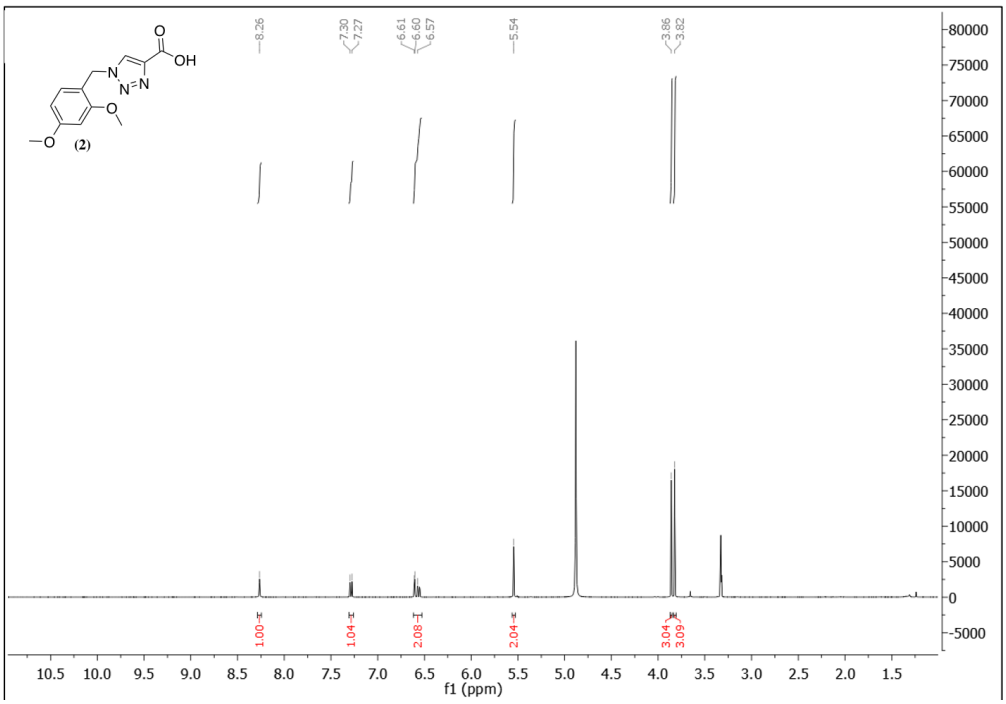

A1.3 [1]H NMR Spectrum of 1-(2,4-dimethoxybenzyl)-1*H*-1,2,3-triazole-5-carboxylic acid **– (2)** in MeOD at 400 MHz.

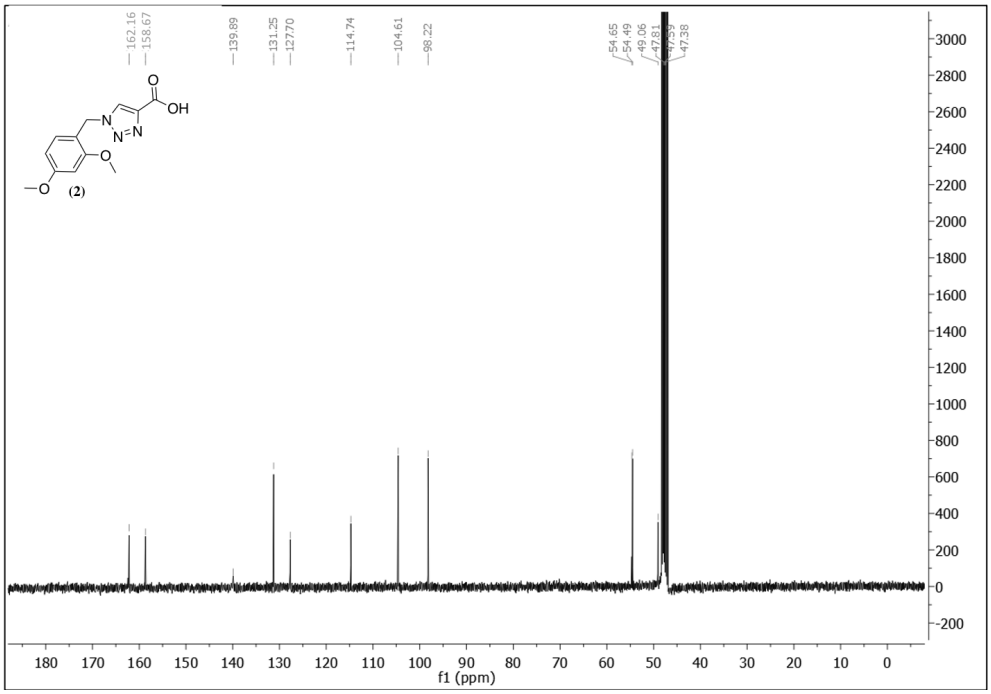

A1.4 [13]C NMR Spectrum of 1-(2,4-dimethoxybenzyl)-1*H*-1,2,3-triazole-5-carboxylic acid **– (2)** in MeOD at 101 MHz

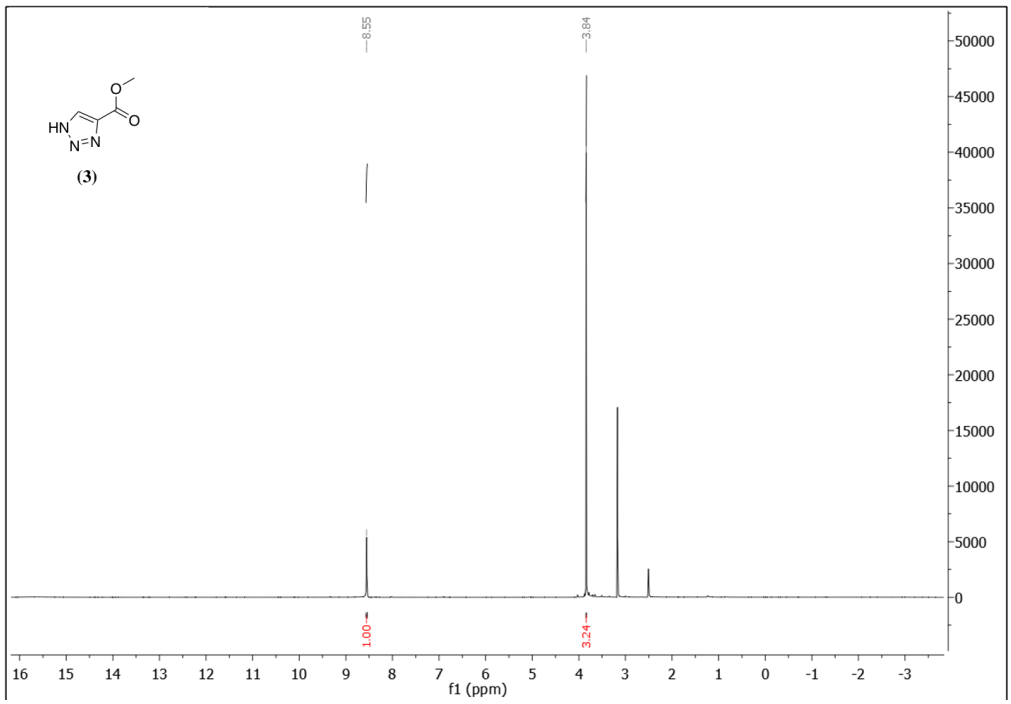

A1.5 ^{1}H NMR Spectrum of Methyl 1*H*-1,2,3-triazole-4-carboxylate **– (3)** in DMSO-d_6 at 400 MHz.

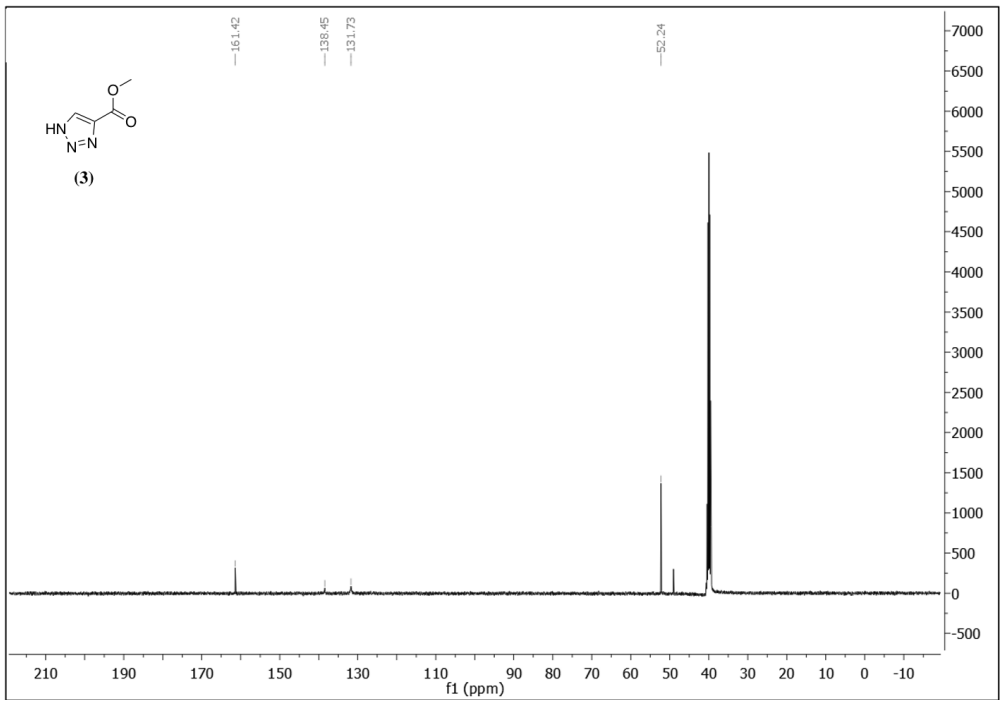

A1.6 ^{13}C NMR Spectrum of Methyl 1*H*-1,2,3-triazole-4-carboxylate **– (3)** in DMSO-d_6 at 101 MHz

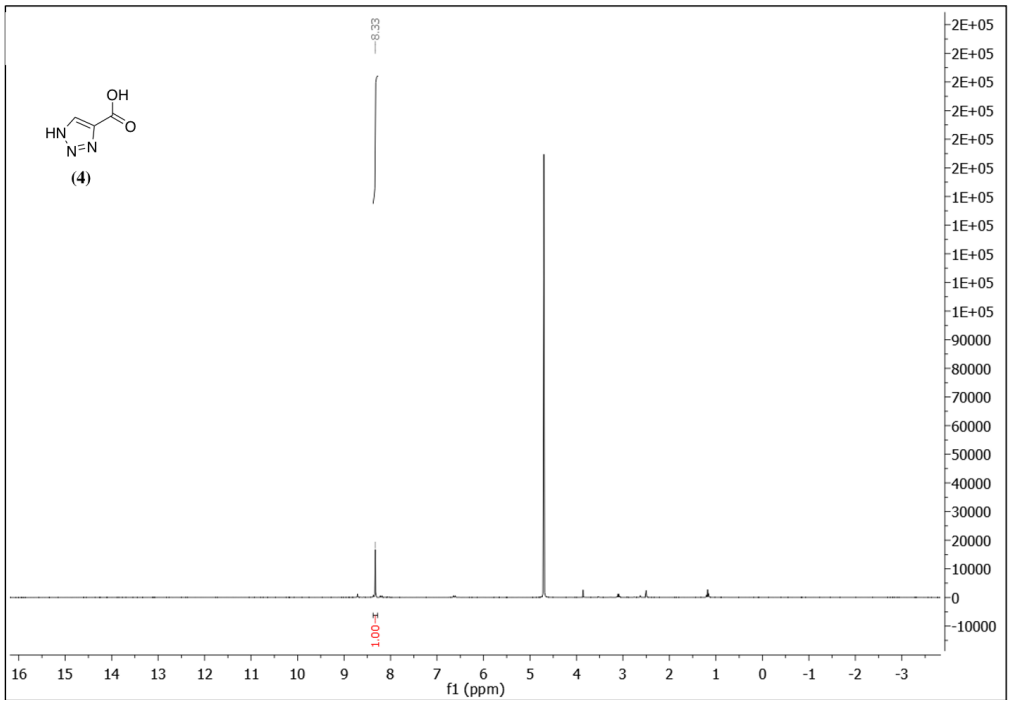

A1.7 ^{1}H NMR Spectrum of 1*H*-1,2,3-triazole-4-carboxylic acid **– (4)** in D_2O at 400 MHz.

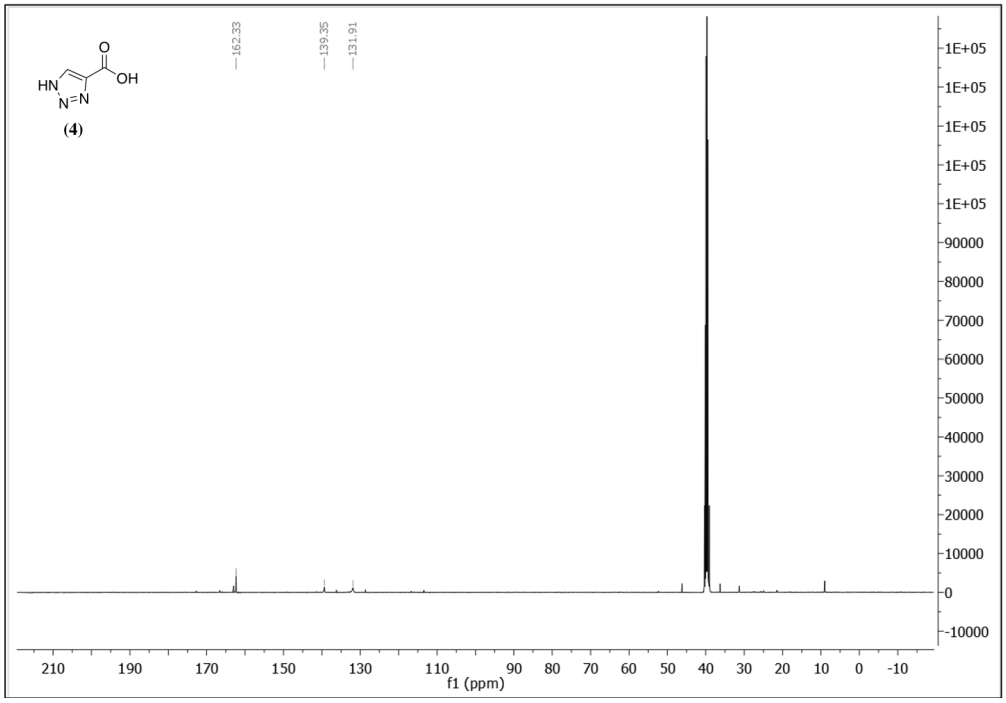

A1.8 ^{13}C NMR Spectrum of 1*H*-1,2,3-triazole-4-carboxylic acid **– (4)** in DMSO-d_6 at 101 MHz

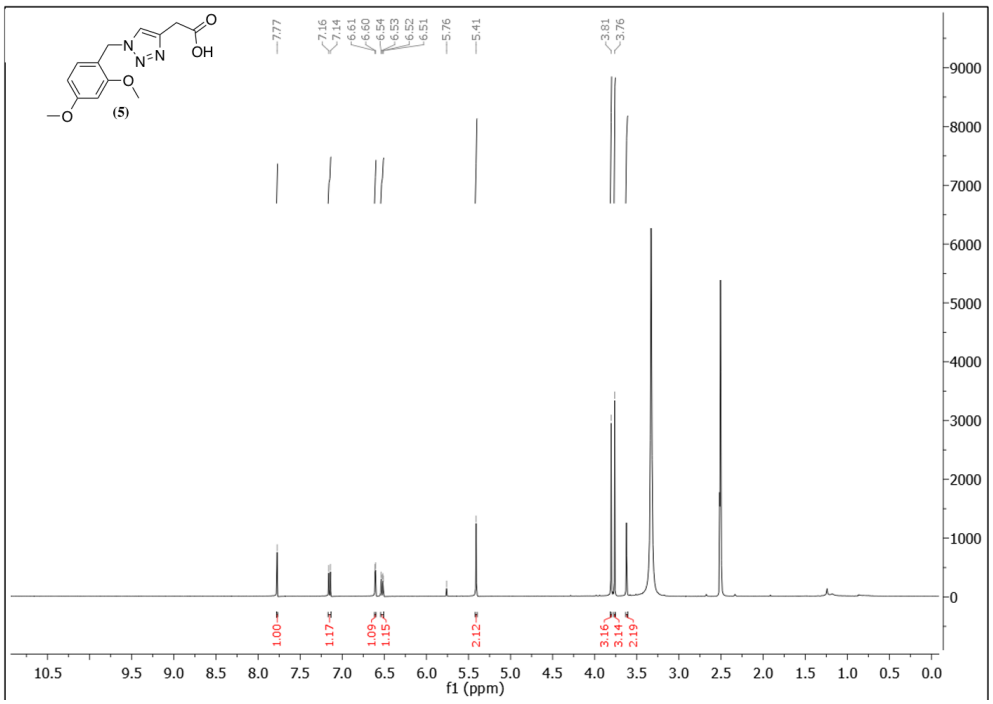

A1.9 [1]H NMR Spectrum of 2-(1-(2,4-dimethoxybenzyl)-1*H*-1,2,3-triazol-5-yl)acetic acid **– (5)** in DMSO-d_6 at 400 MHz.

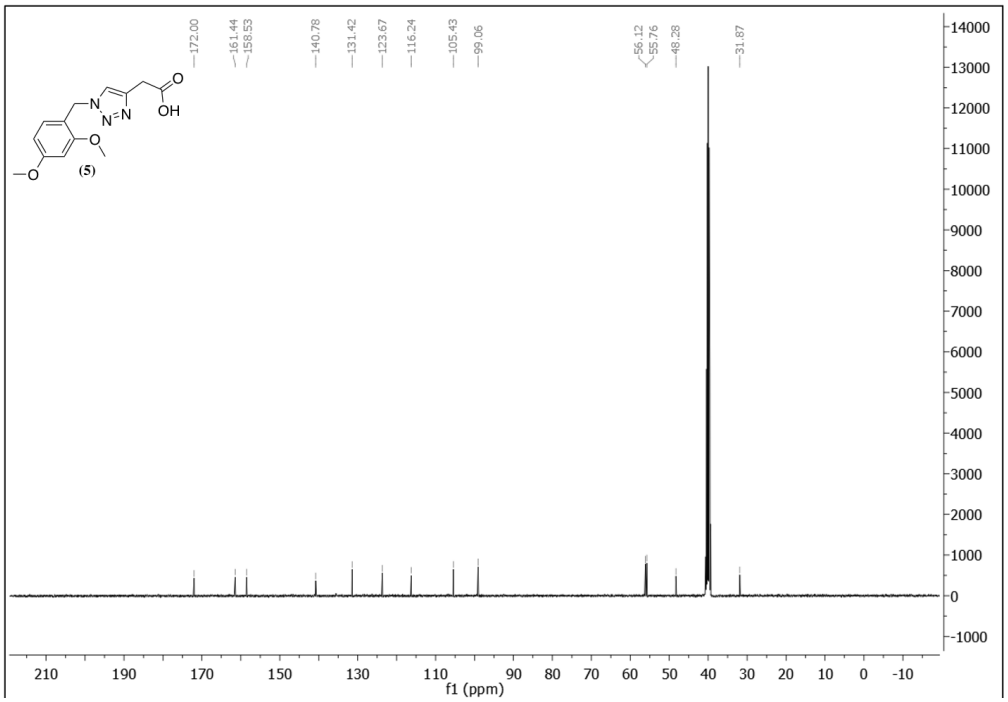

A1.10 [13]C NMR Spectrum of 2-(1-(2,4-dimethoxybenzyl)-1*H*-1,2,3-triazol-5-yl)acetic acid **– (5)** in DMSO-d_6 at 101 MHz

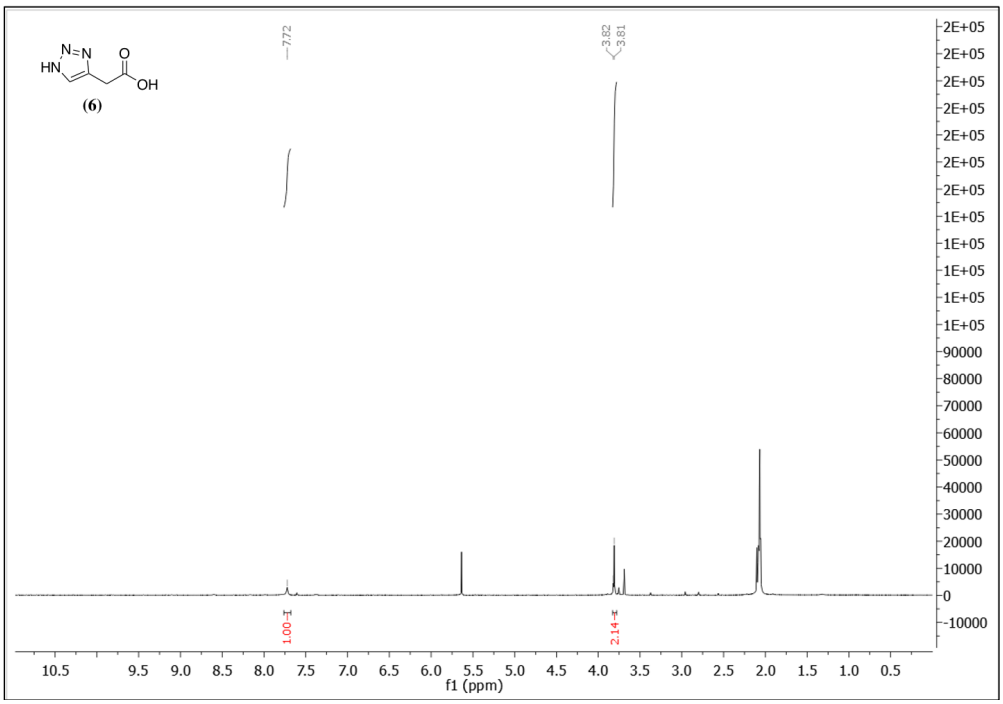

A1.11 [1]H NMR Spectrum of 2-(1*H*-1,2,3-triazol-4-yl)acetic acid **– (6)** in Acetone-d at 400 MHz.

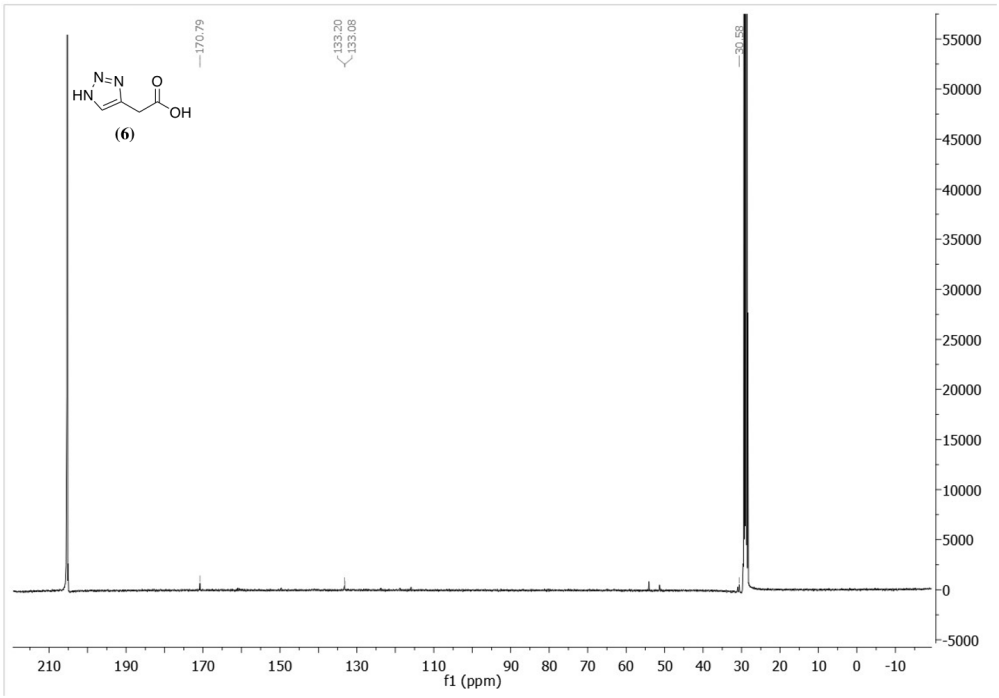

A1.12 [13]C NMR Spectrum of 2-(1*H*-1,2,3-triazol-4-yl)acetic acid **– (6)** in Acetone-d at 101 MHz

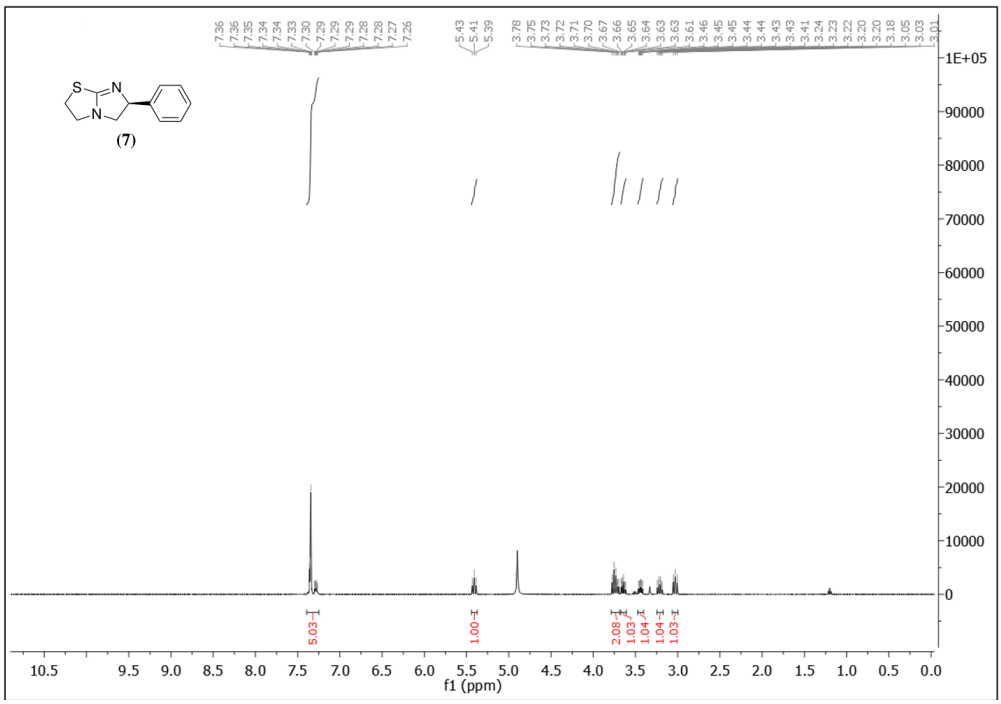

A1.13 [1]H NMR Spectrum of ((S)-6-phenyl-2,3,5,6-tetrahydroimidazo[2,1-b]thiazole) – **(7)** in MeOD at 400 MHz.

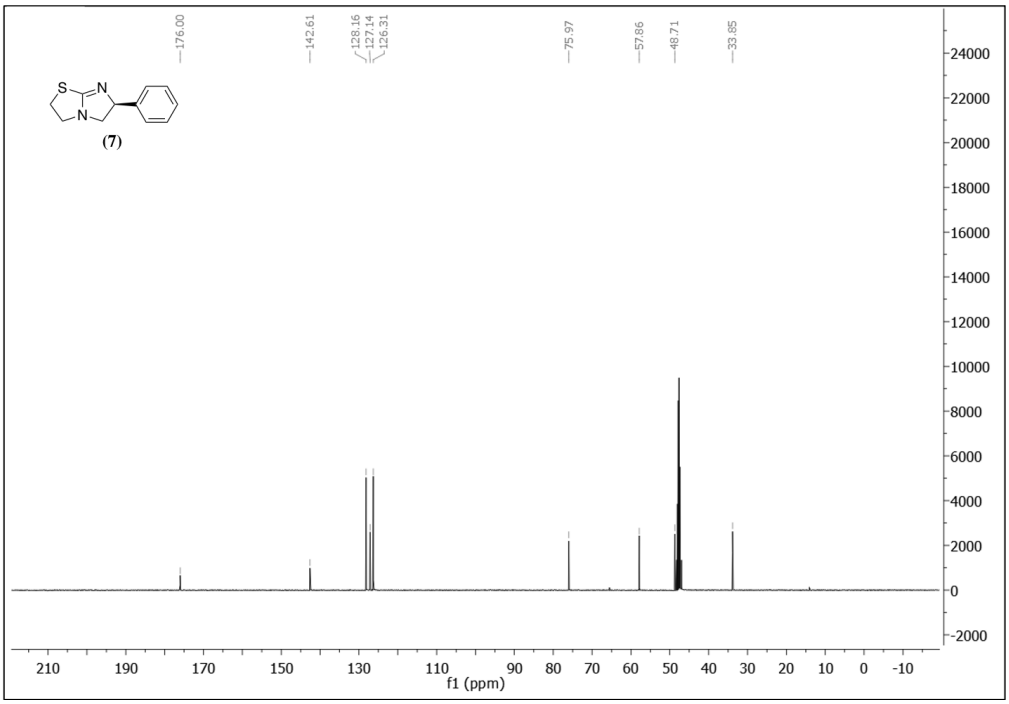

A1.14 [13]C NMR Spectrum of ((S)-6-phenyl-2,3,5,6-tetrahydroimidazo[2,1-b]thiazole) – **(7)** in MeOD at 101 MHz

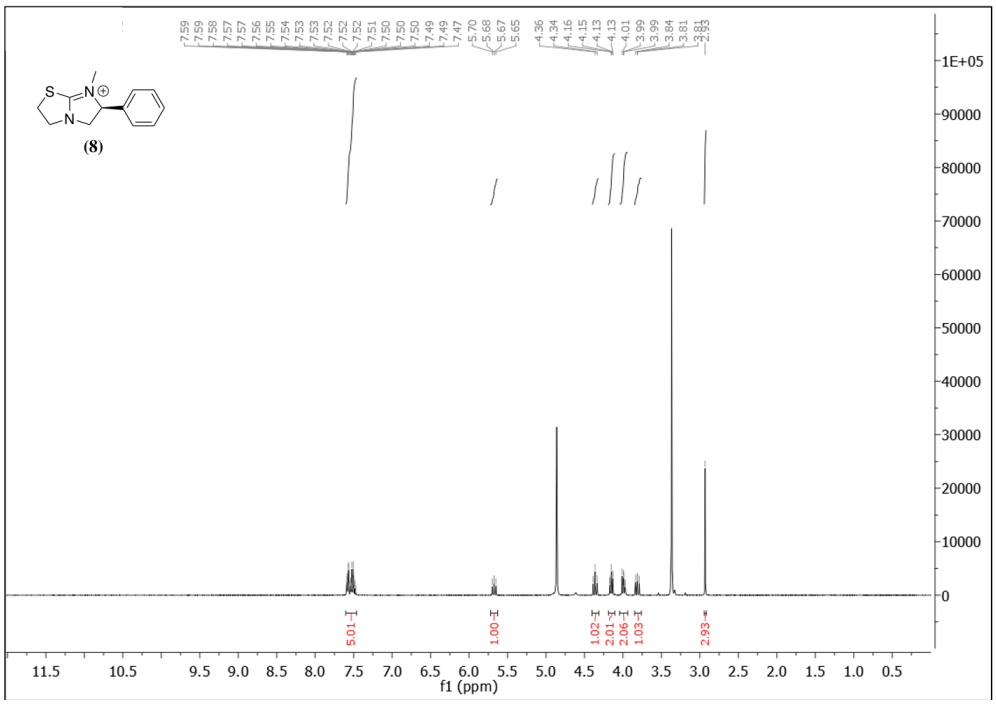

A1.15 [1]H NMR Spectrum of (S)-7-methyl-6-phenyl-2,3,5,6-tetrahydroimidazo[2,1-b]thiazol-7-ium- **(8)** in MeOD at 400 MHz.

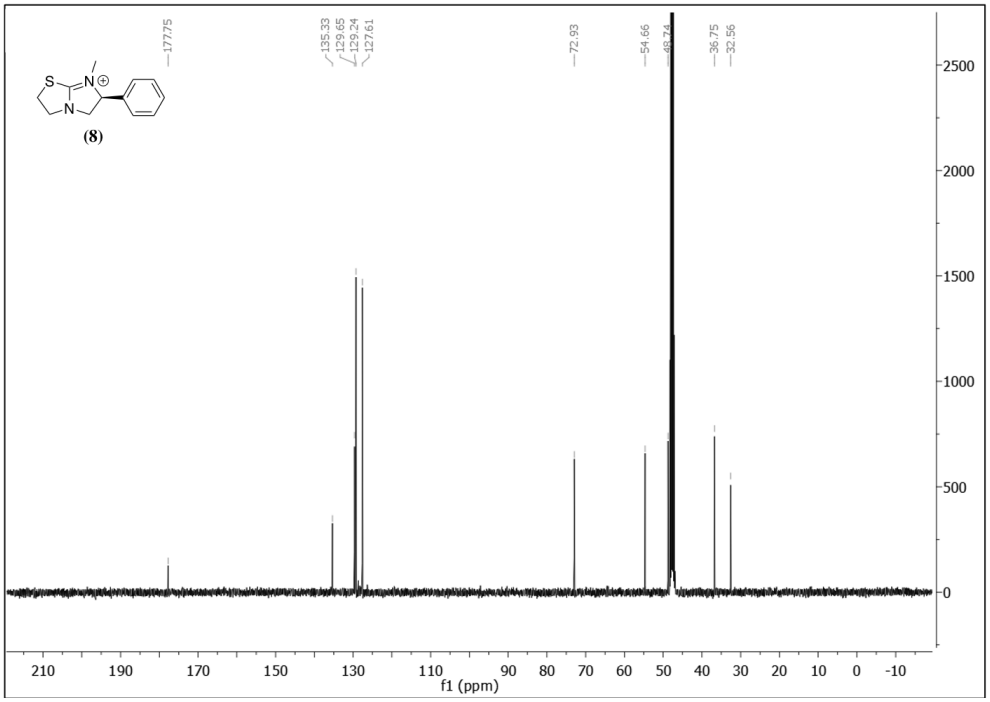

A1.16 [13]C NMR Spectrum of (S)-7-methyl-6-phenyl-2,3,5,6-tetrahydroimidazo[2,1-b]thiazol-7-ium- **(8)** in MeOD at 101 MHz

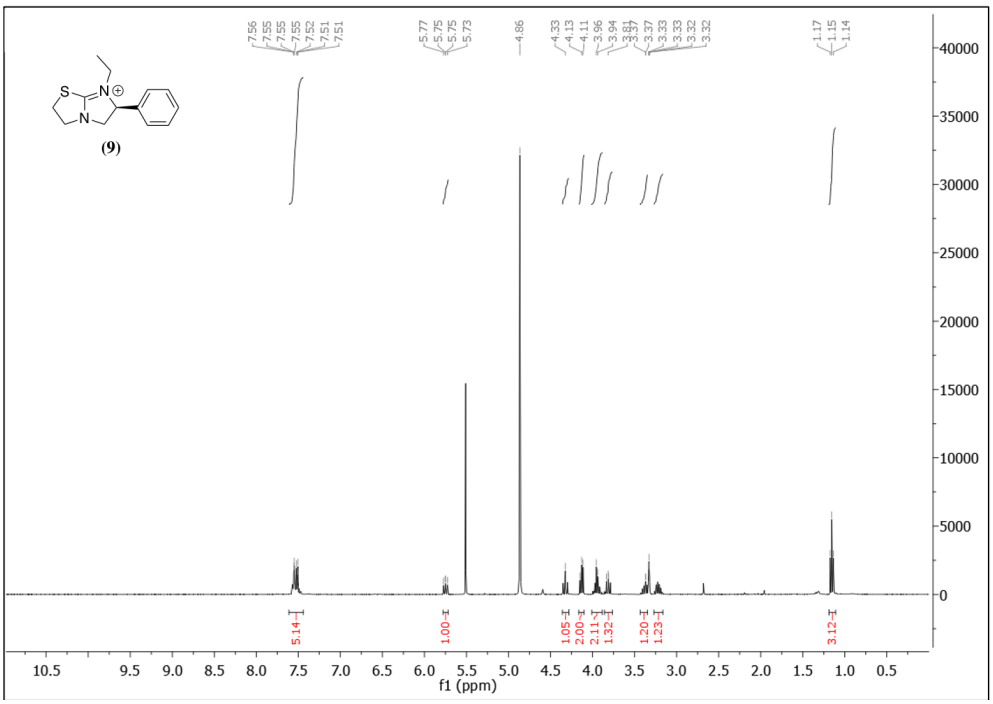

A1.17 ^{1}H NMR Spectrum of (*S*)-7-ethyl-6-phenyl-2,3,5,6-tetrahydroimidazo[2,1-*b*]thiazol-7-ium – **(9)** in MeOD at 400 MHz.

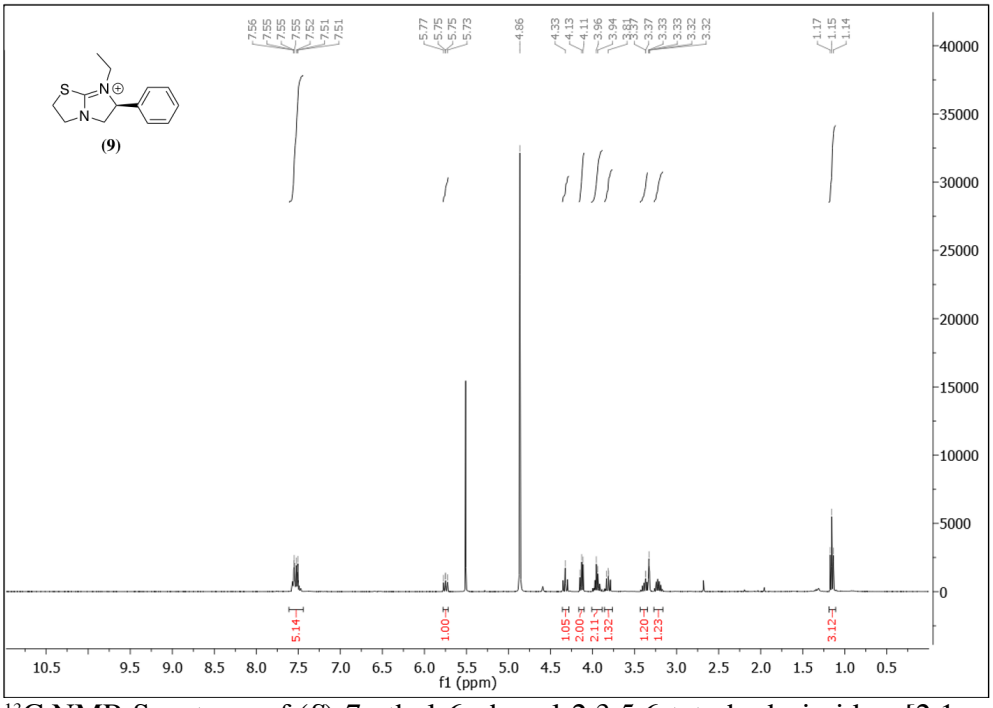

A1.18 ^{13}C NMR Spectrum of (*S*)-7-ethyl-6-phenyl-2,3,5,6-tetrahydroimidazo[2,1-*b*]thiazol-7-ium – **(9)** in MeOD at 101 MHz

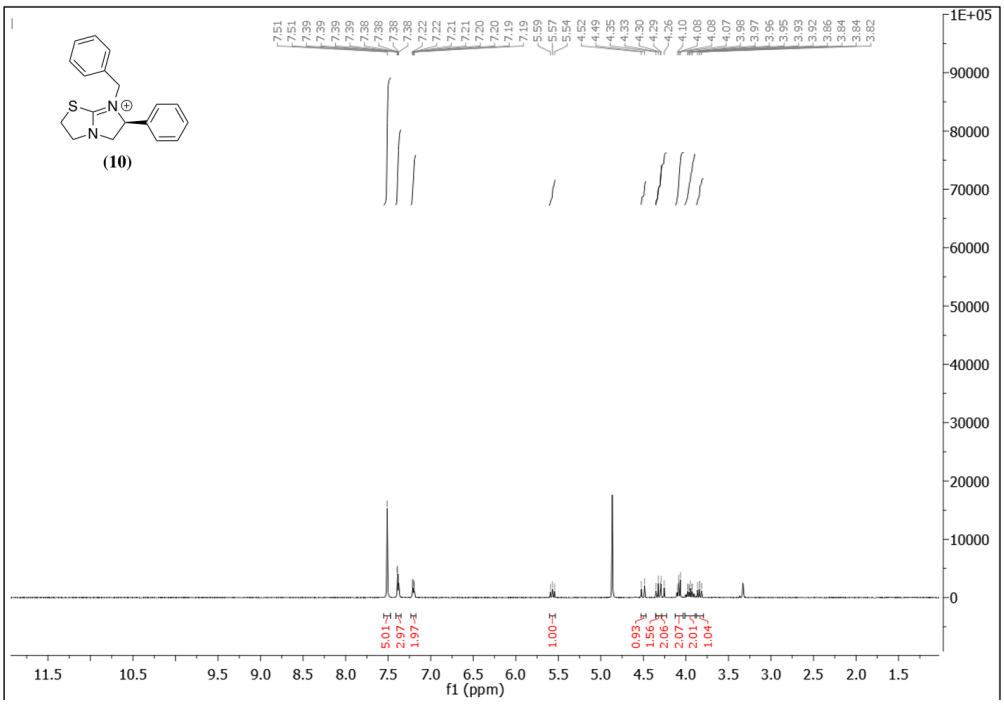

A1.19 [1]H NMR Spectrum of (*S*)-7-benzyl-6-phenyl-2,3,5,6-tetrahydroimidazo[2,1-*b*]thiazol-7-ium- **(10)** in MeOD at 400 MHz.

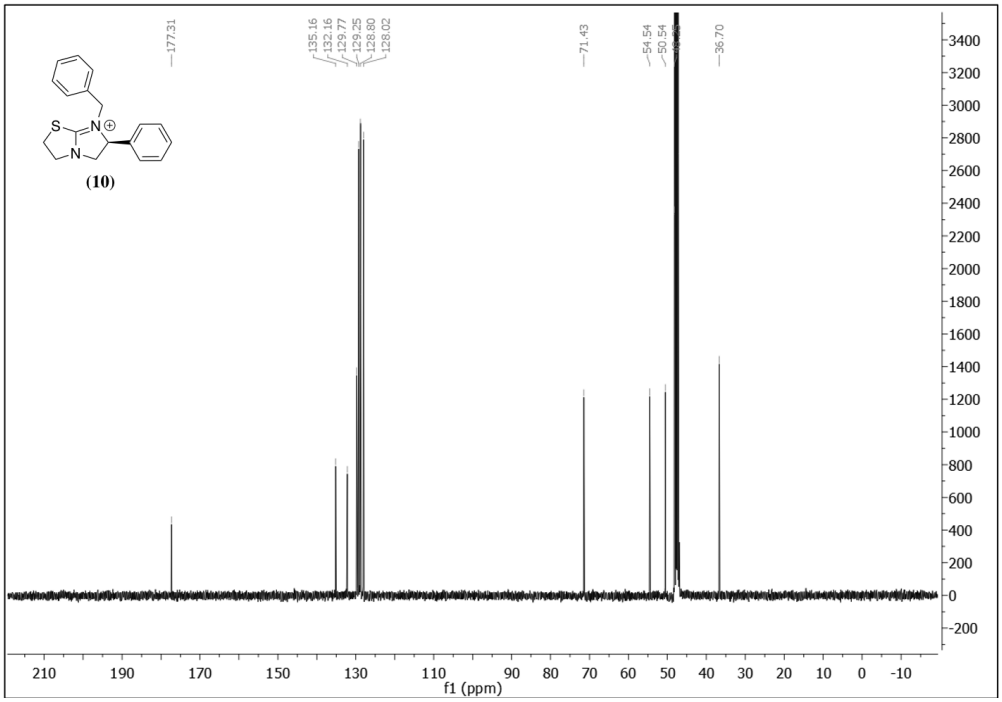

A1.20 [13]C NMR Spectrum of (*S*)-7-benzyl-6-phenyl-2,3,5,6-tetrahydroimidazo[2,1-*b*]thiazol-7-ium- **(10)** in MeOD at 101 MHz

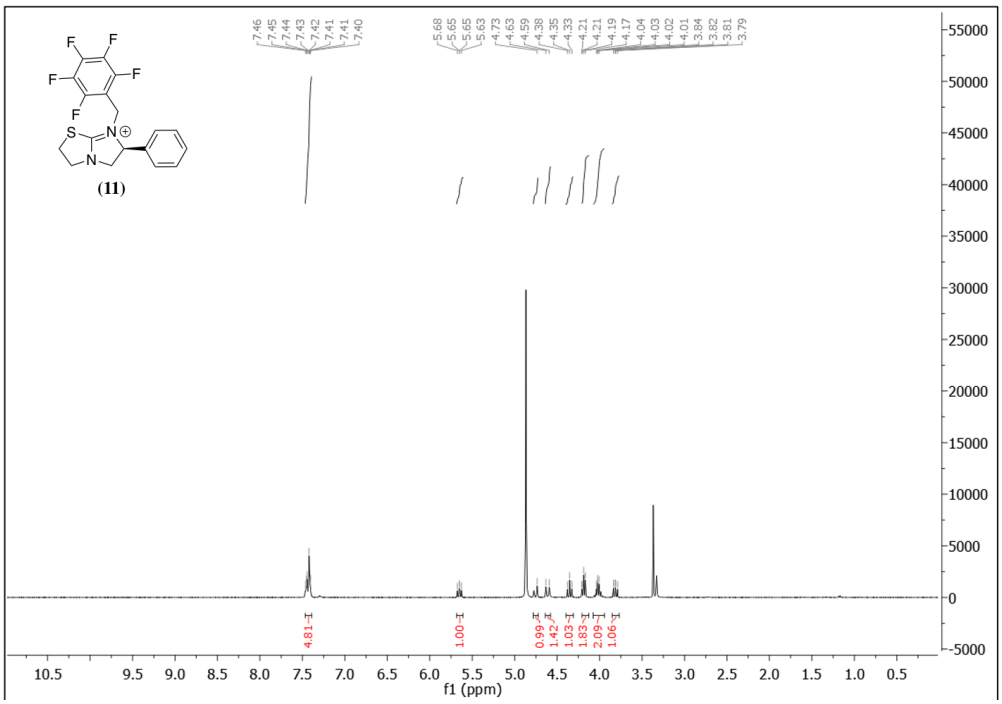

A1.21 [1]H NMR Spectrum of (*S*)-7-((perfluorophenyl)methyl)-6-phenyl-2,3,5,6-tetrahydroimidazo[2,1-*b*]thiazol-7-ium – **(11)** in MeOD at 400 MHz.

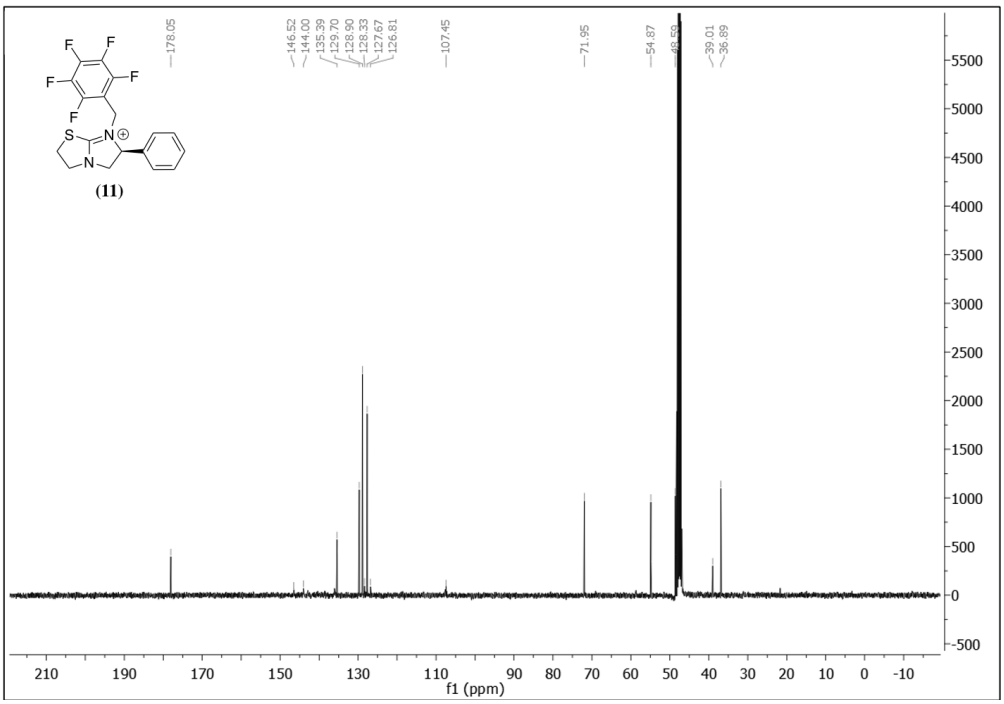

A1.22 [13]C NMR Spectrum of (*S*)-7-((perfluorophenyl)methyl)-6-phenyl-2,3,5,6-tetrahydroimidazo[2,1-*b*]thiazol-7-ium – **(11)** in MeOD at 101 MHz

Confidential and Proprietary Information

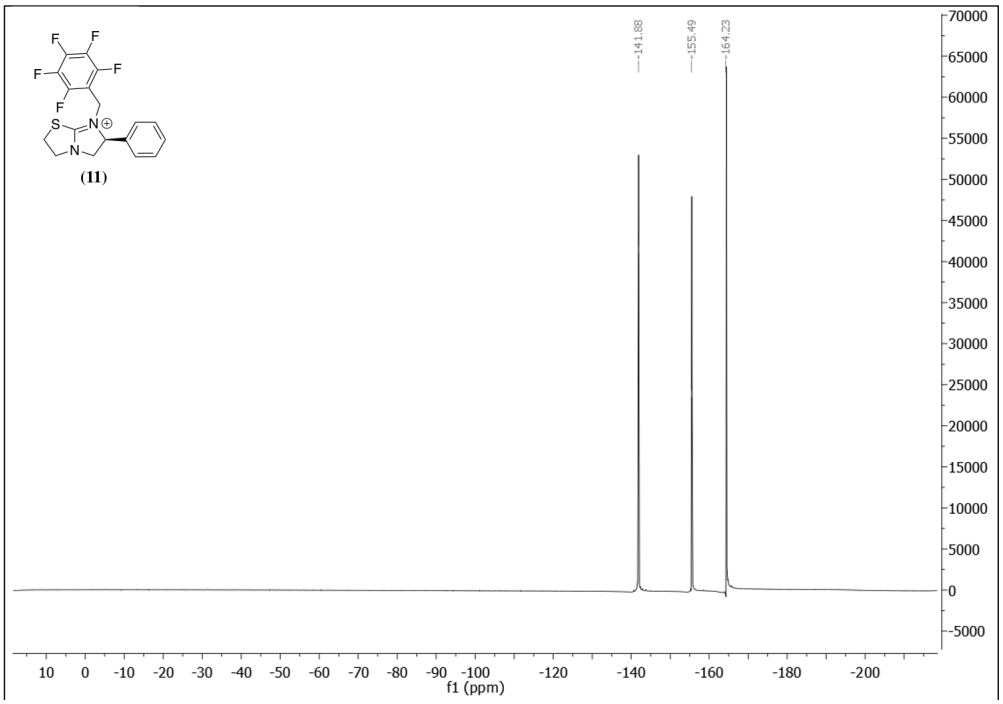

A1.23 ^{19}F NMR Spectrum of (*S*)-7-((perfluorophenyl)methyl)-6-phenyl-2,3,5,6-tetrahydroimidazo[2,1-*b*]thiazol-7-ium – **(11)** in MeOD at 377 MHz.

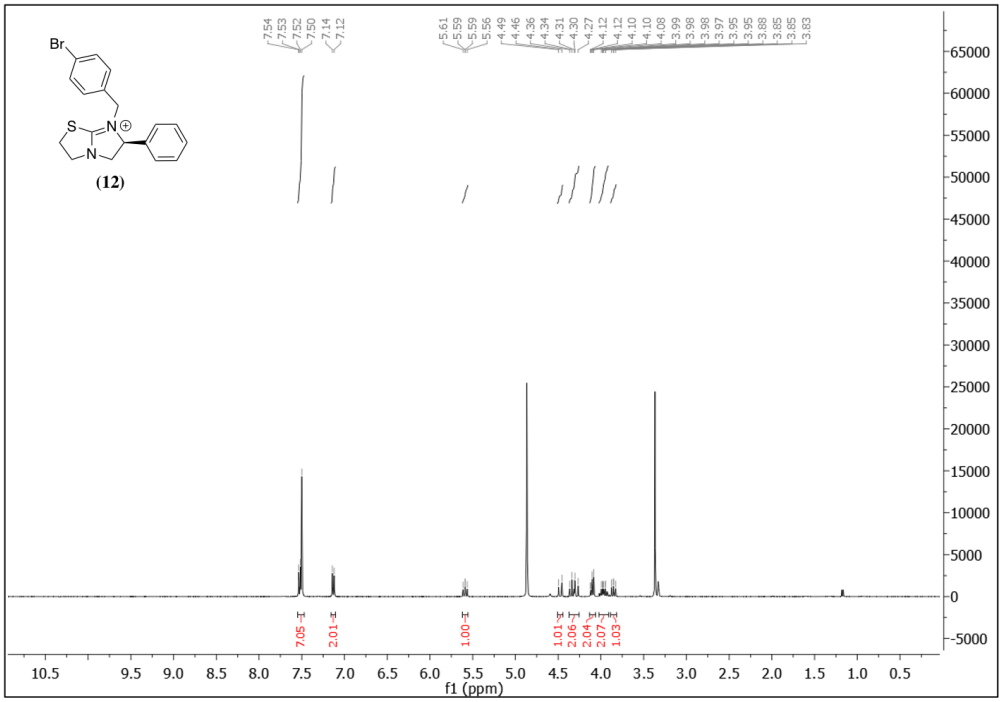

A1.24 ^{1}H NMR Spectrum of (*S*)-7-(4-bromobenzyl)-6-phenyl-2,3,5,6-tetrahydroimidazo[2,1-*b*]thiazol-7-ium – **(12)** in MeOD at 400 MHz.

Confidential and Proprietary Information

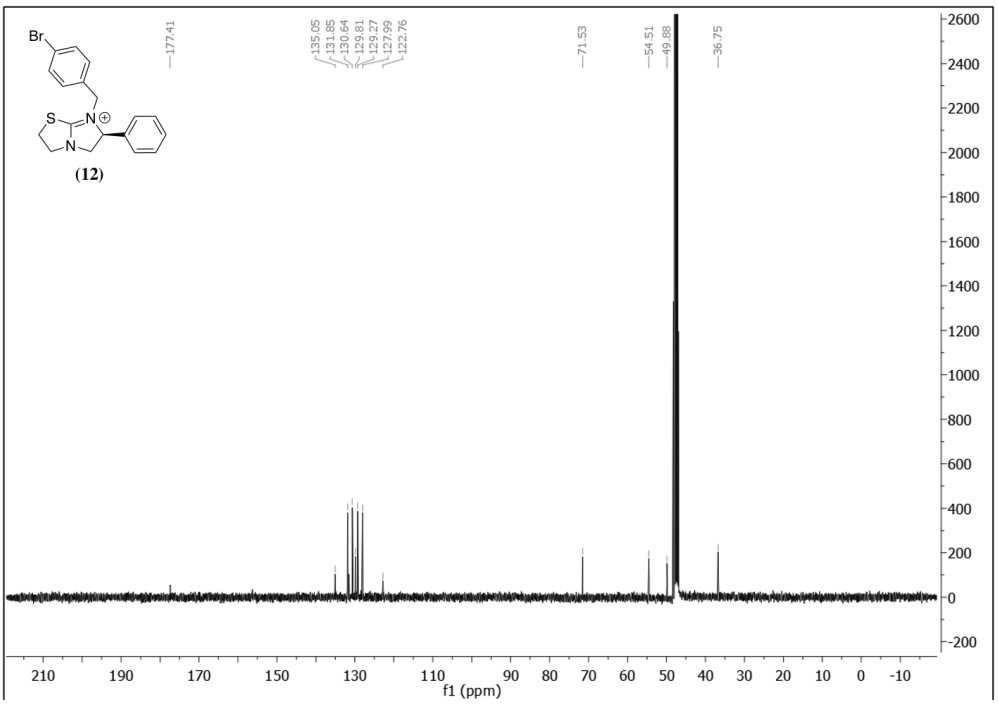

A1.25 ^{13}C NMR Spectrum of (*S*)-7-(4-bromobenzyl)-6-phenyl-2,3,5,6-tetrahydroimidazo[2,1-*b*]thiazol-7-ium – **(12) 3** in MeOD at 101 MHz

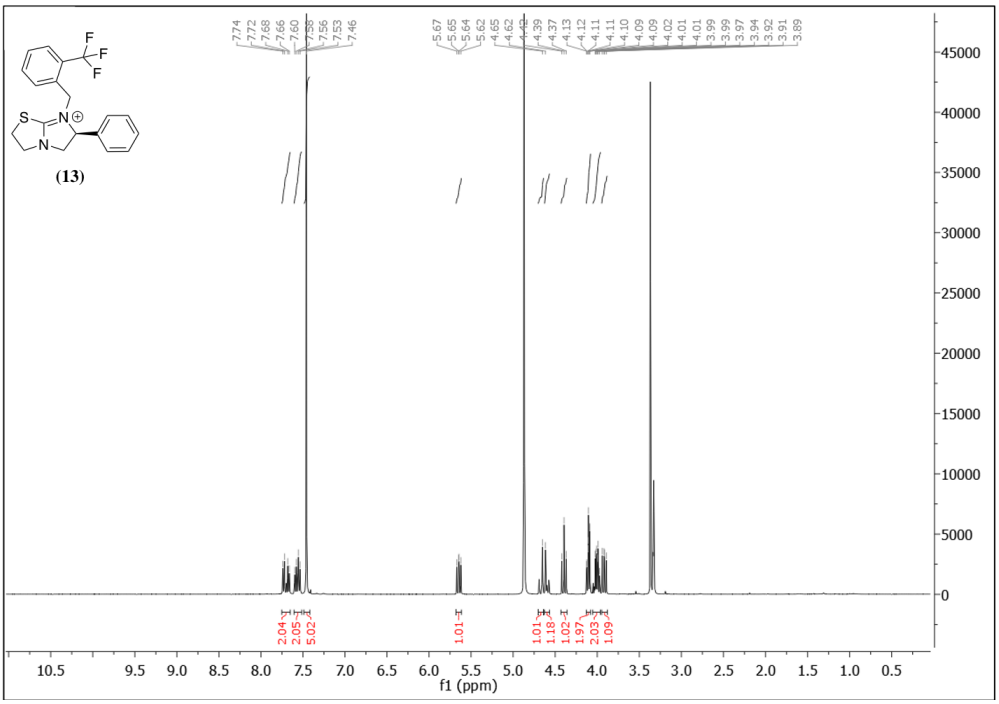

A1.26 ^{1}H NMR Spectrum of (*S*)-6-phenyl-7-(2-(trifluoromethyl)benzyl)-2,3,5,6-tetrahydroimidazo[2,1-*b*]thiazol-7-ium – **(13)** in MeOD at 400 MHz.

Confidential and Proprietary Information

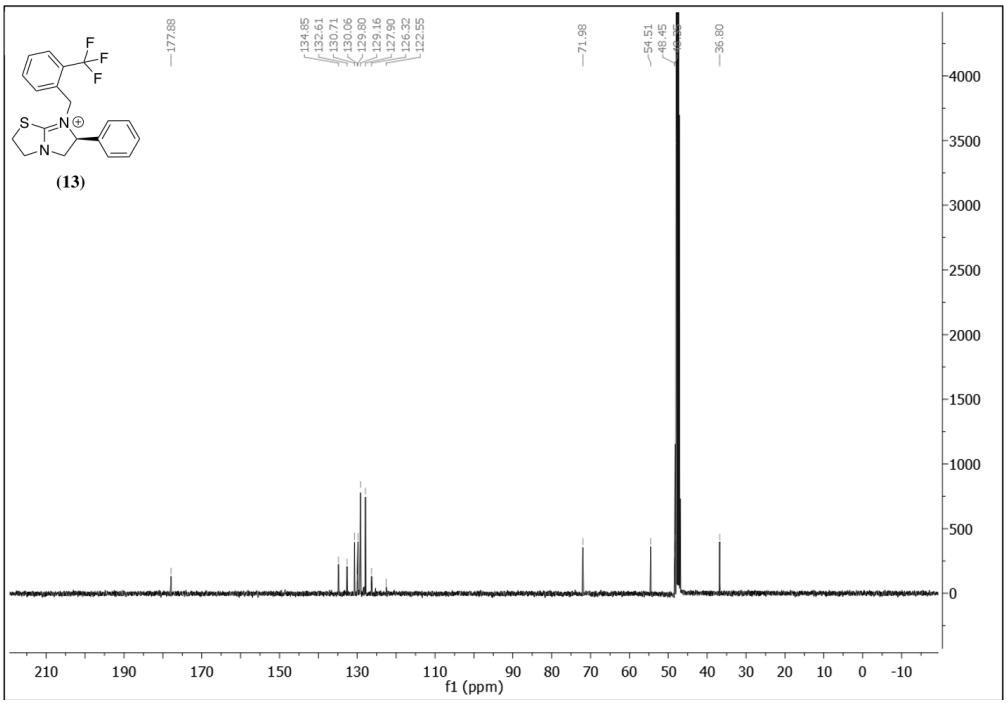

A1.27 ^{13}C NMR Spectrum of (*S*)-6-phenyl-7-(2-(trifluoromethyl)benzyl)-2,3,5,6-tetrahydroimidazo[2,1-*b*]thiazol-7-ium – **(13)** in MeOD at 101 MHz

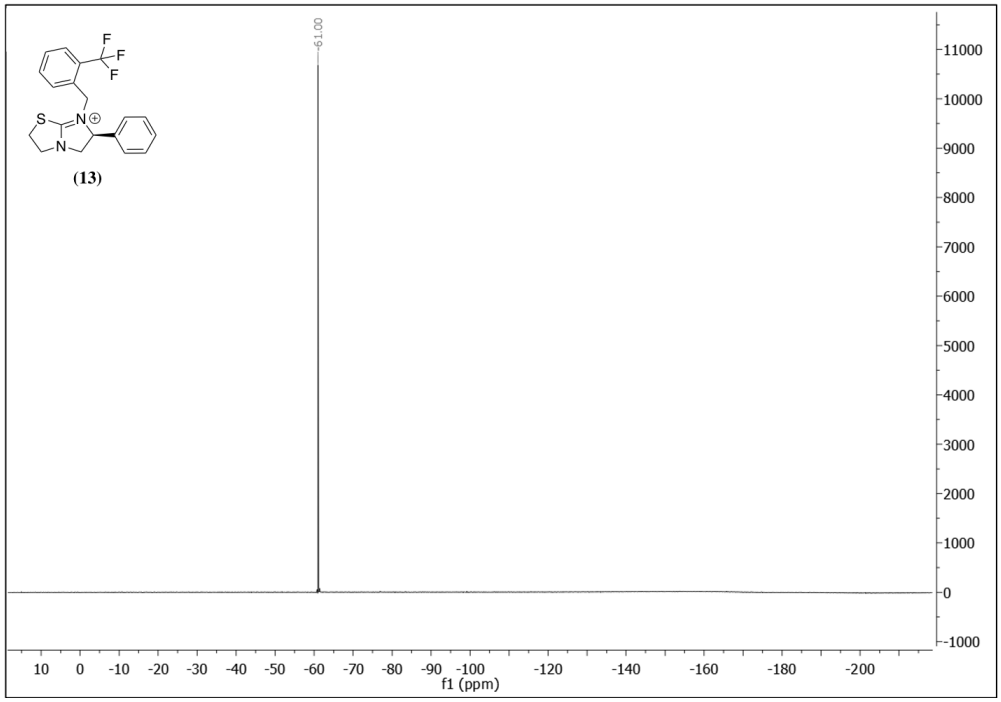

A1.28 ^{19}F NMR Spectrum of (*S*)-6-phenyl-7-(2-(trifluoromethyl)benzyl)-2,3,5,6-tetrahydroimidazo[2,1-*b*]thiazol-7-ium – **(13)** in MeOD at 377 MHz.

Confidential and Proprietary Information

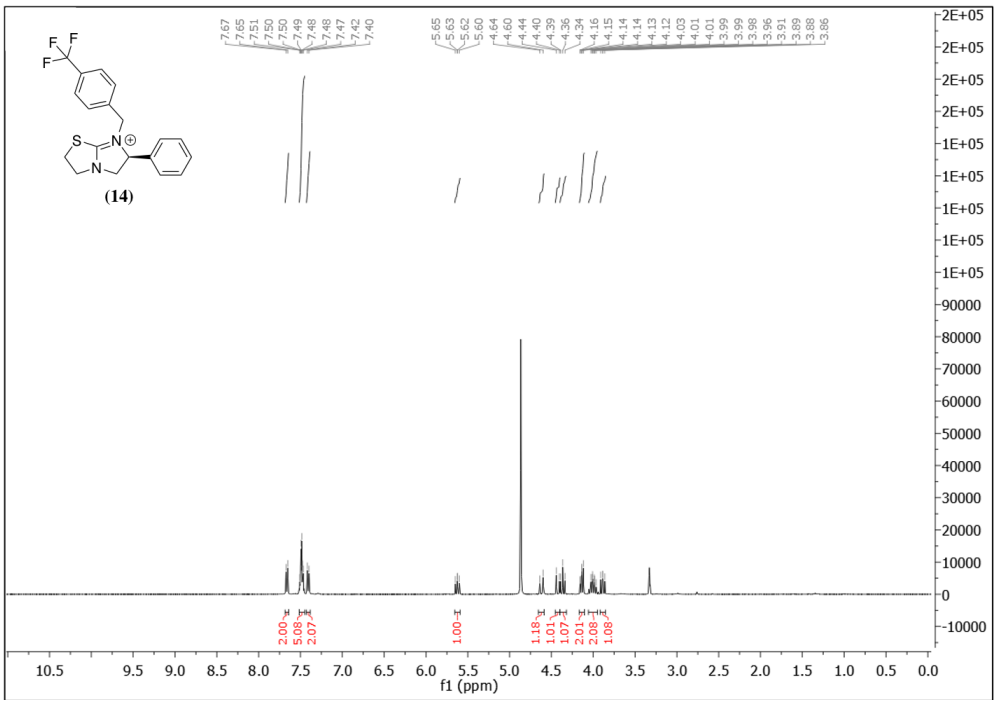

A1.29 [1]H NMR Spectrum of (*S*)-6-phenyl-7-(4-(trifluoromethyl)benzyl)-2,3,5,6-tetrahydroimidazo[2,1-*b*]thiazol-7-ium – **(14)** in MeOD at 400 MHz.

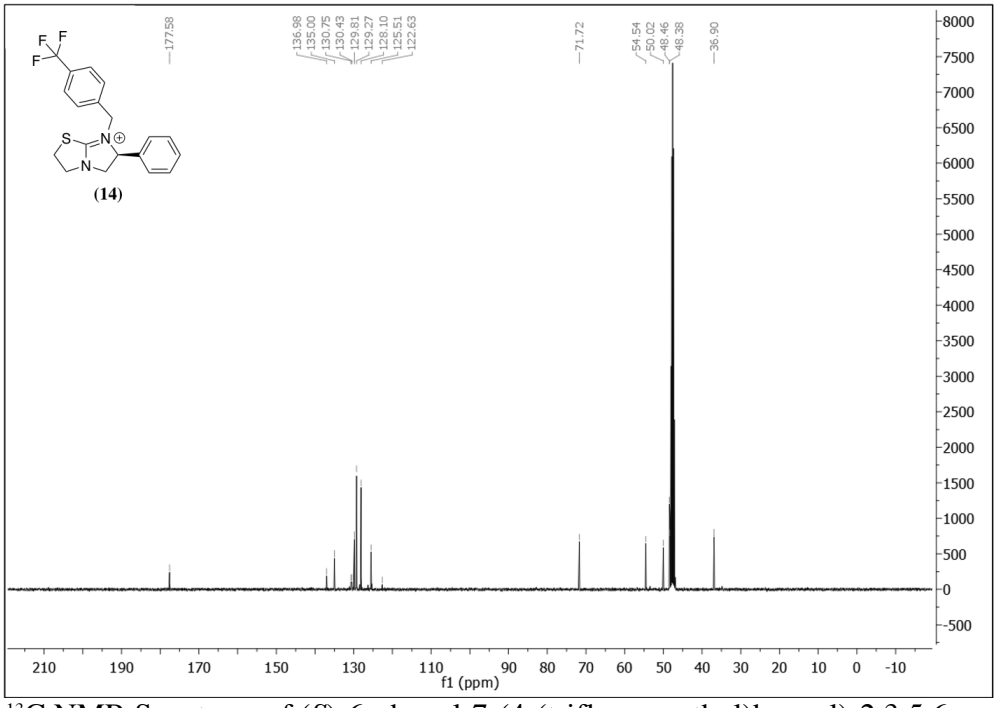

A1.30 [13]C NMR Spectrum of (*S*)-6-phenyl-7-(4-(trifluoromethyl)benzyl)-2,3,5,6-tetrahydroimidazo[2,1-*b*]thiazol-7-ium – **(14)** in MeOD at 101 MHz

Confidential and Proprietary Information

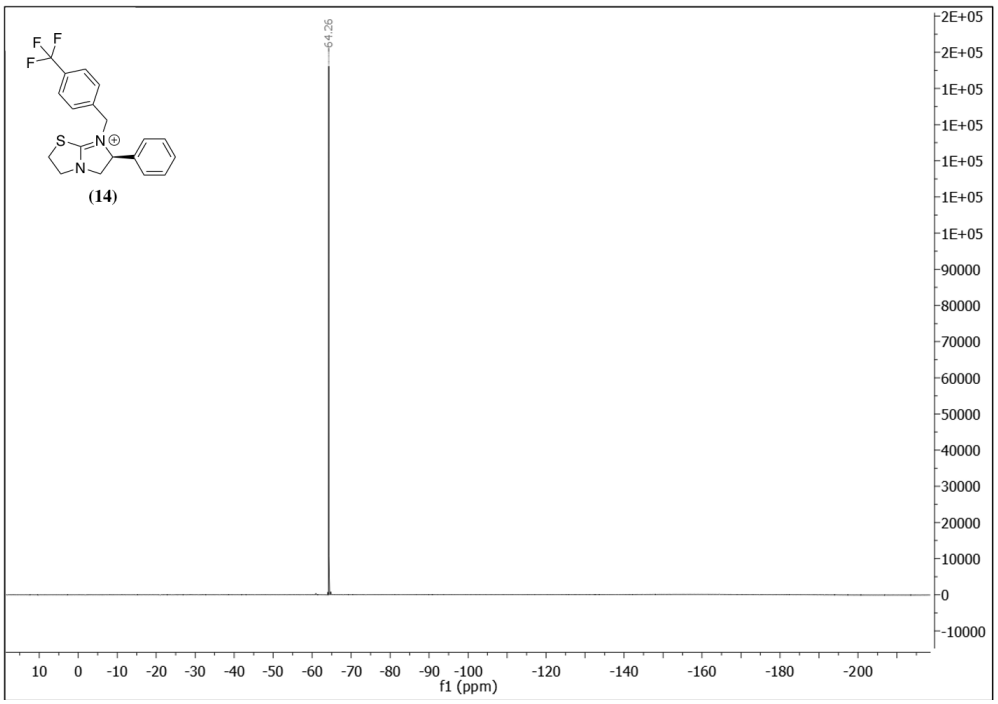

A1.31 [19]F NMR Spectrum of (*S*)-6-phenyl-7-(4-(trifluoromethyl)benzyl)-2,3,5,6-tetrahydroimidazo[2,1-*b*]thiazol-7-ium – **(14)** in MeOD at 377 MHz.

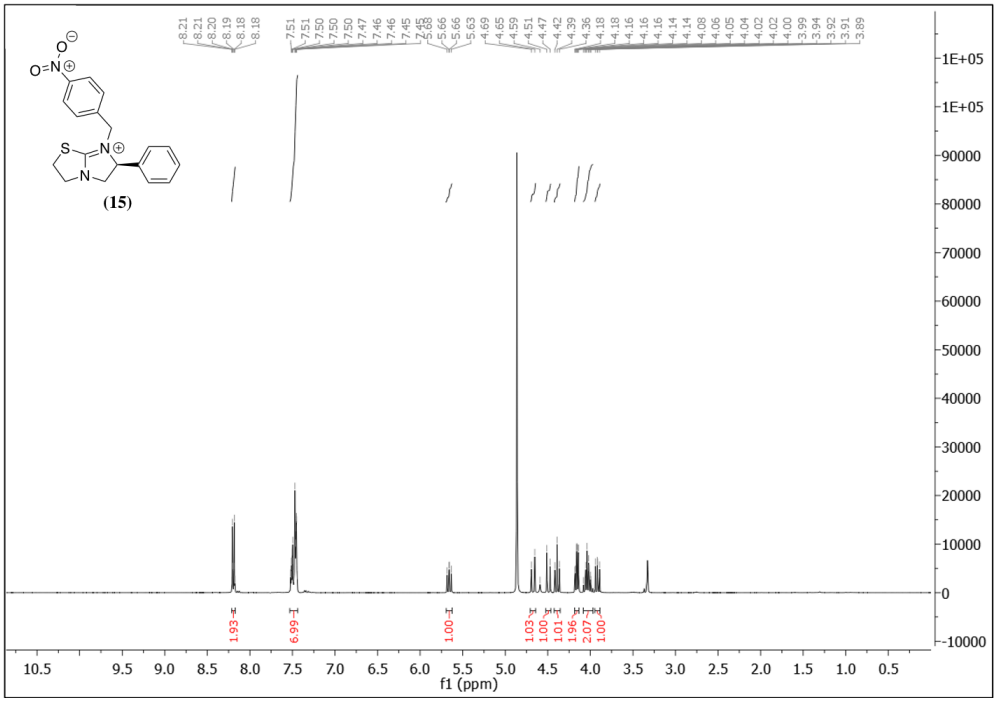

A1.32 [1]H NMR Spectrum of (*S*)-7-(4-nitrobenzyl)-6-phenyl-2,3,5,6-tetrahydroimidazo[2,1-*b*]thiazol-7-ium – **(15)** in MeOD at 400 MHz.

Confidential and Proprietary Information

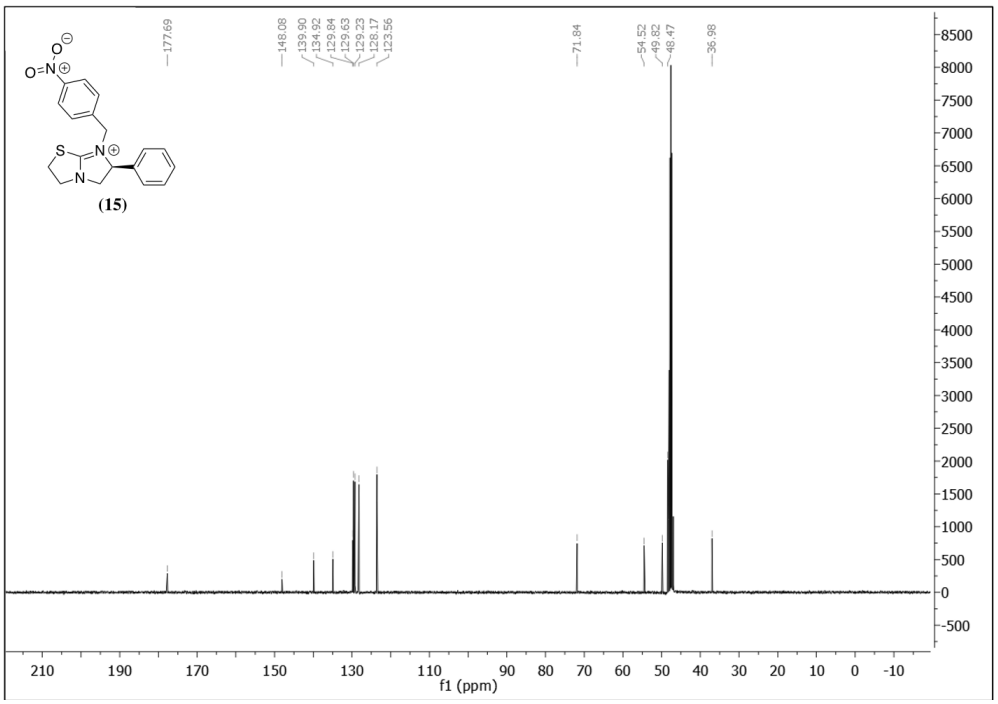

A1.33 ^{13}C NMR Spectrum of (*S*)-7-(4-nitrobenzyl)-6-phenyl-2,3,5,6-tetrahydroimidazo[2,1-*b*]thiazol-7-ium – **(15)** in MeOD at 101 MHz

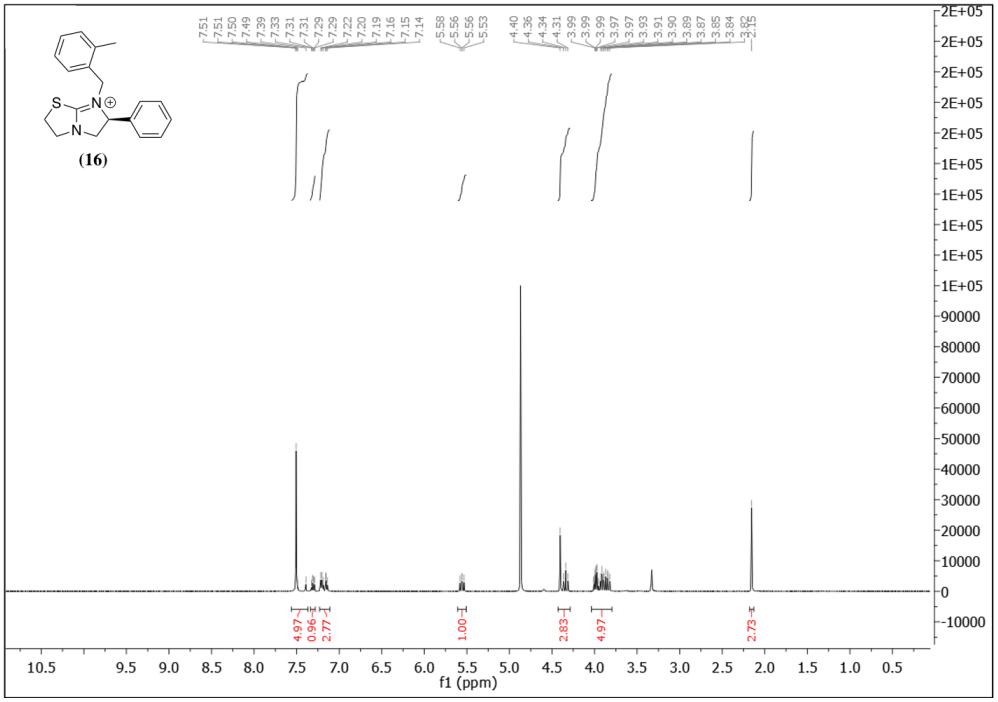

A1.34 ^{1}H NMR Spectrum of (*S*)-7-(2-methylbenzyl)-6-phenyl-2,3,5,6-tetrahydroimidazo[2,1-*b*]thiazol-7-ium – **(16)** in MeOD at 400 MHz.

Confidential and Proprietary Information

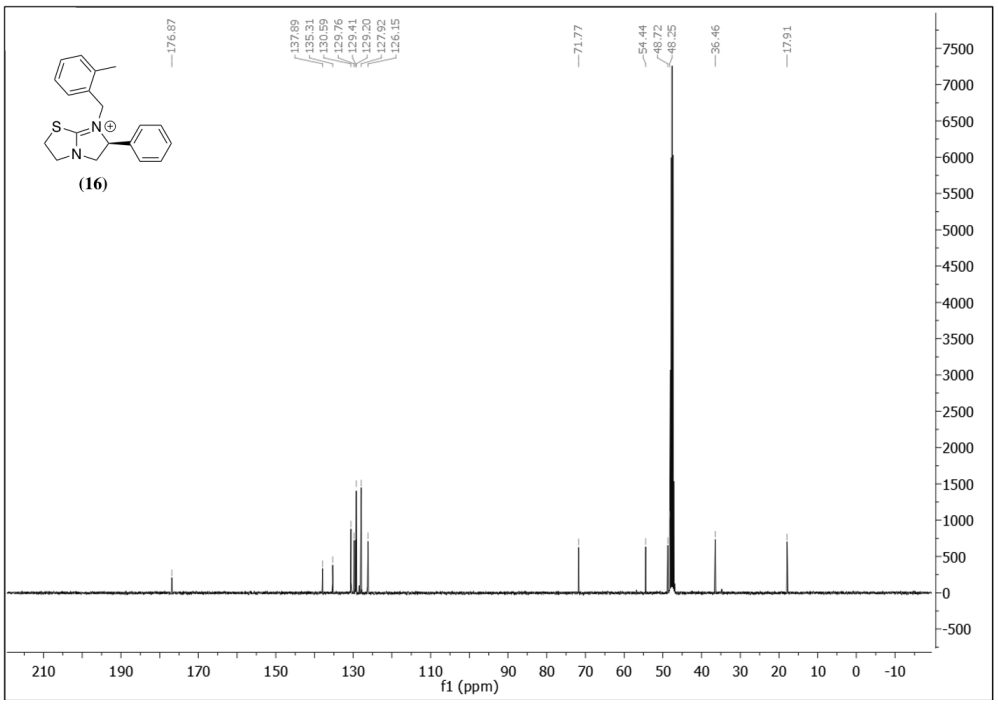

A1.35 ^{13}C NMR Spectrum of (*S*)-7-(2-methylbenzyl)-6-phenyl-2,3,5,6-tetrahydroimidazo[2,1-*b*]thiazol-7-ium – **(16)** in MeOD at 101 MHz

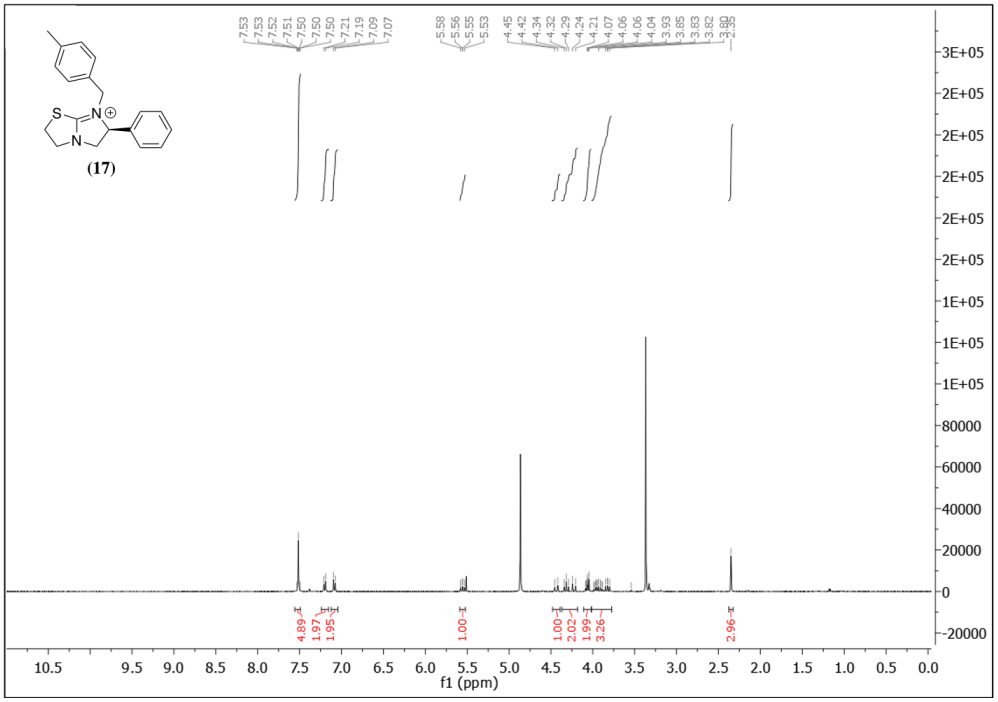

A1.36 ^{1}H NMR Spectrum of (*S*)-7-(4-methylbenzyl)-6-phenyl-2,3,5,6-tetrahydroimidazo[2,1-*b*]thiazol-7-ium – **(17)** in MeOD at 400 MHz.

Confidential and Proprietary Information

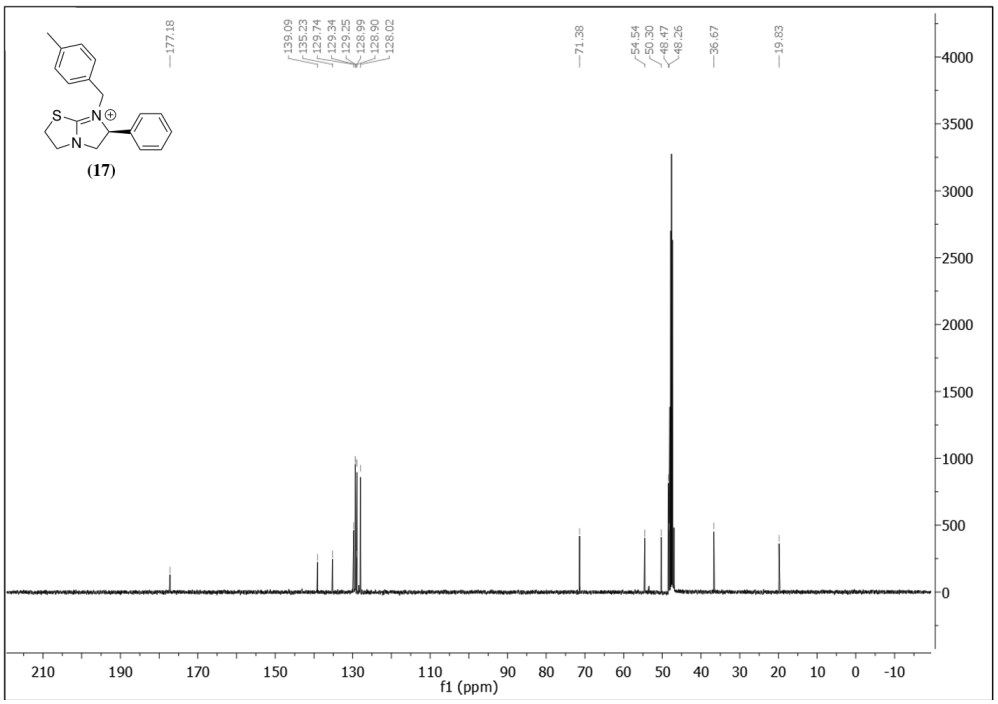

A1.37 ^{13}C NMR Spectrum of (*S*)-7-(4-methylbenzyl)-6-phenyl-2,3,5,6-tetrahydroimidazo[2,1-*b*]thiazol-7-ium – **(17)** in MeOD at 101 MHz

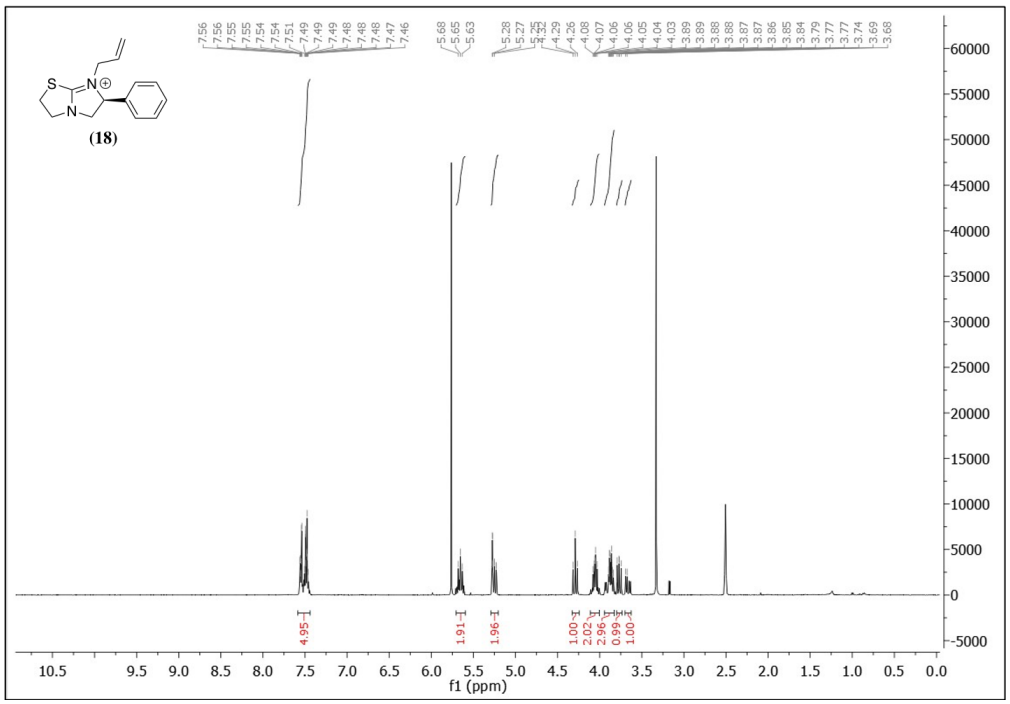

A1.38 ^{1}H NMR Spectrum of (*S*)-7-allyl-6-phenyl-2,3,5,6-tetrahydroimidazo[2,1-*b*]thiazol-7-ium- **(18)**) in DMSO-d_6 at 400 MHz.

Confidential and Proprietary Information

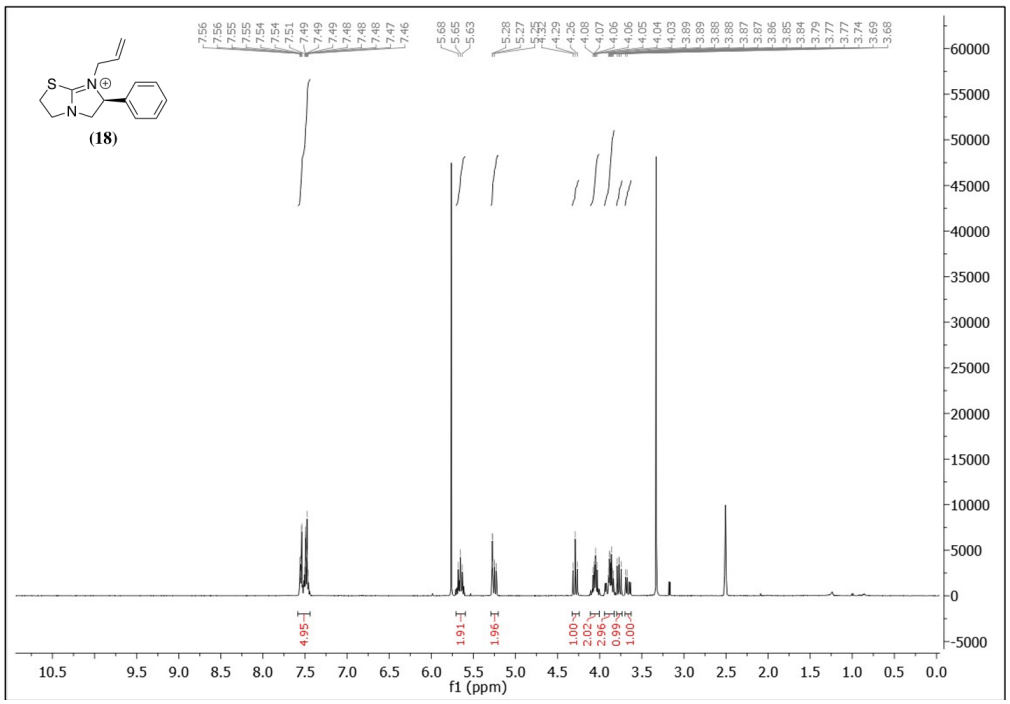

A1.39 ^{13}C NMR Spectrum of (*S*)-7-allyl-6-phenyl-2,3,5,6-tetrahydroimidazo[2,1-*b*]thiazol-7-ium- **(18)** in DMSO-d_6 at 101 MHz

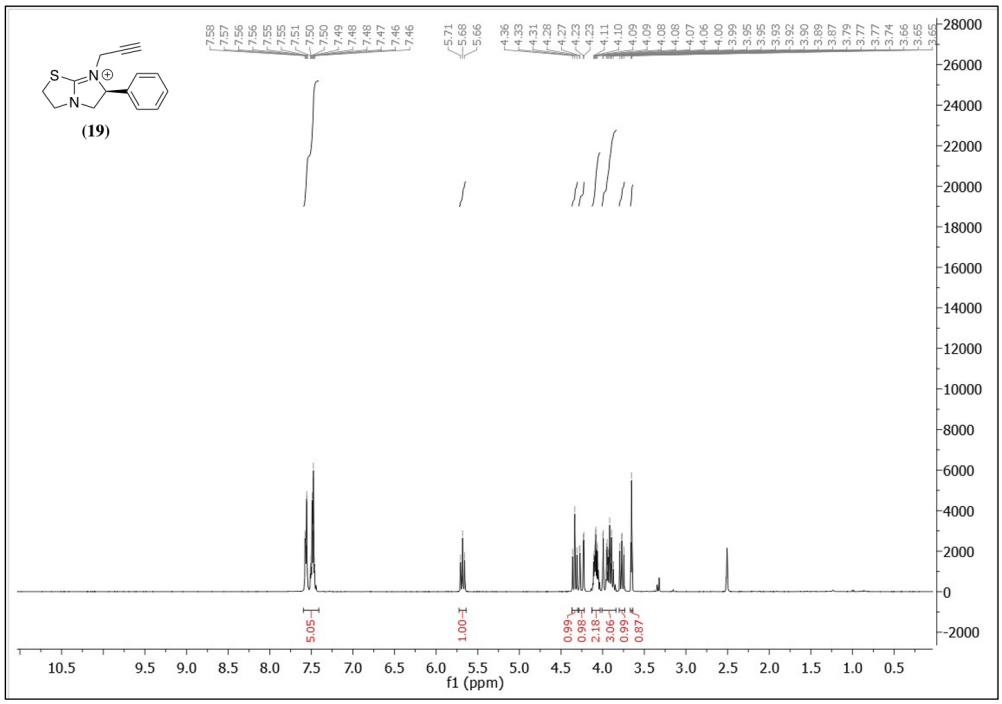

A1.40 ^{1}H NMR Spectrum of (S)-6-phenyl-7-(prop-2-yn-1-yl)-2,3,5,6-tetrahydroimidazo[2,1-b]thiazol-7-ium- **(19))** in DMSO-d_6 at 400 MHz.

Confidential and Proprietary Information

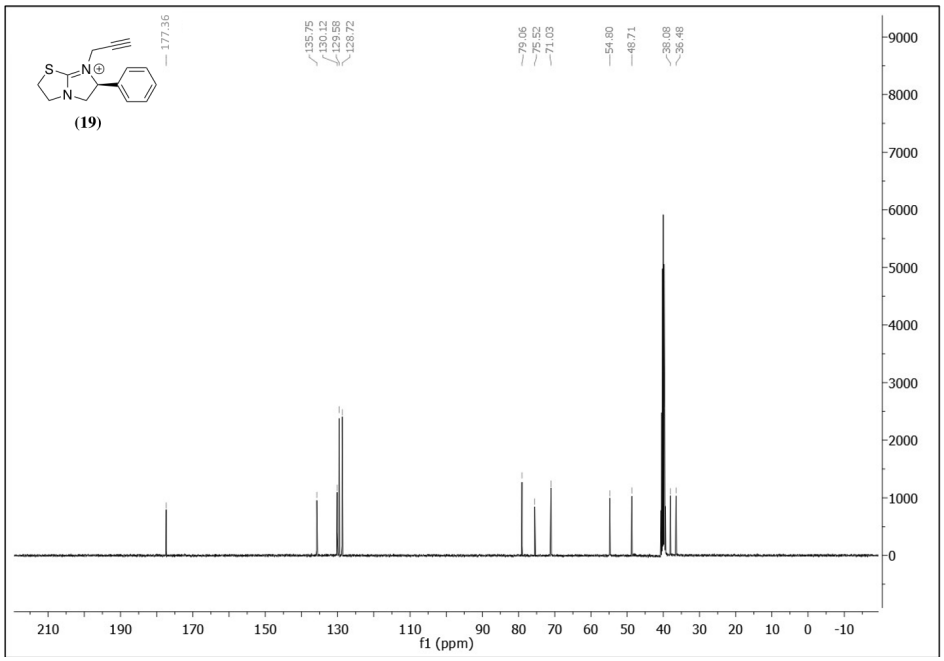

A1.41 ^{13}C NMR Spectrum of (S)-6-phenyl-7-(prop-2-yn-1-yl)-2,3,5,6-tetrahydroimidazo[2,1-b]thiazol-7-ium- **(19)** in DMSO-d_6 at 101 MHz

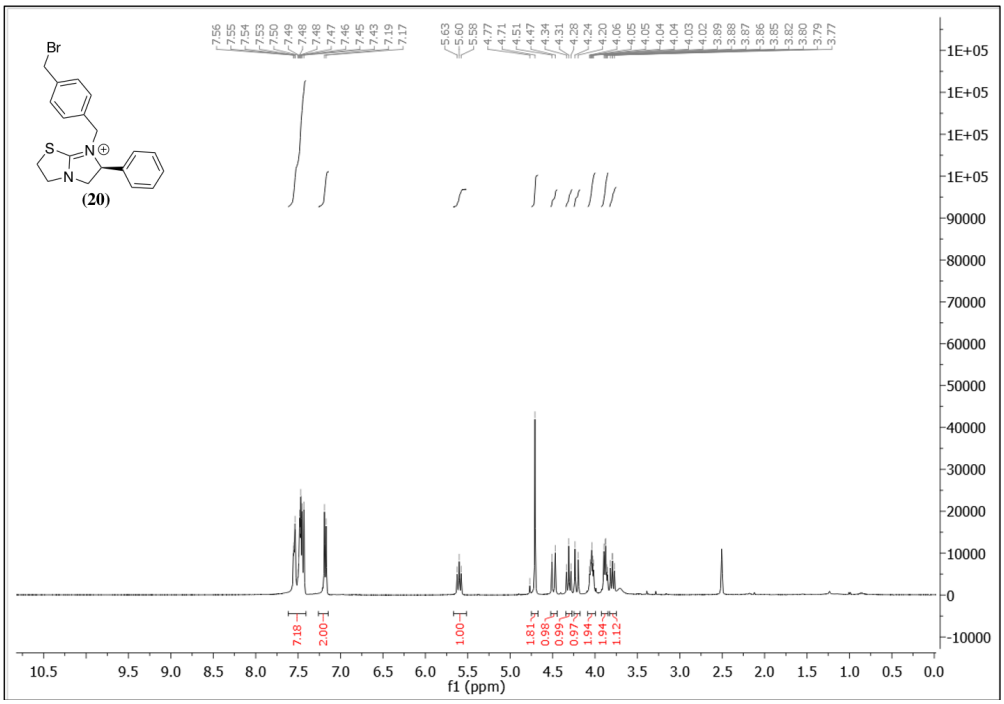

A1.42 ^{1}H NMR Spectrum of (*S*)-7-(4-(bromomethyl)benzyl)-6-phenyl-2,3,5,6-tetrahydroimidazo[2,1-*b*]thiazol-7-ium – **(20)** in MeOD at 400 MHz.

Confidential and Proprietary Information

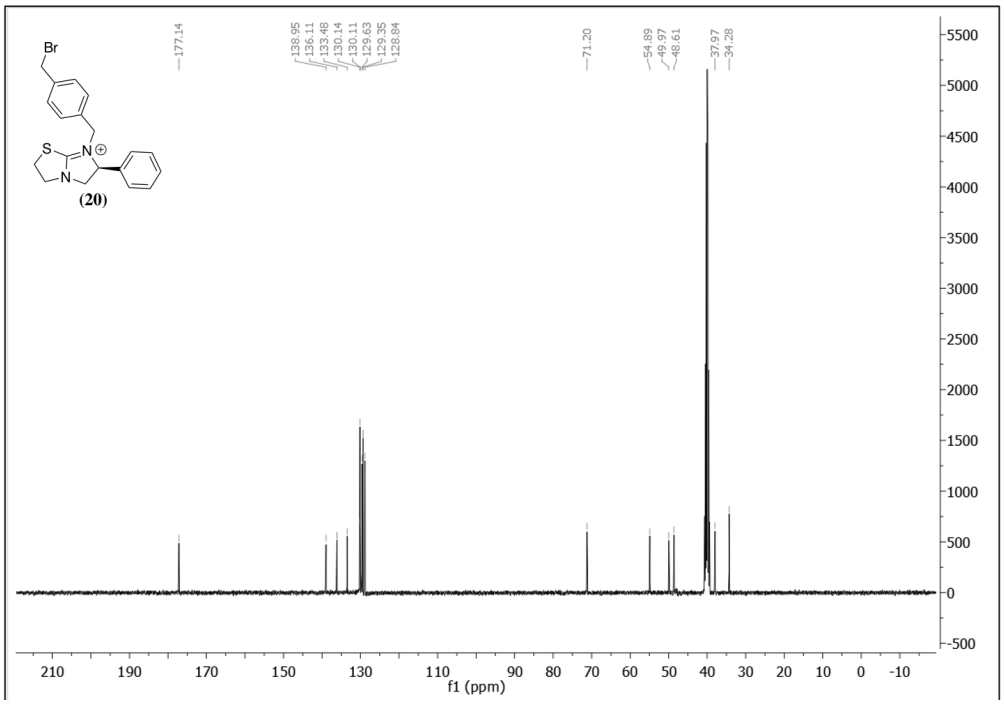

A1.43 ^{13}C NMR Spectrum of (*S*)-7-(4-(bromomethyl)benzyl)-6-phenyl-2,3,5,6-tetrahydroimidazo[2,1-*b*]thiazol-7-ium – **(20)** in MeOD at 101 MHz

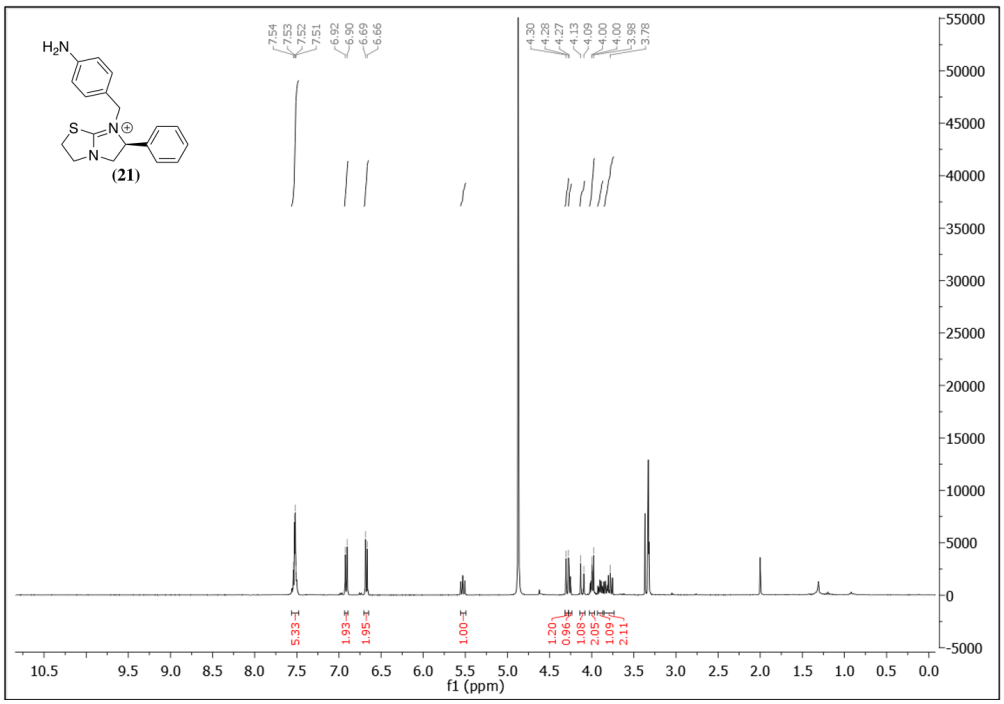

A1.44 ^{1}H NMR Spectrum of (*S*)-7-(4-aminobenzyl)-6-phenyl-2,3,5,6-tetrahydroimidazo[2,1-*b*]thiazol-7-ium – **(21)** in MeOD at 400 MHz.

Confidential and Proprietary Information

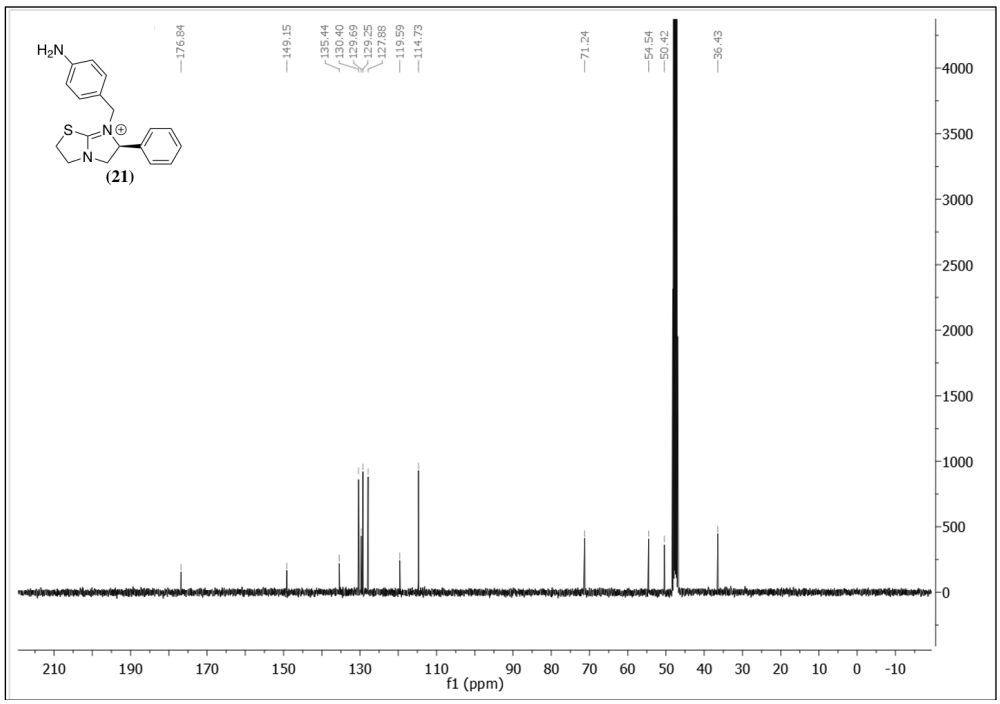

A1.45 ^{13}C NMR Spectrum of (*S*)-7-(4-aminobenzyl)-6-phenyl-2,3,5,6-tetrahydroimidazo[2,1-*b*]thiazol-7-ium – **(21)** in MeOD at 101 MHz

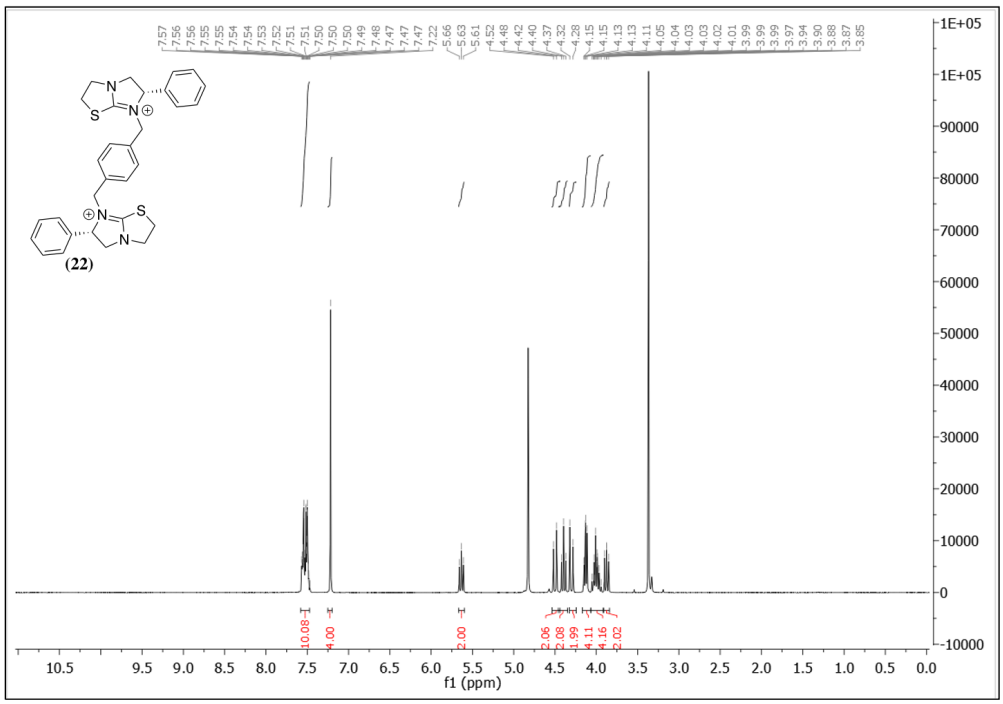

A1.46 ^{1}H NMR Spectrum of (6*R*,6'*R*)-7,7'-(1,4-phenylenebis(methylene))bis(6-phenyl-2,3,5,6-tetrahydroimidazo[2,1-*b*]thiazol-7-ium)– **(22)** in MeOD at 400 MHz.

Confidential and Proprietary Information

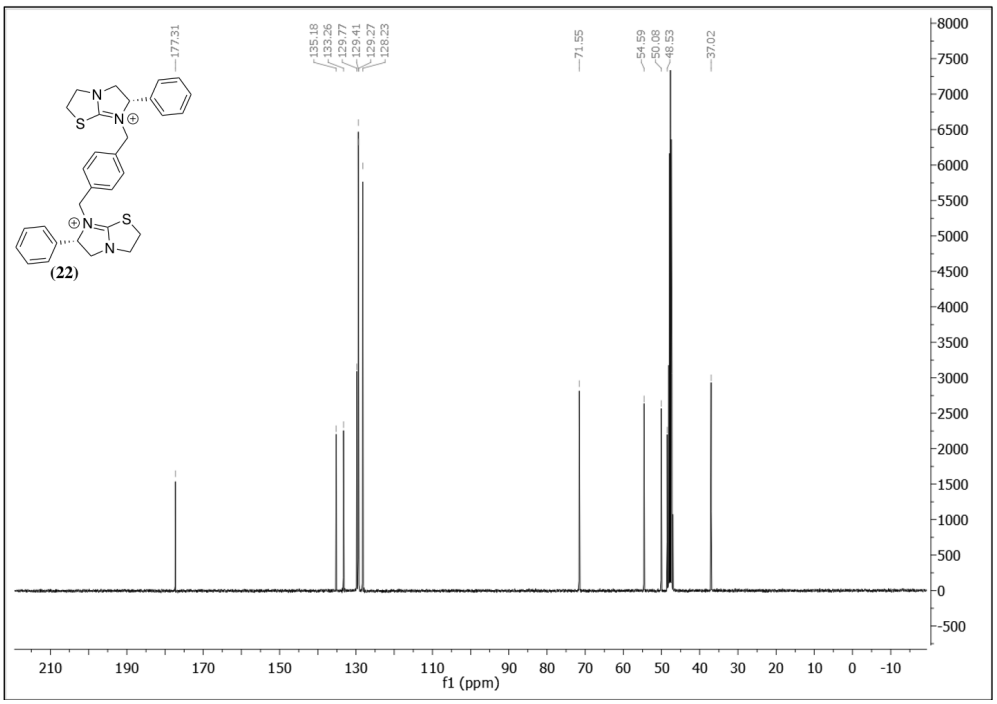

A1.47 ^{13}C NMR Spectrum of (6*R*,6'*R*)-7,7'-(1,4-phenylenebis(methylene))bis(6-phenyl-2,3,5,6-tetrahydroimidazo[2,1-*b*]thiazol-7-ium) – **(22)** in MeOD at 101 MHz

Confidential and Proprietary Information

A2. Conformational MS Spectra

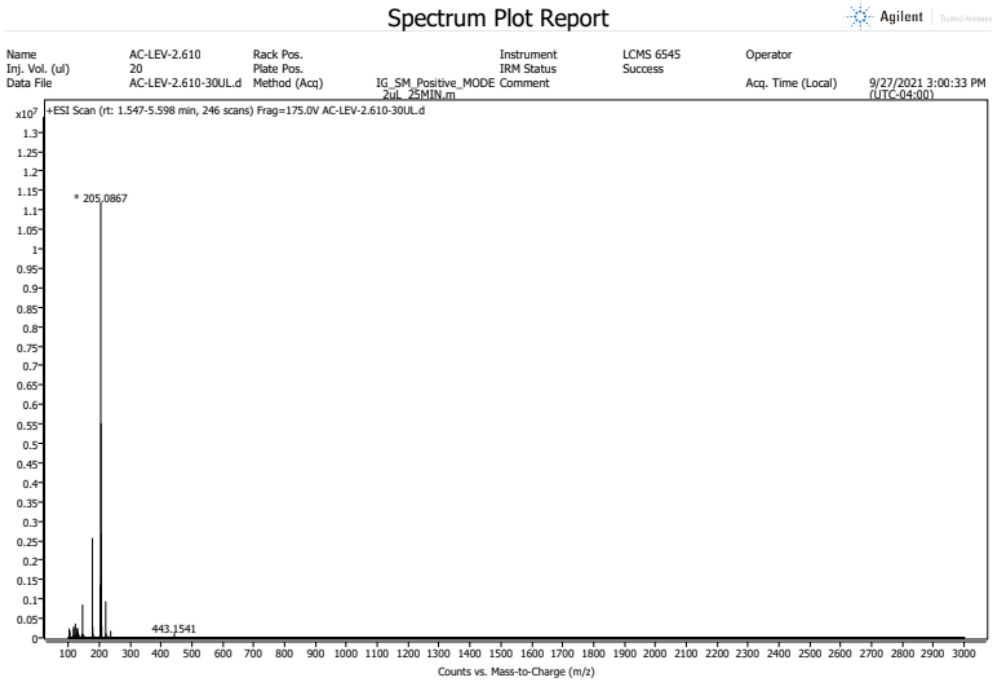

A2.1- Spectrum Plot Report for compound **7** + ESI Scan m/z calculated for compound **7** 205.0799, found 205.0867 [M+H]+

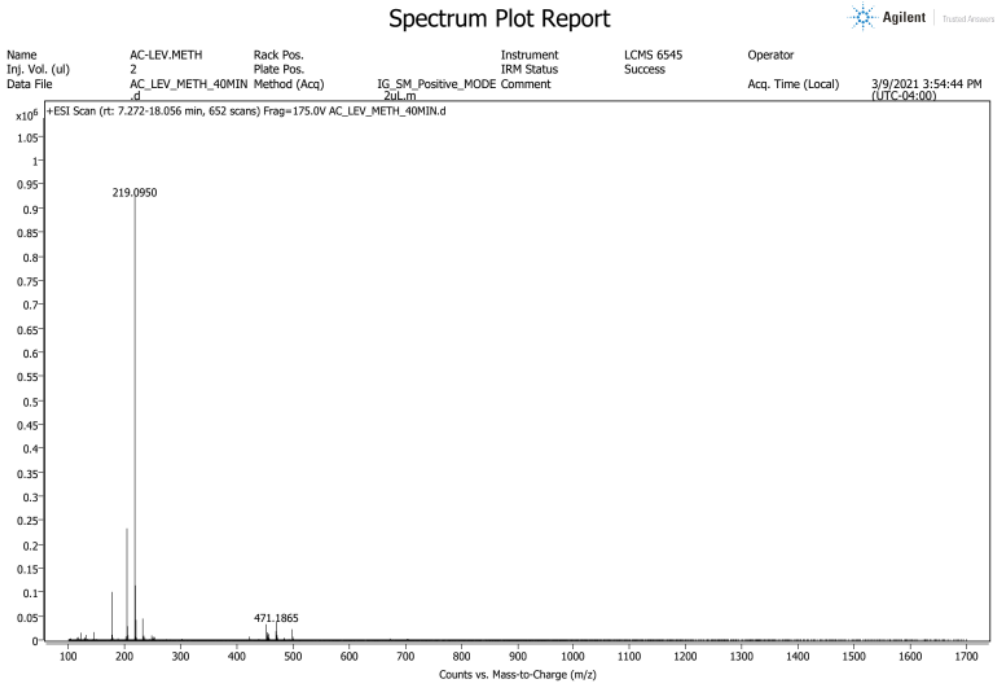

A2.2- Spectrum Plot Report for compound **8** + ESI Scan m/z calculated for compound **8** 219.0956, found 219.0950 [M+H]+

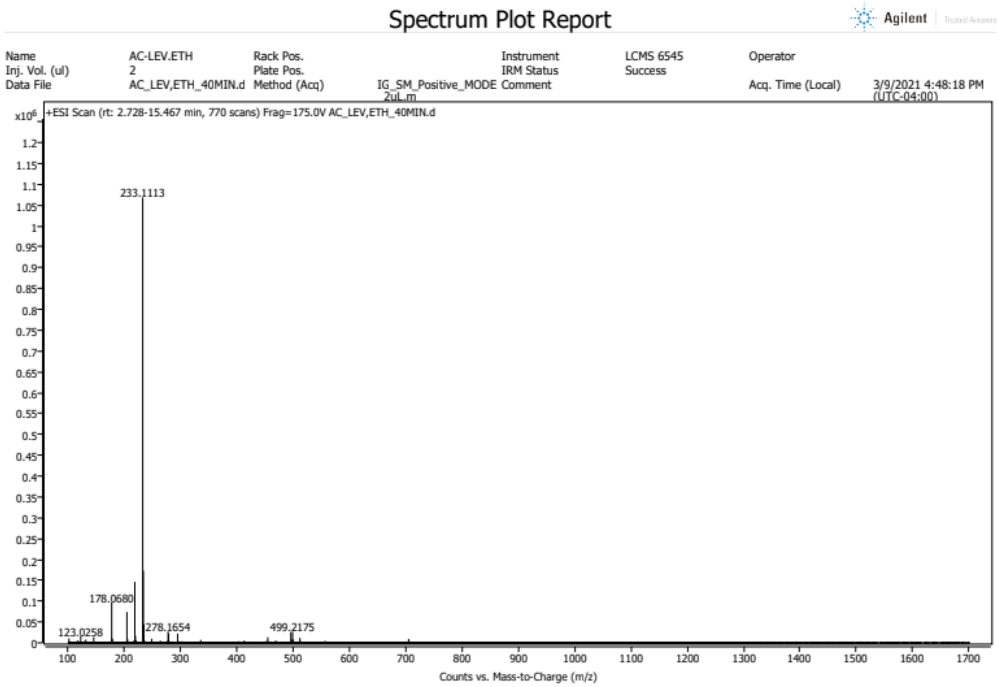

A2.3- Spectrum Plot Report for compound **9** + ESI Scan m/z calculated for compound **9** 233.1112, found 233.1113 [M+H]+

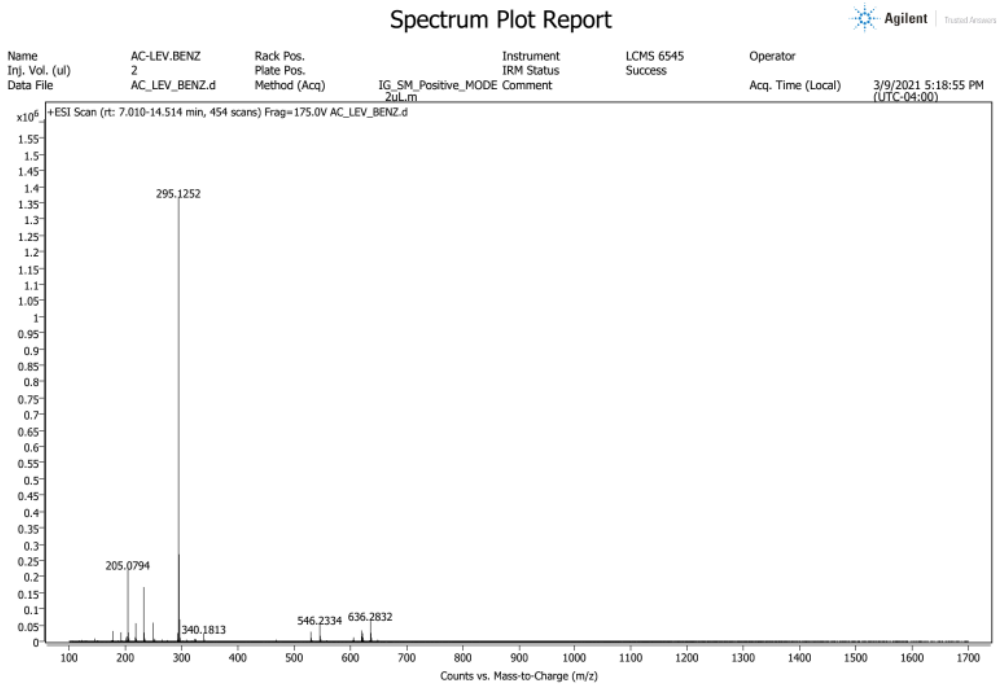

A2.4- Spectrum Plot Report for compound **10** + ESI Scan m/z calculated for compound **10** 295.1269, found 295.1252 [M+H]+

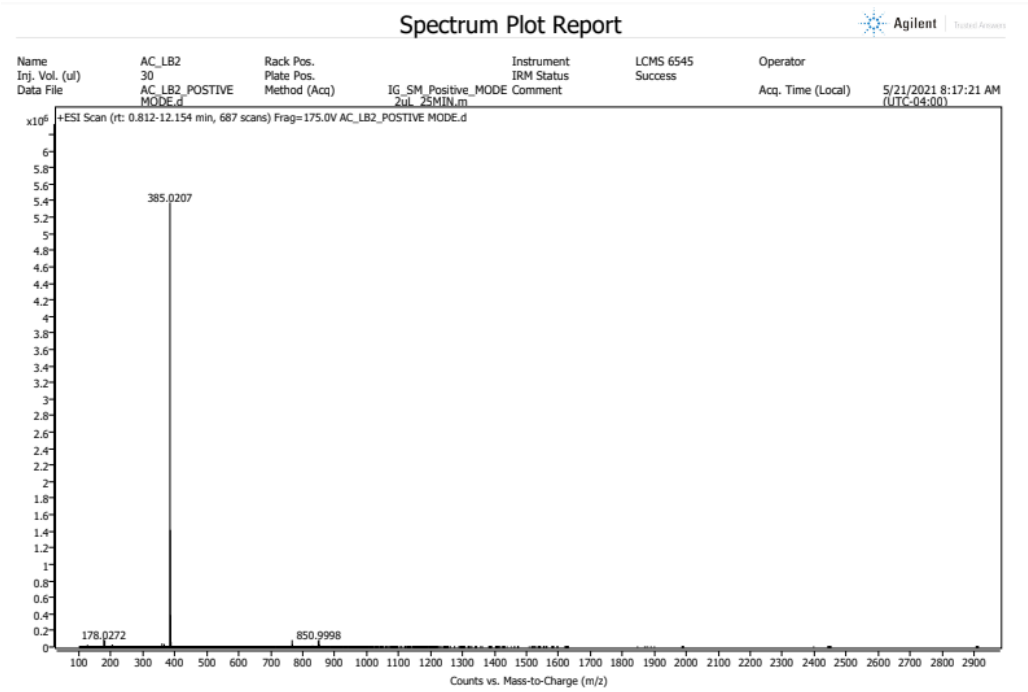

A2.5- Spectrum Plot Report for compound **11** + ESI Scan m/z calculated for compound **11** 385.0798, found 385.0207 [M+H]+

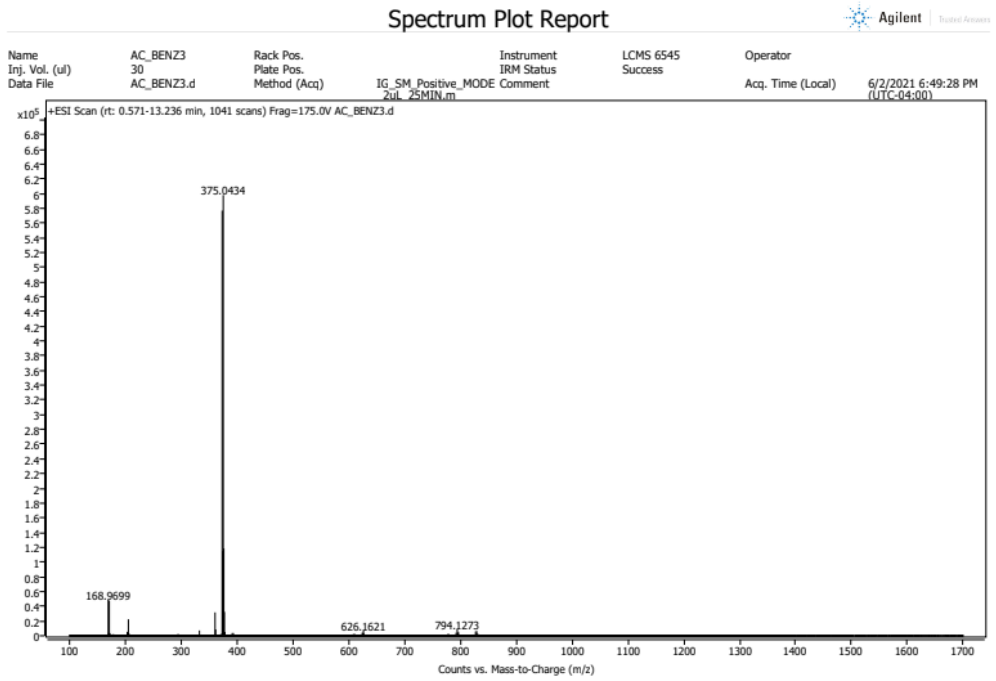

A2.6- Spectrum Plot Report for compound **12** + ESI Scan m/z calculated for compound **12** 373.0374, found 373.0453 and 375.0434 [M+H]+

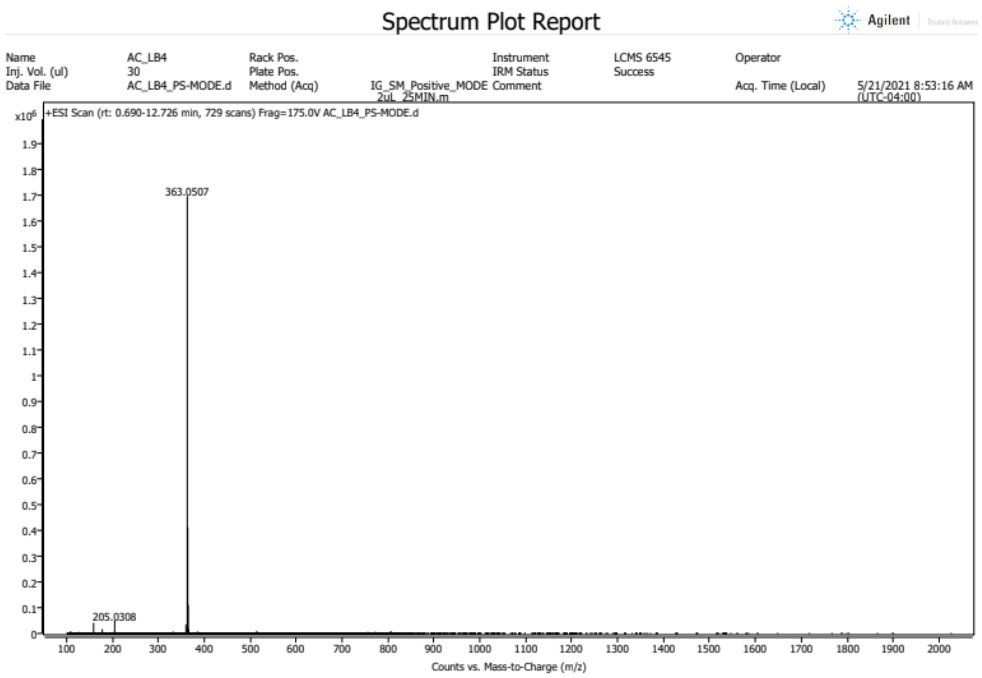

A2.7- Spectrum Plot Report for compound **13** + ESI Scan m/z calculated for compound **13** 363.1143, found 363.0507 [M+H]+

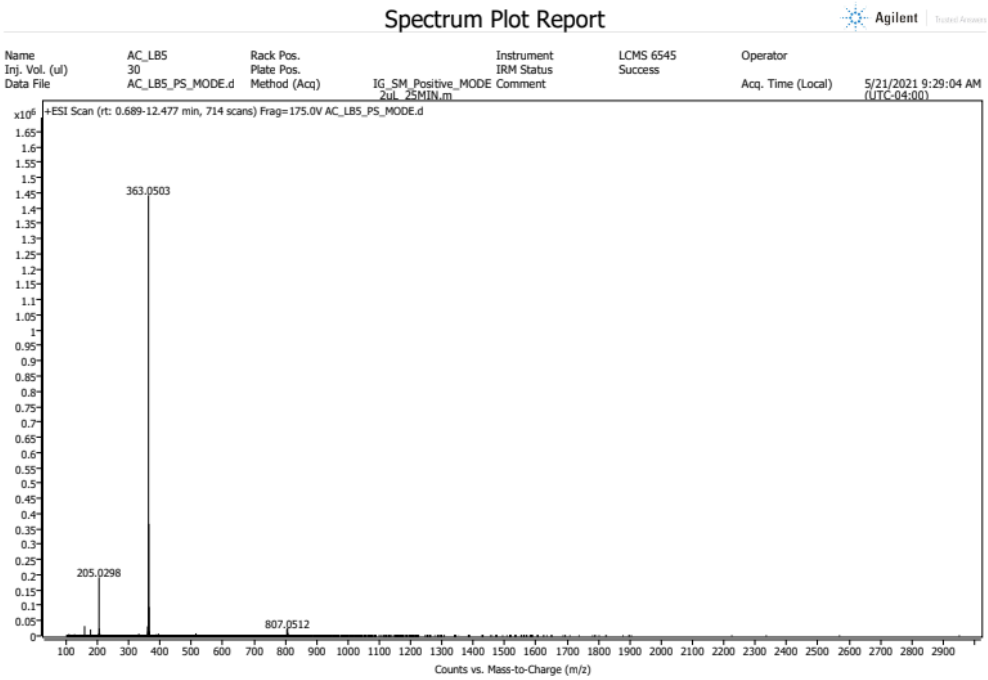

A2.8- Spectrum Plot Report for compound **14** + ESI Scan m/z calculated for compound **14** 363.1143, found 363.0503 [M+H]+

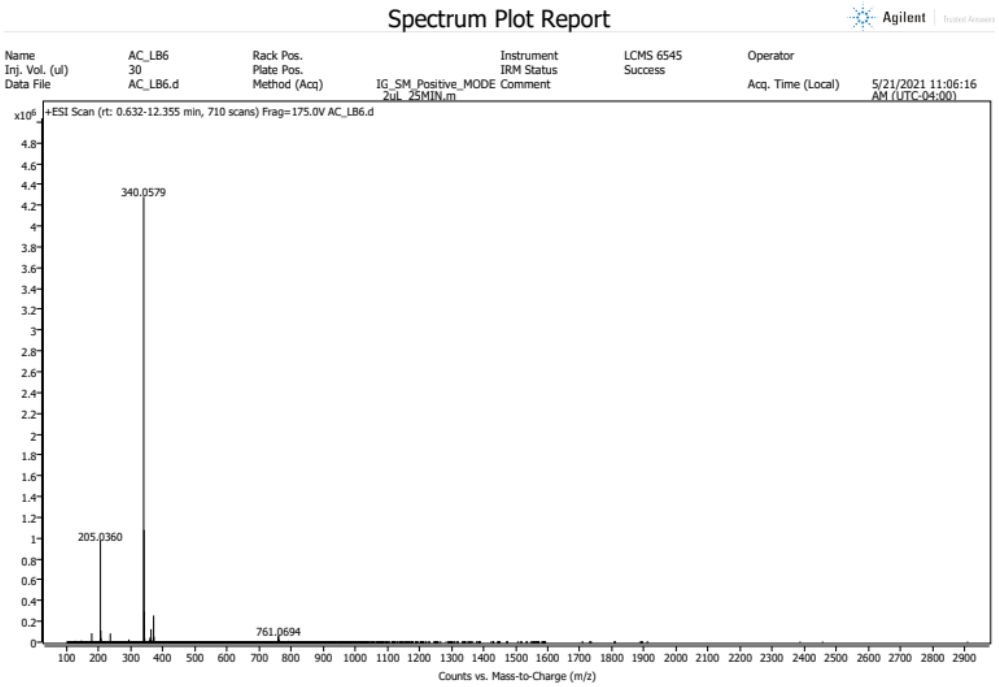

A2.9- Spectrum Plot Report for compound **15** + ESI Scan m/z calculated for compound **15** 340.1120, found 340.0579 [M+H]+

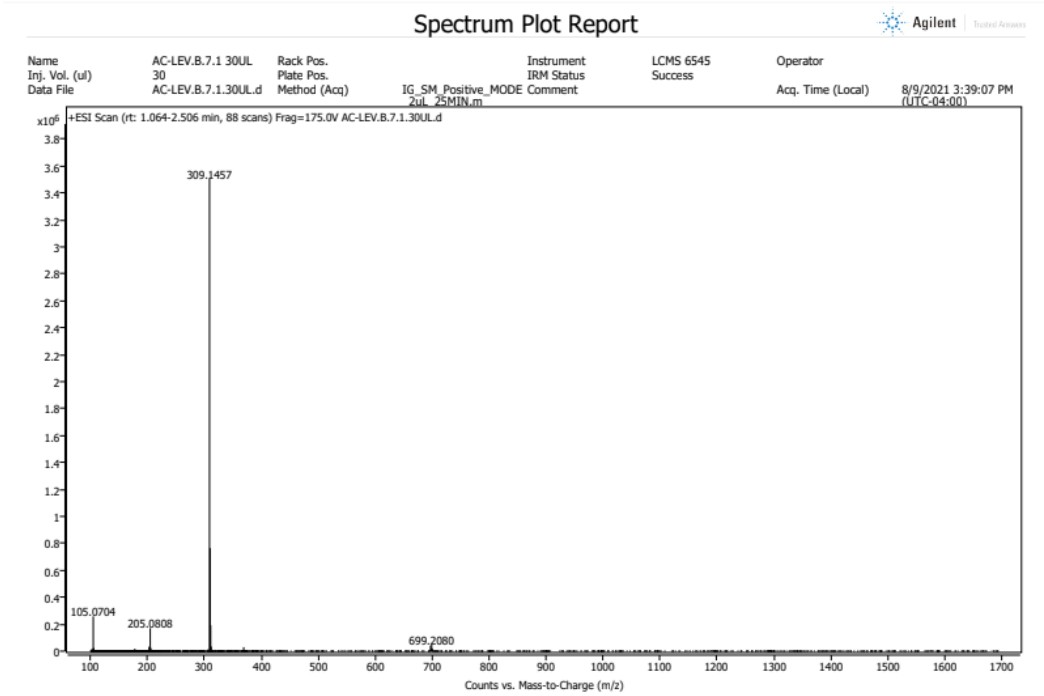

A2.10- Spectrum Plot Report results for compound **16** + ESI Scan m/z calculated for compound **16** 309.1425, found 309.1457 [M+H]+

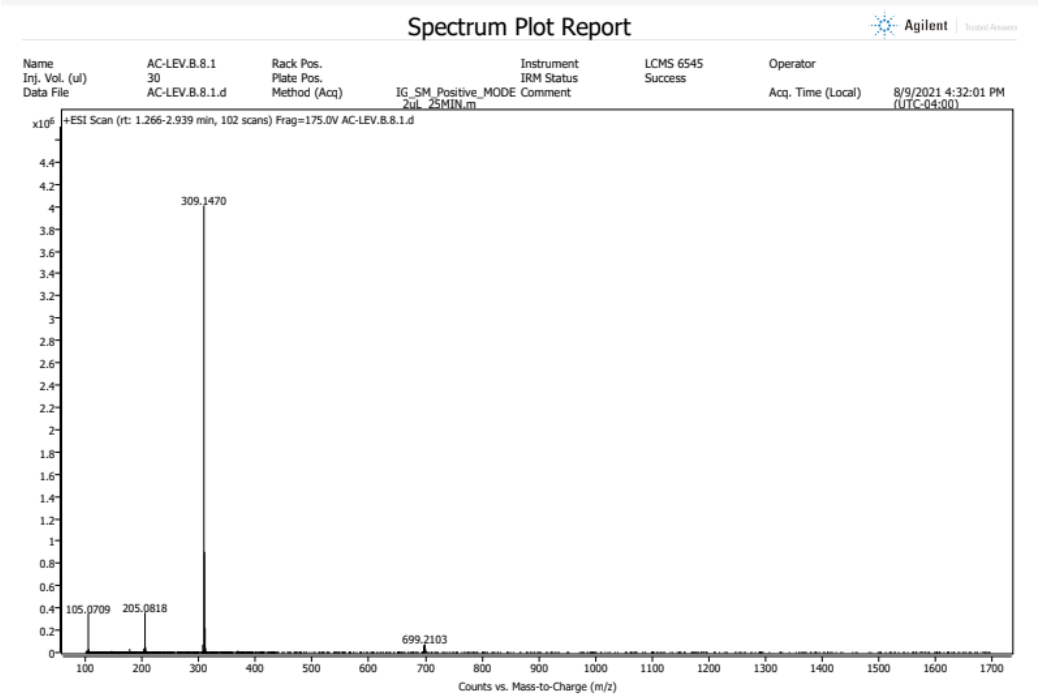

A2.11- Spectrum Plot Report results for compound **17** + ESI Scan m/z calculated for compound 1**7** 309.1425, found 309.1470 [M+H]+

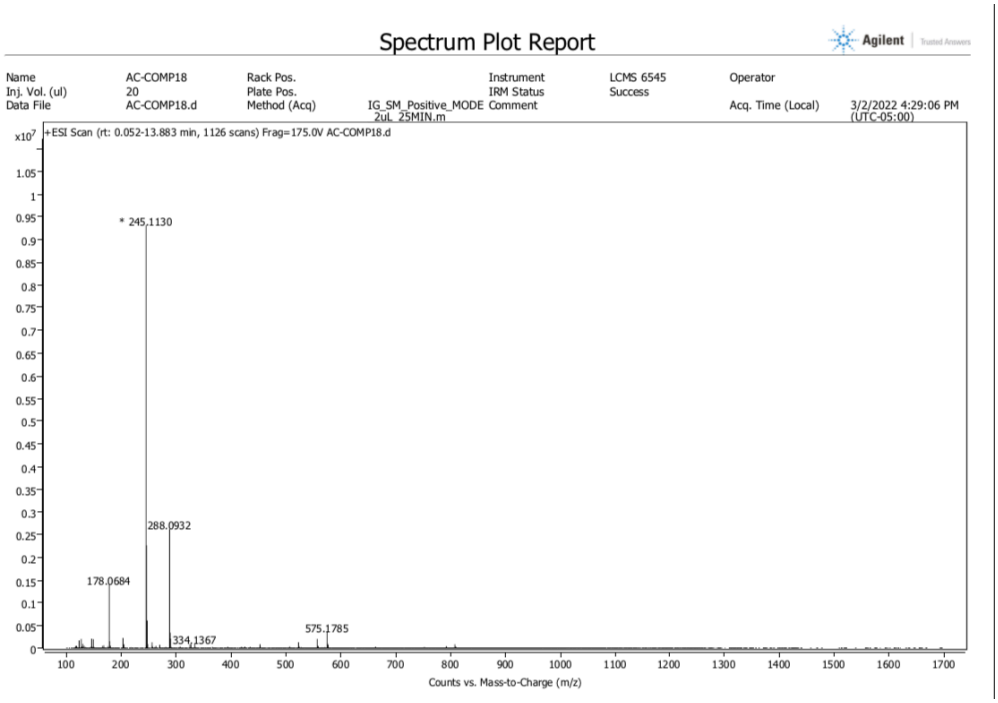

A2.12- Spectrum Plot Report results for compound **18** + ESI Scan m/z calculated for compound **18** 245.1112, found 245.1130 [M+H]+

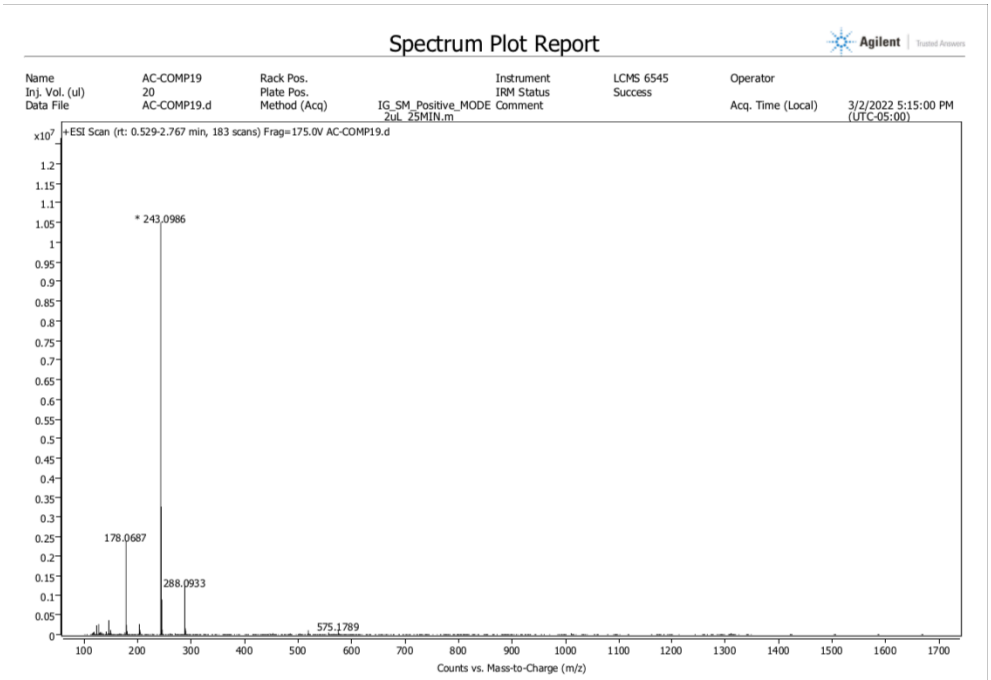

A2.13- Spectrum Plot Report results for compound **19** + ESI Scan m/z calculated for compound **19** 243.0956, found 243.0986 [M+H]+

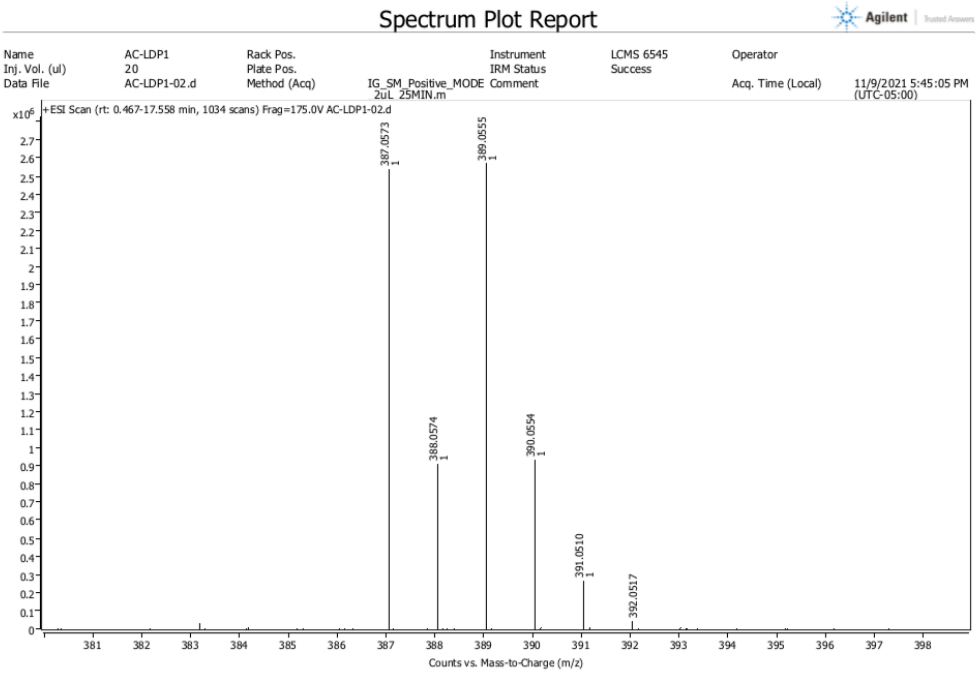

A2.14- Spectrum Plot Report results for compound **20** + ESI Scan m/z calculated for compound **20** 387.0531, found 387.0573 [M+H]+

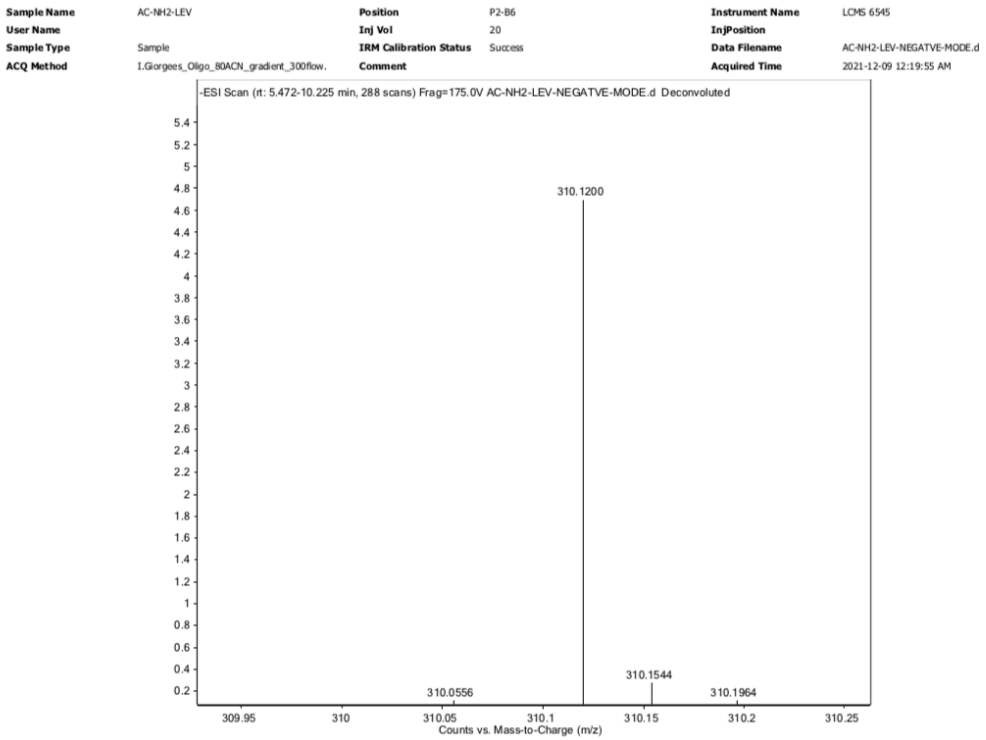

A2.15- Spectrum Plot Report results for compound **21** + ESI Scan m/z calculated for compound **21** 310.1378, found 310.1200 [M+H]+

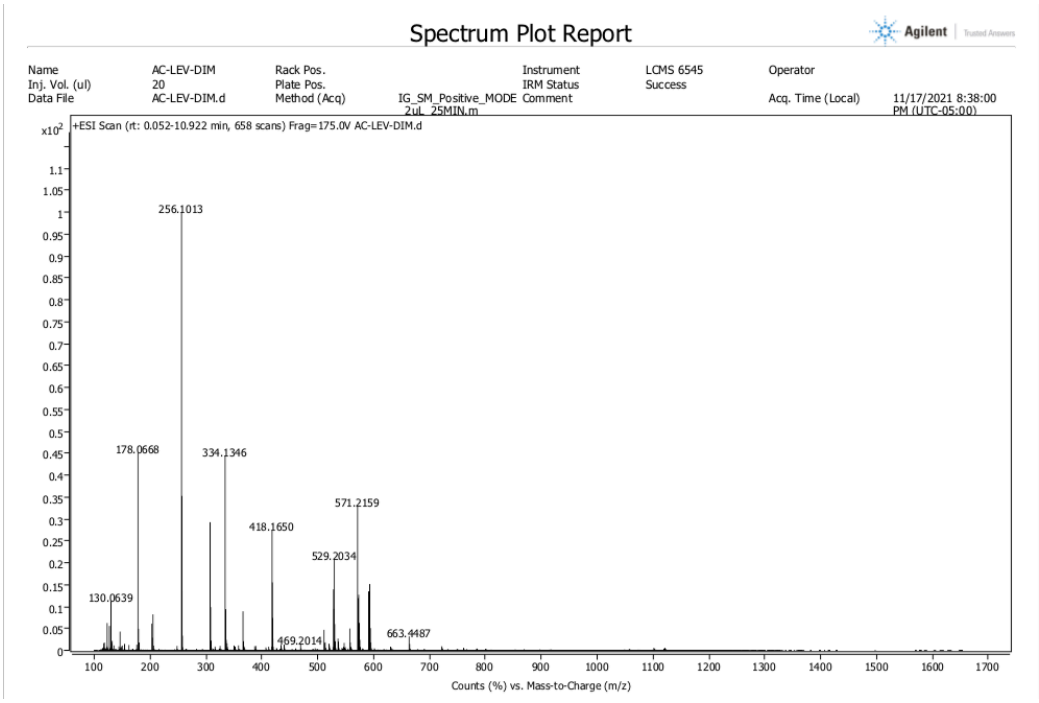

A2.16- Spectrum Plot Report results for compound **22** + ESI Scan m/z calculated for compound **22** 256.1034, found 256.1013[M+H]+

A3. Levamisole Novel Compound Data

Compound Structure and Name	Molecular Weight	Percent response in Hco-ACC-2 when compared to Acetylcholine
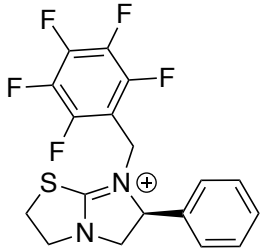 **(11)**	385.38	5.2%
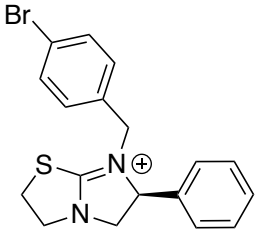 **(12)**	374.32	24.8%
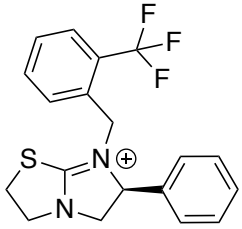 **(13)**	363.42	55.5%
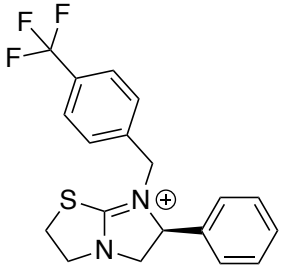 **(14)**	363.38	28.3%

Confidential and Proprietary Information

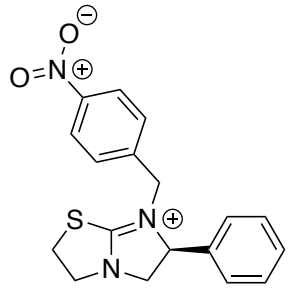 **(15)**	340.32	33.6%
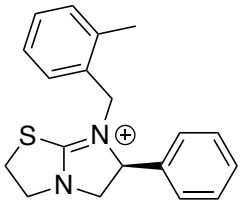 **(16)**	309.45	Not Tested
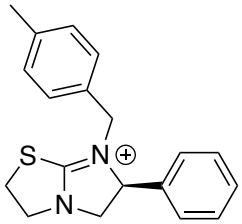 **(17)**	309.45	Not Tested
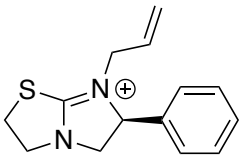 **(18)**	245.36	Not Tested
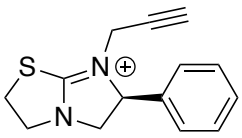 **(19)**	243.35	Not Tested

Confidential and Proprietary Information

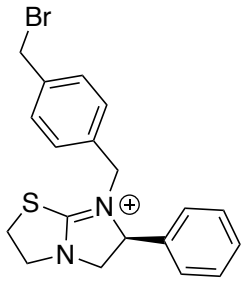 **(20)**	388.35	Not Tested
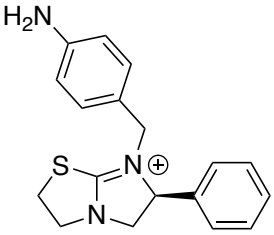 **(21)**	310.44	Not Tested
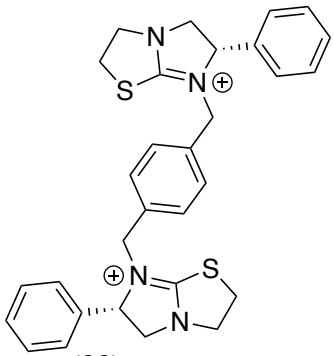 **(22)**	512.73	Not Tested

Confidential and Proprietary Information